NOVEL ECG ANALYSIS WITH APPLICATION TO ATRIAL FIBRILLATION DETECTION

A Thesis Presented to The

CENTRE FOR SIGNAL AND IMAGE PROCESSING,

DEPARTMENT OF ELECTRONIC AND ELECTRICAL ENGINEERING,

UNIVERSITY OF STRATHCLYDE

In Fulfilment of the Requirements for the Degree of

Doctor of Philosophy

By

Fakroul Ridzuan Bin Hashim

2016

Declaration

I declare that this thesis embodies my own research work and that it is composed by me. Where appropriate, I have made acknowledgment to the work of others.

Signed: Date:

Acknowledgements

I would particularly like to express my deepest gratitude here to both my supervisors, Professor John J. Soraghan and Dr Lykourgos Petropoulakis. They imparted invaluable guidance, knowledge and gave me inspiration and encouragement when I needed it the most. They shared my enthusiasm with this research and helped to facilitate my PhD experience by steering my research in the right direction. I am greatly indebted to Professor John and Dr Akis for the support during these periods.

Special thanks to my work place, National Defence University of Malaysia for giving me the opportunity to further my studies up to this point. To the government of Malaysia, I will contribute back to the country after years of sponsoring my studies in the UK. Last but not least, dear staffs and friends in CeSIP, the memories and helps from you guys I will not forget.

My heartfelt gratitude also goes to my parents, siblings and friends whose belief in me never wavered. Finally, I wish to thank the wind beneath my wings, Sya (wife) and Iris & Amanda (daughters), without whose support, love and encouragement this research would have remained just an unrealised dream.

Abstract

A new approach of electrocardiography (ECG) analysis system is developed to process noisy ECG signals leading for improved arrhythmia detection. The system employs two processing units comprising a novel noise reduction unit and a novel pattern recognition unit. Each unit incorporates numbers of processing techniques. In the noise reduction unit, the ECG signal is denoised before proceeding to the next stage. Four main noises contaminating the ECG signal are considered that includes baseline wander (BW), powerline interference (PLI), electromyogram (EMG) and motion artifact (MA). For BW and MA noise reduction, a novel Sqtwolog Threshold and High/Low pass (STHL) wavelet based filter is used. An Improved Proportionate Normalised Least Mean Square (IPNLMS) adaptive filter is used to the effects of EMG noise and a bandstop notch filter is used to cope with PLI.

The pattern recognition unit comprises feature extraction process and classification process. In this research, some features from ECG signals are extracted to be used as the input vector for classification stage. A new Rectangular Pulse Domain (RPD), feature extraction technique is proposed that operates by taking the amplitude of intersection between filtered ECG signal and rectangular pulses. The signal is divided according to R to R peak interval (RRI) before superimposing with the rectangular pulses. The research also investigates the use of the P to T peak interval (PTI) as the signal limiter as an alternative to RRI approach and has shown encouraging performance. The classification process is performed to identify the signal whether it belongs to Atrial Fibrillation (AF) or vice-versa. The extracted features are used as the input vectors to the classifier.

Two novel classifiers are designed which are the Cascade Hybrid Multilayer Perceptron (CHMLP) and the Multi-Classify Hybrid Multilayer Perceptron (MCHMLP) networks which improved version of Hybrid Multilayer Perceptron (HMLP) neural network. The MCHMLP network performs a multiple classification by doing the second classification after the first classification has achieved the optimal point. Compare with the CHMLP network, however, performs the second classification process after the first classification has been done at each iteration and stops after it reaches the optimal structure. Both networks

provide better results than the conventional HMLP network but the CHMLP network gives better accuracy and standard deviation results than the MCHMLP network.

The combination of both the novel noise reduction and the novel pattern recognition units are used to develop the new approach of ECG analysis system in identifying the AF signal. The performance of the new ECG analysis has been tested using the MIT-BIH ECG database.

List of Acronyms

AA	Atrial Activity
AF	Atrial Fibrillation
AHA	American Heart Association
ANFIS	Adaptive Neuro Fuzzy Interference System
ANN	Artificial Neural Network
ARMA	Autoregressive Moving Average
AV	Atrioventricular
aVf	Augmented Vector Foot
aVl	Augmented Vector Left
aVr	Augmented Vector Right
BP	Back propagation
BW	Baseline Wander
CHMLP	Cascade Hybrid Multilayer Perceptron
CLMS	Constrained Least Mean Square
CM	Curve Mapping
CMOS	Complementary Metal-Oxide Semiconductor
Db	Daubechies
DFT	Discrete Fourier Transform
DWT	Discrete Wavelet Transform
EBWS	Energy Based Wavelet Transform
ECG	Electrocardiography
EMD	Empirical Mode Decomposition
ESC	European Society of Cardiology
FFT	Fast Fourier Transform
FIR	Finite Impulse Response
FSA	Frequency Spectrum Analysis
GA	Genetic Algorithm
GMM	Gaussian Mixture Model
HT	Heursure Threshold
HTHL	Heursure Threshold & High/Low pass
ICA	Independent Component Analysis

IIR	Infinite Impulse Response
IMF	Intrinsic Mode Function
IPNLMS	Improved Proportionate Normalised Least Mean Square
K-Mean	K-Mean Clustering
KNN	K-Nearest Neighbourhood
LADT	Linear Approximation Data Transfer
LCAD	Low Cost Access cum Computing Device
LDA	Linear Discriminant Analysis
LM	Levenberg Marquardt
LMS	Least Mean Square
LVE	Left Ventricle Event
MA	Motion Artifact
MCHMLP	Multi-Classify Hybrid Multilayer Perceptron
MIT-BIH	Massachusetts Institute of Technology Beth Israel Hospital
MLP	Multilayer Perceptron
MM	Markov Model
MRBF	Multiple Radial Basis Function
MRPE	Modified Recursive Prediction Error
MSE	Mean Square Error
MT	Minimax Threshold
MTHL	Minimax Threshold & High/Low pass
NLMS	Normalised Least Mean Square
NSR	Normal Sinus Rhythm
NSRLMS	Normalised Signed Regressor Least Mean Square
PAR	Pulse Active Ratio
PD	Partial Discharge
PLI	Powerline Interference
PRD	Pulse Rectangular Domain
PRSA	Phase Rectified Signal Averaging
PTB	Physikalisch-Technische Bundesanstalt Diagnostic
PTI	P to T Peak Interval
PVC	Premature Ventricular Contraction
PWM	Pulse Width Modulation
QDA	Quadratic Discriminant Analysis

RBF	Radial Basis Function
RLS	Recursive Least Square
RMS	Root Mean Square
RPE	Recursive Prediction Error
RRI	R to R Peak Interval
RT	Rigrsure Threshold
RTHL	Rigrsure Threshold & High/Low pass
SA	Sino-Atrial
SD-LMS	Sign Data Least Mean Square
SG	Savitzky Golay
SMW	Signal Matching Wavelet
SNR	Signal to Noise Ratio
ST	Sqtwolog Threshold
STHL	Sqtwolog Threshold & High/Low pass
SVM	Support Vector Machine
SWT	Stationary Wavelet Transform
TDMG	Time Domain Morphology and Gradient
TVCF	Time-Varying Coherence Functions
TVTF	Time-Varying Transfer Functions
UCI	University of California at Irvine
UFD	Ultrasonic Flaw Detection
VFD	Variable Fraction Delay

List of Figures

Figure 2.1:	The basic human heart anatomy.	9
Figure 2.2:	ECG output with cardiac activities.	10
Figure 2.3:	The electric impulses movement in the heart.	11
Figure 2.4:	ECG signal complex.	13
Figure 2.5:	The fiducial points taken from a complex ECG signal.	14
Figure 2.6:	The placement of 10 leads in the standard 12 Leads configuration.	15
Figure 2.7:	The Einthoven's triangle configuration setting at the limb.	16
Figure 2.8:	The Holter monitoring system.	17
Figure 2.9:	The Holter system used to record ECG signals.	19
Figure 2.10:	Holter monitor in use.	19
Figure 2.11:	A screenshot of the Holter ECG.	20
Figure 2.12:	The AF ECG signal in the heart.	22
Figure 2.13:	The normal ECG signal in the heart	23
Figure 3.1(a):	Normal ECG signal.	26
Figure 3.1(b):	BW noise.	26
Figure 3.1(c):	PLI noise.	27
Figure 3.1(d):	EMG noise.	27
Figure 3.1(e):	MA noise.	28
Figure 3.1(f)	Corrupted normal ECG with BW, PLI, EMG and MA noises.	28
Figure 3.2:	Adaptive filter block set.	32
Figure 3.3:	Block diagram of filter analysis.	37
Figure 3.4:	A 3 level filter bank.	38
Figure 3.5:	PAR pulse generation.	46
Figure 3.6:	Nonlinear neuron model.	51
Figure 3.7:	A schematic diagram of a HMLP network with one hidden layer.	54
Figure 4.1:	The novel noise reduction unit with different filters of each noise.	58
Figure 4.2:	Adaptive filter structure.	59
Figure 4.3:	Block diagram for the filtering process of BW and MA noises.	62
Figure 4.4(a):	Normal signal with PLI noise.	65
Figure 4.4(b):	Result after PLI noise removal from normal signal.	65
Figure 4.5(a):	AF signal with PLI noise.	66

Figure 4.5(b):	Result after PLI noise removal from AF signal.	66
Figure 4.6:	The MSE performances for normal subjects.	67
Figure 4.7:	The MSE performances for AF subjects.	68
Figure 4.8(a):	Result of EMG noise removal from normal ECG filtered by NLMS.	69
Figure 4.8(b):	Result of EMG noise removal from normal ECG filtered by PNLMS.	70
Figure 4.8(c):	Result of EMG noise removal from normal ECG filtered by IPNLMS.	70
Figure 4.8(d):	Result of EMG noise removal from normal ECG filtered by MPNLMS.	71
Figure 4.9(a):	Result of EMG noise removal from AF ECG filtered by NLMS.	72
Figure 4.9(b):	Result of EMG noise removal from AF ECG filtered by PNLMS.	72
Figure 4.9(c):	Result of EMG noise removal from AF ECG filtered by IPNLMS.	73
Figure 4.9(d):	Result of EMG noise removal from AF ECG filtered by MPNLMS.	73
Figure 4.10(a):	Normal signal with BW and MA noises.	77
Figure 4.10(b):	Result of MA noise removal from normal signal after ST is applied.	77
Figure 4.10(c):	Result of MA and BW noises removal from normal signal after STHL is applied.	78
Figure 4.10(a):	AF signal with BW and MA noises.	79
Figure 4.10(b):	Result of MA noise removal from AF signal after ST is applied.	79
Figure 4.10(c):	Result of MA and BW noises removal from AF signal after STHL is applied.	80
Figure 5.1:	The pattern recognition unit; (a) extraction feature process by using RRI and PTI morphology and (b) classification process using MCHMLP and CHMLP networks.	85
Figure 5.2:	The flowchart of the feature extraction process.	86
Figure 5.3:	Extraction of irregularity of PTI and rest time removal.	87
Figure 5.4(a):	ECG feature extraction based on RRI (AF signal).	88
Figure 5.4(b):	ECG feature extraction based on PTI (AF signal).	89
Figure 5.4(c):	ECG feature extraction based on RRI (normal signal).	89

Figure 5.4(d):	ECG feature extraction based on PTI (normal signal).	90
Figure 5.5:	Block diagram of the proposed network architecture.	92
Figure 5.6:	A schematic diagram of CHMLP network with one hidden layer.	93
Figure 6.1:	The flowcharts of the ECG analysis system.	104
Figure 6.2(a):	Normal signal corrupted with BW, PLI, EMG and MA noises.	107
Figure 6.2(b):	Normal signal after PLI elimination.	107
Figure 6.2(c):	Normal signal after EMG removal.	108
Figure 6.2(d):	A clean normal signal generated after BW and MA been reduced.	108
Figure 6.3(a):	AF signal corrupted with BW, PLI, EMG and MA noises.	109
Figure 6.3(b):	AF signal after PLI elimination.	109
Figure 6.3(c):	AF signal after EMG removal.	110
Figure 6.3(d):	A clean AF signal generated after BW and MA been reduced.	110

List of Tables

Table 3.1:	Summary of contaminating noises in ECG signal.	25
Table 3.2:	Summary of ECG noise reduction using IIR/FIR.	30
Table 3.3:	Summary of ECG noise reduction using adaptive filter.	33
Table 3.4:	Summary of ECG noise reduction using wavelet.	39
Table 3.5:	Summary of ECG characteristic detection techniques.	42
Table 3.6:	Summary of waveform based feature detection techniques.	44
Table 3.7:	The comparative results of AF classification using various techniques.	47
Table 4.1:	PLI removal from normal and AF signal.	63
Table 4.2:	EMG removal from normal and AF signal.	68
Table 4.3:	The comparative study on denoising the EMG noise from ECG signals.	74
Table 4.4:	BW and MA removal from normal and AF signals.	76
Table 4.5:	The comparative study on denoising the BW and MA noises from ECG signals.	81
Table 5.1:	The HMLP classification performance by using extracted features from RRI morphology as the input vector.	90
Table 5.2:	The HMLP classification performance by using extracted features from RRI morphology as the input vector.	91
Table 5.3:	Dataset descriptions.	94
Table 5.4:	Classification performance of the CHMLP, MCHMLP and other classifiers on several datasets.	96
Table 5.5:	The comparative results of AF classification using various technique.	99
Table 6.1:	Performance of the noise reduction unit.	105
Table 6.2:	The results of AF classification using CHMLP and MCHMLP networks.	111

Table of Contents

Declaration		i
Acknowledgements		ii
Abstract		iii
List of Acronyms		v
List of Figures		viii
List of Tables		xi
Chapter 1	**Introduction**	
1.1	Overview	1
1.2	Research Motivation	2
1.3	Summary of Original Contributions	3
1.4	Thesis Organization	5
	Author Publications	7
Chapter 2	**ECG Acquisition**	
2.1	Introduction	8
2.2	Cardiac Rhythm Abnormality	8
2.2.1	Type of Cardiac Abnormality	9
2.3	Electrocardiography (ECG)	10
2.3.1	Electrical Conductivity of The Heart	11
2.3.2	ECG Signal Morphology	12
2.3.3	Ficidual Point Detection	13
2.3.4	ECG Lead Configuration	15
2.4	Holter Monitor	16
2.4.1	History of Development	17
2.4.2	Component of Holter Monitor	18
2.4.2.1	ECG Recorder	18
2.4.2.2	ECG Analysis Software	20
2.5	Atrial Fibrillation (AF)	22
2.5.1	AF Diagnosis	23
2.6	Conclusion	23

Chapter 3	**ECG Analysis**	
3.1	Introduction	24
3.2	ECG Database	24
3.3	ECG Filtering	25
3.4	Noise Reduction Method	29
3.4.1	IIR and FIR Filters	29
3.4.2	Adaptive Filter	32
3.4.3	Wavelet Transform	35
3.5	ECG Feature Extraction	41
3.5.1	Characteristic Based Feature	42
3.5.2	Waveform Based Feature	44
3.5.3	AF Detection Algorithms	46
3.6	ECG Pattern Recognition using Neural Network	51
3.6.1	Hybrid Multilayer Perceptron (HMLP)	52
3.6.2	Training Process	55
3.7	Conclusion	56
Chapter 4	**Novel ECG Noise Reduction Unit**	
4.1	Introduction	57
4.2	Noise Reduction Unit	57
4.2.1	Bandstop Notch Filter in Eliminating PLI Noise	58
4.2.2	LMS based Adaptive Filter in Removing EMG Noise	58
4.2.3	Wavelet based Filter in Reducing BW and MA Noise	62
4.3	Experiment Results	63
4.3.1	PLI Elimination	63
4.3.2	EMG Removal	67
4.3.3	BW and MA Denoising	75
4.4	Discussion	82
4.5	Conclusion	83
Chapter 5	**Novel Pattern Recognition Unit**	
5.1	Introduction	84
5.2	Pattern Recognition Unit	85
5.2.1	Rectangular Pulse Domain (RPD) Feature Extraction Process	86
5.2.2	Neural Network Classification	91

5.2.3	Improvement on HMLP Network Performance	95
5.3	Atrial Fibrillation Classification	98
5.3.1	RPD Feature Extraction	98
5.4	Discussion	100
5.5	Conclusion	101
Chapter 6	**ECG Analysis System**	
6.1	Introduction	103
6.2	ECG Analysis System	103
6.3	System Performance	105
6.4	Discussion	112
6.5	Conclusion	113
Chapter 7	**Conclusions and Future Work**	
7.1	Conclusions	114
7.2	Future Work	115
References		118

Chapter 1

Introduction

1.1 Overview

Atrial fibrillation (AF) is an arrhythmia which can progress to a chronic condition. AF treatment could be enhanced if better prediction methods were available. The factors which contribute to the risk of AF include hypertension, myocardial infarction, congestive heart failure, as well as increasing age. The number of cases of AF increases with age and approximately 10% of people aged over 80 are diagnosed with AF [1]. Some reports [2] state that the mortality rates recorded for AF patients are higher than those diagnosed as having a normal sinus rhythm (NSR). More accurate AF prediction would lead to a faster initiation of treatment that could save lives. AF is often asymptomatic, thus is not suspected by the patient by any sensation of irregular heartbeat or pulse. AF episodes occurring intermittently, known as paroxysmal AF also contribute to making an AF diagnosis particularly challenging [3].

For AF early detection, a new electrocardiography (ECG) analysis system is developed to obtain the preliminary information before the results are transmitted to the local hospital for further analysis. The system involves two processing units (Noise Reduction and Pattern Recognition) before the detection results can be obtained. In the first unit the ECG signals are collected from patients. Before the ECG signals being proceeded to the pattern recognition unit the noise contaminating in the ECG signals are removed by using several noise cancellation techniques since the ECG contained with number of noises.

In the pattern recognition stage the filtered ECG signals are processed and several features are extracted from the signal. The features are then fed to the classifier as the input vector before the AF or non-AF episode could be detected.

1.2 Research Motivation

In this study noise reduction techniques for removing the unwanted noise from ECG signals are investigated. Noise in the ECG signal can be divided broadly into two groups which are correlated and uncorrelated noise [4, 5]. In uncorrelated noise, the noise frequencies are not correlated with ECG signal, and can be got rid of easily (i.e. baseline wander (BW) and powerline interference (PLI)). The BW and PLI noises are comes from medical equipment and power supply which easily can be identified and removed [6, 7]. The electromyogram (EMG) is the electric activity in muscle [8]. The electrical impulse activity from muscle is needed to be measured and used as reference signal for denoising techniques. In the case of correlated noise, the motion artifact (MA) is contributed by the movement of patient's body and difficult to be identified[9, 10]. The MA noise frequency is completely overlapped and correlated with the ECG signal. In MA denoising works, a signal/model of MA noise has to be identified before the MA noise in the ECG signal could been reduced. The model of the MA signal is hard to be identified since a lot of muscle movement in patient's body in one time. In this study, we attempt to minimise the noise in the ECG signal by developing a novel ECG denoising unit.

The feature extraction is the main process before any classification is performed. In AF pattern recognition, numbers of techniques have been used in the detection as summarize by Larburu in [11]. In previous researches, characteristic waveform based features are widely used for extracting each ECG complex. Most of them used the amplitude of the P, QRS and T peaks and the durations of segmentation as the detection indicator. However, the results provided in [11] still leaves room for improvement to be made. On the other hands, most of ECG data is taken from stationary patient (at rest) or while performing a constant movement (i.e. while on the treadmill with constant velocity). ECG data collection on the non-stationary patient is performed at minimum frequencies whilst overlooks the high mortality rate during having sport or active activities [11]. In this research we are investigating the best technique to extract the ECG features and try to solve the non-stationary issue.

A lot of classifiers are available to be used in the AF pattern recognition process [11]. The capability of classifiers to give high accuracy depends on how the classifier is trained. The matched selection of the classifier structure and training algorithm also allow good classification results to be produced [12] and the suitability of input vector also contributes to the performance of classifier. The hybrid multilayer perceptron (HMLP) neural network has shown the ability to perform good classification [12]. However, the network has its own limitations and fails to converge once reaching the highest optimum point. In this research, we attempt to improve the classification ability of the HMLP network by extending the network's optimum point.

1.3 Summary of Original Contributions

Several novel contributions are identified in the research work. The contributions comprise two units that include a noise reduction unit and a pattern recognition unit that are utilised to form a new ECG Analysis system that is used for AF detection.

1) Noise Reduction Unit

Novel ECG denoising methods have been proposed in filtering the unwanted noises. The new technique employed is the improved proportionate normalized least mean square (IPNLMS) adaptive filter for removing the EMG effect. The IPNLMS adaptive filter has been used before in echo cancellation and limited uses of medical signal. The EMG noise can be measured from standard ECG lead system as the reference. The normalized least mean square (NLMS) based adaptive filters have the capability to reduce the EMG noise from both stationary and non-stationary conditions. The IPNLMS provides significant result to be compared with other NLMS based adaptive filter and other filtering techniques.

Novel wavelet based filters in reducing the BW and MA noise signals also has been designed by combining two wavelet based filters. The novel Sqtwolog Threshold & High/Low pass (STHL) wavelet based filters is used to reduce the effect of BW and MA noises without using any model/pattern signal as the references. Both BW and the MA noises are non-stationary and immeasurable signals, so application of wavelet threshold techniques and wavelet high-pass/low-pass filter are used to reduce the BW and the MA effects. The performance of new filters (IPNLMS and STHL) have been tested by datasets (ECG signals and noises) taken from Massachusetts Institute of Technology Beth Israel Hospital (MIT-BIH) database with encouraging results.

2) Pattern Recognition Unit

A novel feature extraction process is presented that uses the rectangular pulse domain (RPD) approach. Differ from conventional feature which are based on duration and amplitude of P, QRS and T peaks, the RPD try to extract information from others point. The RPD use several rectangular pulses that are superimposed with an ECG complex. The intersection points between RPD and ECG complex are extracted and used as the input vectors to the classifier. In this research, the R to R peak interval (RRI) and P to T peak interval (PTI) morphologies are used to segregate each complex of ECG signal. A comparative performance study is conducted and demonstrated the RPD extracted feature capable to perform well by using HMLP network for RRI and PTI morphology compare to others classifier. In the other hands, the PTI morphology is important for the non-stationary cases since the different of the rest time happen for each non-stationary subjects. Information from P to T peak for each ECG complex are used for PTI morphology, leaving the rest time behind.

In the part of classification, improvement to the HMLP network is done by performing multi-classify (first and second classify) of classification process. The novel multi-classify hybrid multilayer perceptron (MCHMLP) network doing the first stage classification until achieved the optimal point, then starts the second classification process. Here, the output of the first HMLP network will be fed as the input of the second HMLP network. In the other hand, a new arrangement on second classification of MCHMLP network gave better classification results, and known as cascade hybrid multilayer perceptron (CHMLP) network. In CHMLP network, the second classification starts after the first HMLP network is done at each iteration. A comparative study of the classifier performance is conducted, both MCHMLP and CHMLP networks gives high accuracy results. However, the CHMLP network provides better accuracy and faster to reach the optimal point than MCHMLP network. In order to investigate the performance of MCHMLP and CHMLP networks, several samples are taken from the machine learning repository, University of California - Irvine (UCI) [13] (Pima Indian Diabetes , Iris, Glass, Lung Cancer, Ionosphere and Hayes-Roth) and used to test the network's classification ability.

3) ECG Analysis System for AF Detection

The study developed a new ECG analysis system, the complete combination of the noise reduction unit (to perform filtering of the ECG signal) and the pattern recognition unit (to recognize features and perform the classification). The system is able to identify the presence of AF or non-AF with high accuracy and at the same time false positive occurrence can be reduced. Several datasets are taken from MIT-BIH database to test the capability of the system. It is shown that the occurrence of AF and non-AF are identified correctly by the system with a superior accuracy compared to conventional approaches.

1.4 Thesis Organization

The thesis is organised as follows. Chapter 1 provides an introduction to this research. The chapter covers the research motivation and introduces the novel techniques which are presented in the following chapters. A summary of the original contributions is also provided.

Chapter 2 reviews cardiac rhythm abnormalities with a brief description of each condition. The chapter also highlights the importance AF, with in-depth explanation of this condition. The development of the Holter monitoring system is explained. The development of Holter monitor components that have been used and ECG acquisition method need to be understood completely since the aim of the study is to develop an intelligent Holter monitoring system. In this study, AF activity is chosen to be detected and classified. A detailed discussion on the characteristic, the classification, the symptoms and the diagnosis of AF are being done in Chapter 2.

Chapter 3 reviews the approach used in processing the raw signal until the AF is identified. First of all, the source of datasets and unwanted noises to be filtered are clarified.

Techniques such as digital filters, adaptive filters and wavelet transform used to reduce contaminating noise in the signal, are explained. In performing the feature extraction process, the characteristic and waveform based features are discussed. Some review of previous researches on AF detection is done in Chapter 3. The neural network pattern recognition technique in doing the classification process is also reviewed in the chapter.

Chapter 4 introduces the novel ECG denoising technique which is applied to reduce the EMG, BW and MA noise from the ECG signals. The IPNLMS adaptive filter is used for filtering the EMG noise while wavelet based filters are used for reducing the effect of BW and MA noise. In removing the PLI noise, a bandstop notch filter is designed. The evaluation processes are done by comparing the techniques used with others filter.

Chapter 5 reveals the performance of RPD feature extraction technique which is able to provide significant information to the classifier. This study also proposes the use of PTI morphology as an alternative to RRI morphology in AF detection. Chapter 5 also shows the performance of two modified HMLP networks (MCHMLP and CHMLP) as useful classifiers. Both networks are shown to be able to obtain high accuracy results during the classification process with CHMLP network doing better classification than the MCHMLP network.

Chapter 6 present a new ECG analysis system which start by injecting ECG signal to the system and end after AF or non-AF have been detected. The system includes the noise reducing process, the feature extraction phase and last but not least the classification stage. The system attempted to reduce as much as possible the noises contaminating the ECG signals. The system then extracted the filtered signal and the extracted features are used to be the input vectors to the classifier in identifying AF.

Chapter 7 concludes the thesis along with discussion and some future works. Some suggestions in improving the reliability of the system are made since the system is still at the initial stage and has scope for improvement.

Author Publications

[1] F. R. Hashim, J. J. Soraghan and L. Petropoulakis (2012) “Multi-classify Hybrid Multilayered Perceptron for Pattern Recognition Applications,” in Artificial Intelligent Applications and Innovation, Springer-Heidelberg, vol. 1, pp. 19-27.

[2] F. R. Hashim, J. J. Soraghan, L. Petropoulakis and S. I. Safie (2012) “Wavelet Based Motion Artifact Removal for ECG Signals,” *IEEE EMBS International Conference on Biomedical Engineering and Sciences,* pp. 339-342.

[3] F. R. Hashim, J. J. Soraghan, L. Petropoulakis and N. G. N. Daud (2014) “EMG Cancellation from ECG Signals using Modified NLMS Adaptive Filters,” *Biomedical Engineering and Sciences (IECBES), 2014 IEEE Conference on,* pp. 735-739.

[4] F. R. Hashim, J. J. Soraghan and L. Petropoulakis “Cascade Hybrid Multilayer Perceptron (CHMLP) Network for Pattern Recognition Applications,” (Submitted to International Journal of Applied Engineering Research (IJAER)).

[5] F. R. Hashim, J. J. Soraghan and L. Petropoulakis “Atrial Fibrillation Classification using Pulse Rectangular Domain and Cascade Hybrid Multilayer Perceptron Network,” (Submitted to Australian Journal of Basic and Applied Science).

Chapter 2

ECG Acquisition

2.1 Introduction

AF is an abnormality of cardiac rhythm, detected by ECG. The cardiac structure, anatomy and physiology, and associated abnormalities have to be understood before the arising of AF can be detected. Detailed explanation of electrocardiography and the use of the ECG in detecting and diagnosing cardiac rhythm abnormalities are presented. The use of the Holter monitor allows continuous detection and recording of cardiac rhythm for several days. A review of Holter monitor development and its use in medical practice today is provided. The latest technology used in the development of the Holter monitor in accordance with present modernization is also discussed.

2.2 Cardiac Rhythm Abnormality

Cardiac rhythm abnormality refers to a large group of conditions where the electrical activity in the heart is abnormal. Abnormality of rhythm may be regular or irregular, fast or slow, or combinations of these[14-16]. The spectrum of abnormality of rhythm ranges from asymptomatic innocent criteria such as isolated irregular beats, to conditions causing major symptoms such as breathlessness, blackouts, and even sudden death.

There are four chambers of human heart: right atrium, left atrium, right ventricle and left ventricle [17-19]. The heart functions as two parallel pumps; both ventricles contract simultaneously, the right ventricle pumps de-oxygenated blood to the lungs while the left ventricle pumps oxygenated blood to the rest of the body. The atria also contract simultaneously; they function mainly as collecting chambers, and contract to fill their respective ventricle; the sequence and timing of all this is controlled by an electrical conducting system running throughout the heart

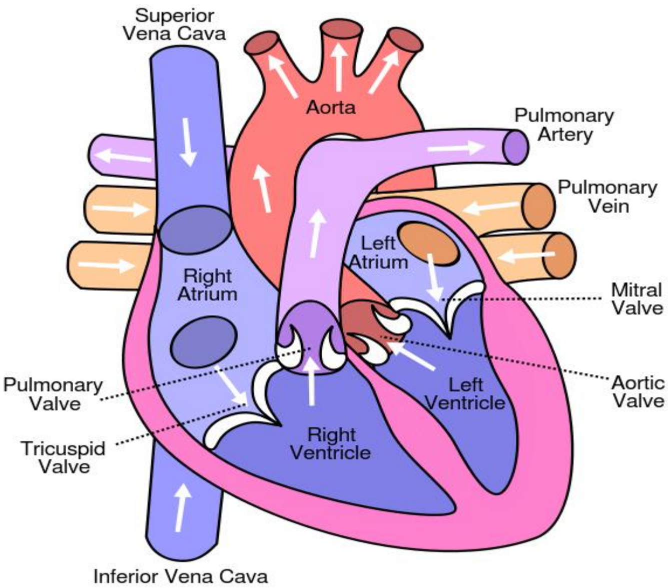

Figure 2.1: The basic human heart anatomy [17].

2.2.1 Types of Cardiac Abnormality

The cardiac abnormality, known as arrhythmia, is an irregular heartbeat. Arrhythmia involves the abnormal electrical activity in the heart. The heart beat may be too fast or too slow, and may be regular or irregular. If the acceleration of the heart rate is too high this is known as tachycardia while if the heartbeat is too slow it is known as bradycardia [20, 21]. Several life-threatening arrhythmias can cause heart attacks. In fact, sudden cardiac arrhythmias are among the most common causes of death.

Generally, for an adult, the normal heart rate during rest time is 60-80 beats per minute. The bradycardia is a slow heart rate of less than 60 beats per minute while the heart rate at rest is 100-120 beats per minute, then this is labelled as tachycardia [21, 22]. The fibrillation occurs when the abnormal activity of electrical impulses in the entire chamber of the heart chamber. Fibrillation could be life-threatening and when it affects the function of the atria is known as AF [23-25]. AF may be caused by a serious medical condition that underlies and should be evaluated by a doctor.

2.3 Electrocardiography (ECG)

ECG is an interpretation of the electrical signal of the heart and recorded using electrodes that are attached to the skin [14, 15, 26]. The recording phase is obtained by using an electrocardiographic device. The ECG detects and amplifies the small electrical changes which occur when the heart conducting tissue and muscle depolarises and repolarises. Electric charge crosses the cell membrane during the depolarisation and repolarisation process. A small change in voltage between two electrodes is displayed as a wave on a screen or paper [14, 27, 28] as shown in Figure 2.2.

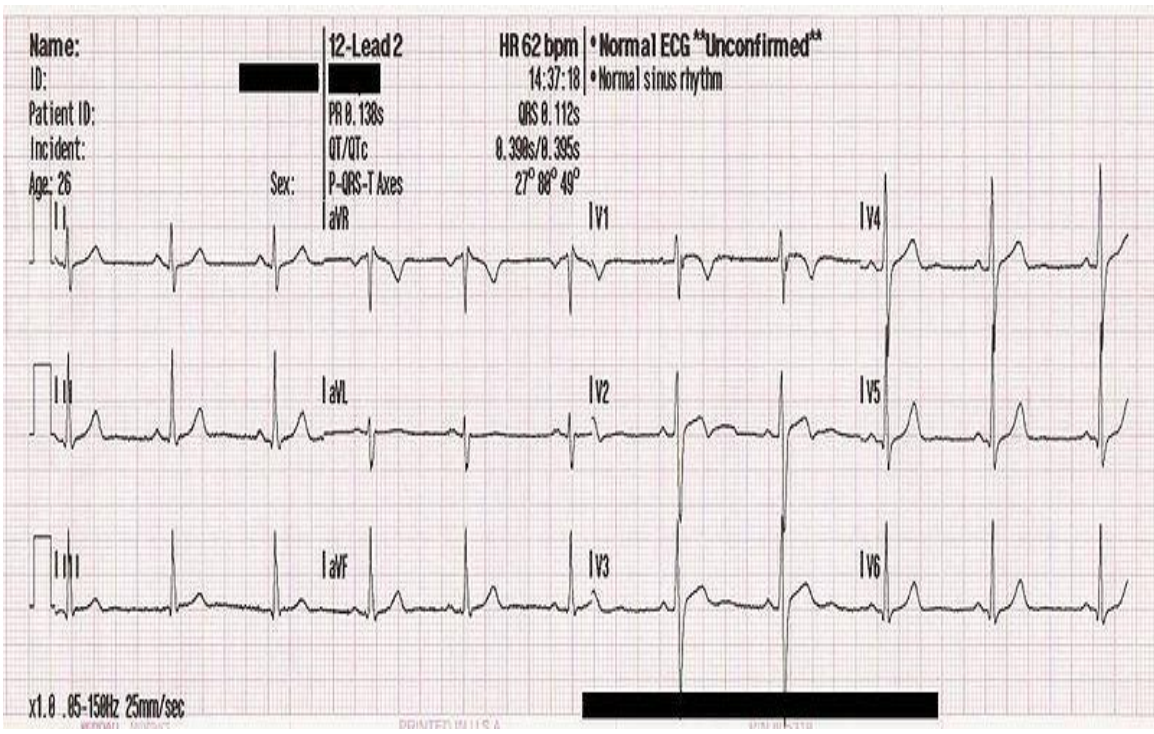

Figure 2.2: ECG output with cardiac activities [14].

2.3.1 Electrical Conductivity of the Heart

The spread of electrical impulses in the heart begins when the impulses arise in the sinoatrial (SA) node before spreading to both atria. After that, the electrical impulses arrive at the atrioventricular (AV) node. The electrical impulses from the AV node are directed to the ventricles via the Bundle of His. The arrival of the electrical signal at the individual cells of the myocardium allows them to contract in unison, thus allowing the ventricles to contract, producing a systemic circulation via left ventricle and a pulmonary circulation via the right ventricle [29-31]. Figure 2.3 shows the electrical conduction system throughout the heart.

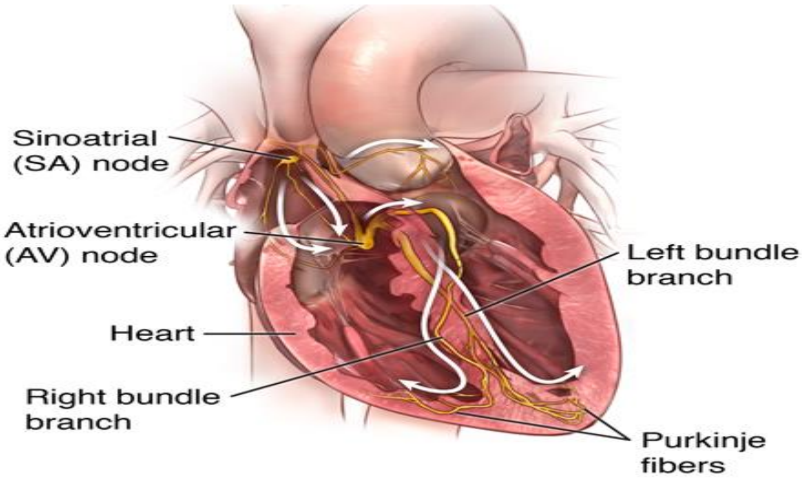

Figure 2.3: The electric impulses movement in the heart [30].

In normal condition, the electrical impulses in the heart are spontaneously generated at SA node which acts as a physiological pacemaker. Each electrical impulse is transmitted through the left atrium to the right atria passing through the Bachmann bundle (right and left bundle branch). This electrical activity stimulates the atria to contract. The movement of electrical impulses from the left atrium into the right atria is observed in the peak P of the ECG signals as in Figure 2.4. The intermodal tracts are a specific pathway of electrical impulses throughout the atria - the motion is from the SA node to the AV node.

The AV node serves as a regulator to delay the conduction of electrical impulses into the ventricle. The AV node controls the contraction of the heart thus making sure no simultaneous contraction occurs between the atria and the ventricles. The activity carried out by the AV node is observed by the P-R segment in the ECG signal. The P-R segment also reflects repolarization activity in the atria. The electrical impulses at AV node spread to the ventricles through the Purkinje fibres and finally stimulate the ventricular myocardium. The stimulation of ventricular myocardium produces the QRS complex of the ECG, representing complete depolarisation of the ventricles. The T peak (and sometimes U) represents repolarisation of the myocardium and is influenced by the nervous system that is driven by an integrated brainstem [31].

2.3.2 ECG Signal Morphology

A healthy individual with a normal heart cycle is capable of displaying an ECG complex that consists of three main waves P, QRS and T. Put simply, the P wave corresponds to atrial contraction, the QRS wave corresponds to the electrical signal travelling through the ventricular muscle which causes ventricles contraction, and the T wave corresponds to repolarisation of the ventricles. In AF, the electrical actually through the atria is disorganized. Therefore, the two atria do not contract in unison; therefore, there is no P wave on the ECG. Figure 2.4 shows the ECG signal morphology that occurs in the heart.

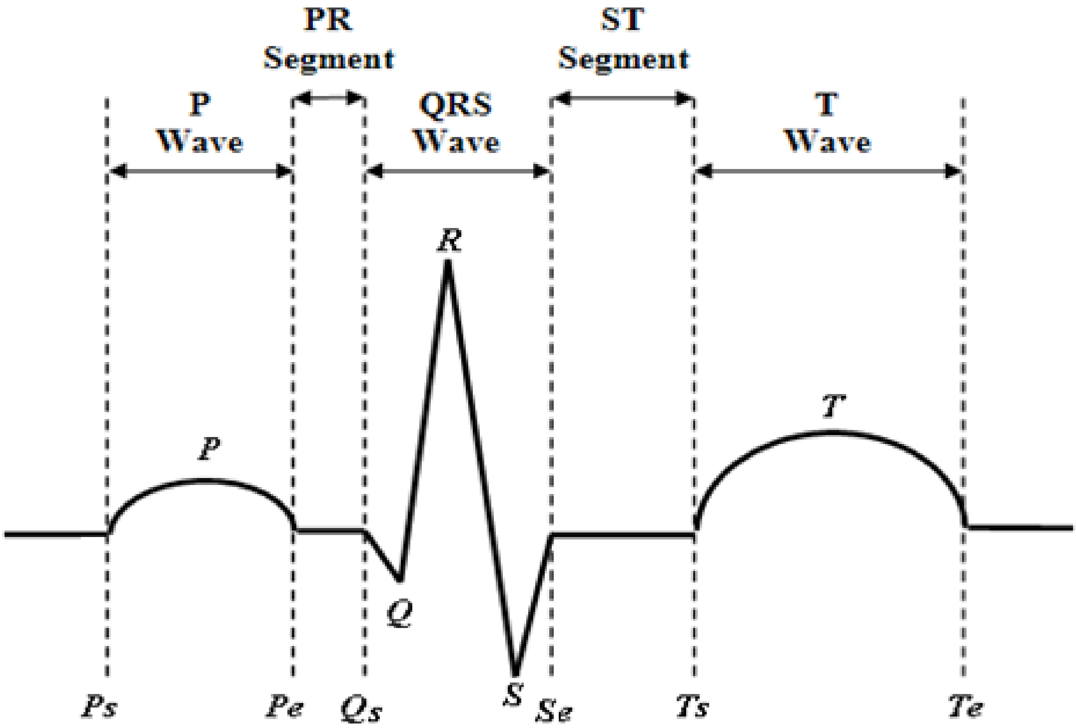

Wave	*Start*	*Peak*	*End*
P	*Ps* : Starting point of P wave	*P* : Peak of P wave	*Pe*: Ending point of P wave
QRS	*Qs*: Starting point of Q wave	*R* : Peak of R wave	*Se* : Ending point of S wave
T	*Ts*: Starting point of T wave	*T* : Peak of T wave	*Te*: Ending point of T wave

Figure 2.4: ECG signal complex.

2.3.3 Fiducial Point Detection

A fiducial point is a point corresponding to the peak or a location of the three main waves in an ECG complex, which can be used as a reference point. In an ideal complex, there are at least nine fiducial points which can be identified. However, the boundaries of each wave cannot be distinguished by the human eye and therefore no clear definition can be given regarding the beginning or end of each of the main waves. Pan and Tompkins in [32] proposed a technique to detect the locations of the three major waves in the ECG signal by calculating the signal amplitude and width as well as the slope. Boulgouris et al. [33] also proposed tracking the local maximum and minimum radius of curvature. The combination of these two methods is able to improve the sensitivity and accuracy of ECG wave detection.

Many manufacturers of ECG recording equipment apply a combination of these techniques into their devices.

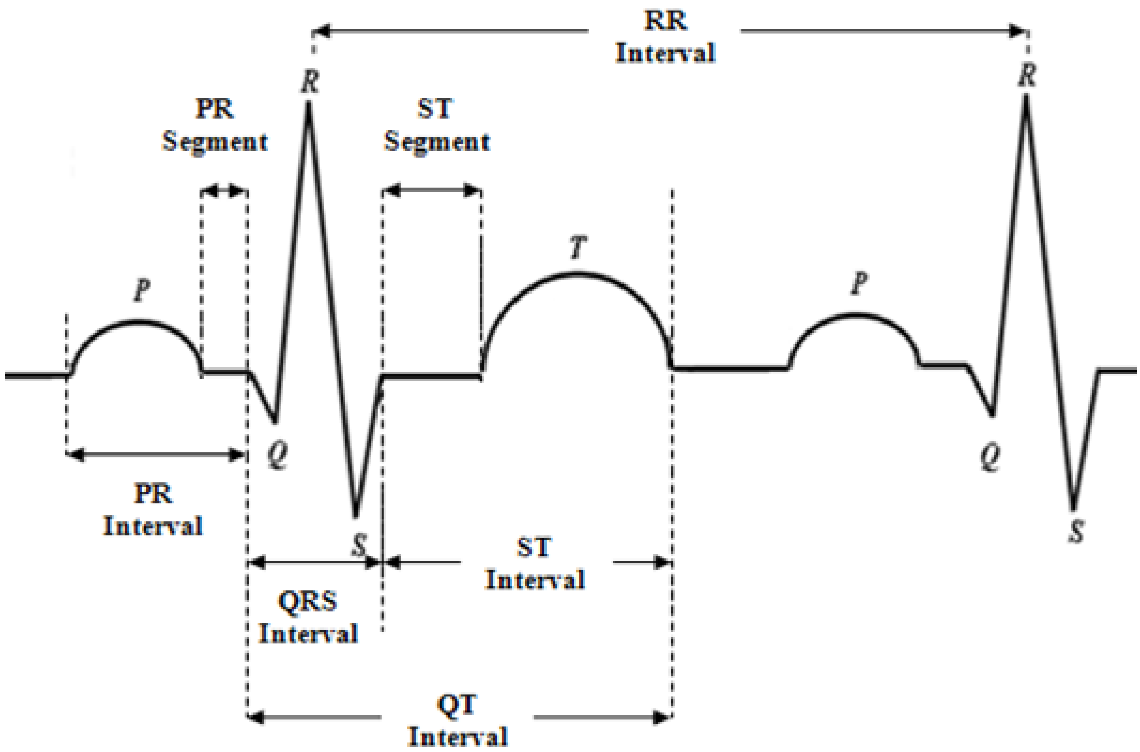

Figure 2.5: The fiducial points taken from a complex ECG signal.

Figure 2.5 shows the identified fiducial points of a complex of ECG signal. These fiducial points are often used in classifying cardiac abnormalities including PR interval, i.e. the distance measured from beginning of point P to peak R. The PR segment is measured starting at endpoint of P to the starting point of Q. The QRS interval is measured starting at point Q up to end of point S. Next, the QT interval and the ST intervals are measured based on the distances from beginning of point Q to end of point T and from end of point S to end of point T, respectively. The ST segment is measured from the endpoint of S to the start point of T. The RR interval is measured from the R peak to the next R peak. In addition, the amplitudes of the P, QRS and T peaks also contribute to the fiducial points.

2.3.4 ECG Lead Configuration

In activity related to ECG, in this thesis the terms of 'lead' and 'Lead' define two different meanings. The 'lead' is defined as a cable or wire connecting the electrocardiograph machine with surface electrode to the user. On the other hand, the 'Lead' is defined as the potential difference between two points on the human body. There are two types of Lead configurations: bipolar (two electrodes with opposite polarity) and unipolar (combination of several electrodes with an electrode as the reference point) [34].

Limb leads	Chest leads
RA: Right Arm	V1: Fourth intercostals space at the right border of the sternum
LA: Left Arm	V2: Fourth intercostal space at the left border of the sternum
RL: Right Leg	V3: Midway between location V2 and V4
LL: Left Leg	V4: At the mid-clavicular line in the fifth intercostal space
	V5: At the anterior axillary line on the same horizontal level as V4
	V6: At the mid-axillary line on the same horizontal level as V4 and V5

Figure 2.6: The placement of 10 leads in the standard 12 Leads configuration.

Figure 2.6 shows the common used standard, the 12 Leads surface ECG which consists of ten leads with four leads connected to the limb (both hands and legs) and while another six leads connected to the chest [34].

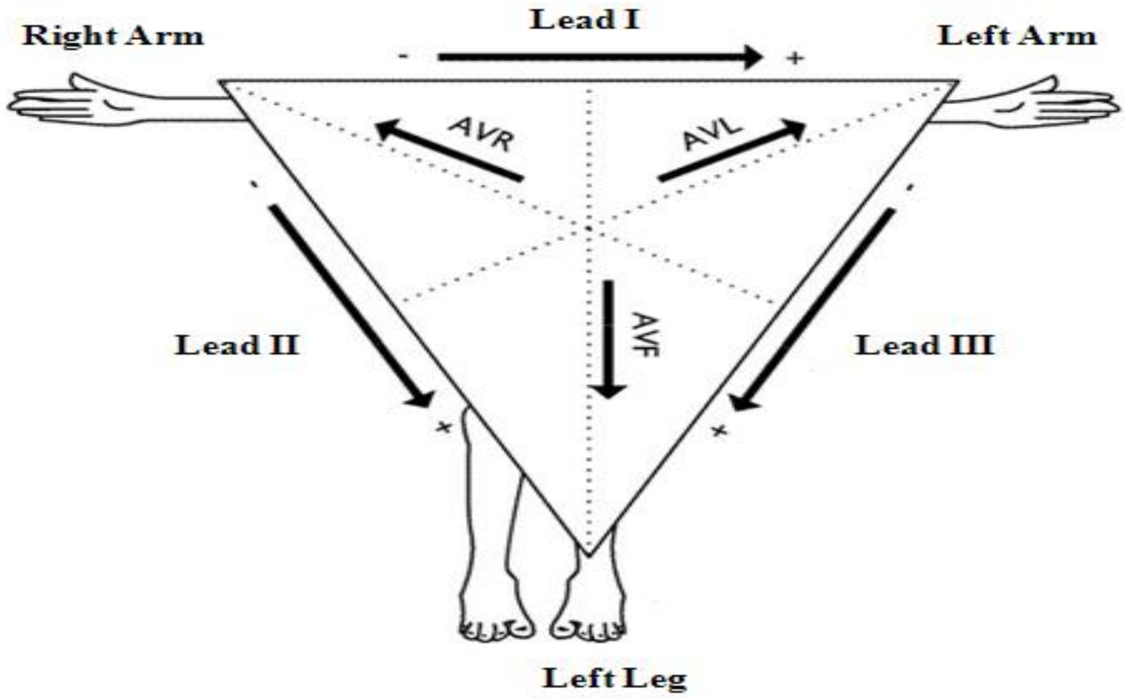

Bipolar Leads	Unipolar Leads
Lead I = LA – RA	$aV_R = RA - \frac{1}{2}(LA+LL)$
Lead II = LL – RA	$aV_L = LA - \frac{1}{2}(RA+LL)$
Lead III = LL – LA	$aV_F = RA - \frac{1}{2}(RA+LA)$

Figure 2.7: The Einthoven's triangle configuration setting at the limb [35].

Figure 2.7 shows the Einthoven setting configuration. Three bipolar configuration generates Lead I, Lead II and Lead III while the three unipolar configuration generates Lead augmented vector foot (aVf), Lead augmented vector left (aVl) and Lead augmented vector right (aVr) [35].

2.4 Holter Monitor

A Holter monitor is a portable device for continuous monitoring of electrical activity of the cardiovascular system for up to 48 hours. Its continuously recording period is very useful for detecting occasional or short episodes of cardiac arrhythmia [16, 36, 37].

2.4.1 History of Development

The Holter monitor was invented by Dr. Norman J. Holter. Cardiac telemetric monitoring was invented in 1949 but clinical use only started in the early 1960s [36, 37]. Holter monitor records electrical changes from the heart through a series of electrodes which attached to the body. Electrodes are located over bones to minimise interference from muscle activity when breathing. Attachment locations and number of electrodes differ depending on the model. Commonly, though, most Holter monitors employ between three and eight electrodes [15, 38]. Being a small piece of equipment, it is usually attached to the patient's belt or it is hung around the neck. This equipment is connected to electrodes and works as a log keeper of the heart's electrical activities. Previous devices used reel tapes which ran at a 1.7mm or 2mm/s speed to record the electrical activity. When the recording was completed, it could be played back and analysed at 60x speed. Thus 24 hours of recording can be analysed in 24 minutes. The latest technology allows modern recorders to record the cardiac activities onto digital flash memory devices. Data from flash memory is downloaded to a computer and analysed. Cardiac activity is processed automatically by counting the number of ECG complexes, computing heart rate, P, Q, R, S and T peak's location, PR interval, QRS complexes and etc. Figure 2.8 shows a Holter monitoring system.

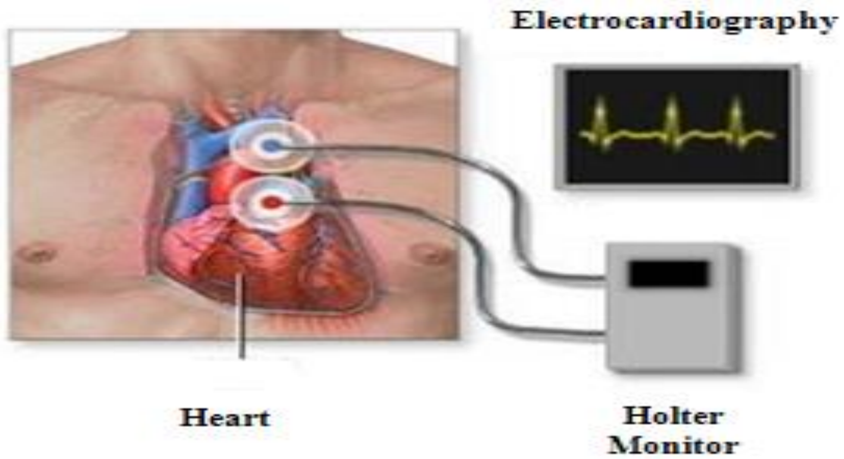

Figure 2.8: The Holter monitoring system [39].

2.4.2 Components of Holter Monitor

Each Holter system consists of two main parts, namely hardware which consists of a monitor and recorder and software to analyse the recorded signals. The latest Holter recorders are able to display signals and at the same time check the quality of the signal and perform analysis on the signal, whilst they also record the signal for future use. The Holter system is designed with patient operated buttons. Patients push the button when feeling ill, before going to sleep, or while taking medication, for example, because heart rate may change from the normal situation. The Holter system was designed to identify any changes of the signal and facilitate the task of the doctor or technicians to determine key areas to analyse.

2.4.2.1 ECG Recorder

Recorders have different sizes depending on the requirements and the manufacturers. The average dimensions of the device on the market are about 110mm x 70mm x 30mm. Most of the devices operate using a direct connection from a source of electricity or by using the battery according to the needs and circumstances. Most Holter monitors have two to three channels depending on the model from the manufacturer. The system to monitor ECGs and perform calculations may differ between models depending on the indicators set by the manufacturer and also the implementation in the Holter system. Nowadays, most of the Holter systems are designed with the comfort of the wearer in mind, so as to ensure the recorded ECG signal is free of any noise caused by movement due to discomfort. Due to technological progress, the Holter systems have more channels now compared to the conventional Holter system originally developed.

Although the classical Mason-Likar lead system is still used, a better system has been designed in order to represent ECG signals. By using the new system, the recorded ECG signal is able to represent a similar signal during rest time or under stress. Figure 2.9 shows the portable Holter monitor system currently on the market.

Figure 2.9: The Holter system used to record ECG signals [39].

A Holter system is able to detect whether the patient is standing, walking or is in bed by adding a triaxial sensor into the system. The software available at the Holter system will activate the mode whether it is standing, walking or sleeping on the recommendation provided by the sensors. This invention could help cardiologists in collecting ECG analysis with records recorded in a patient’s diary. The recording device can be worn on the belt or the strap across the chest. Patients being monitored do not need to limit the normal daily activities. The device should be stored in a dry place and activities involving water whilst wearing the device should be avoided (i.e. bathing or swimming). The monitor’s battery can be removed for a few minutes without affecting the data signal collector and be replaced if long term monitoring is needed. Figure 2.10 shows the Holter monitor attached to the human body.

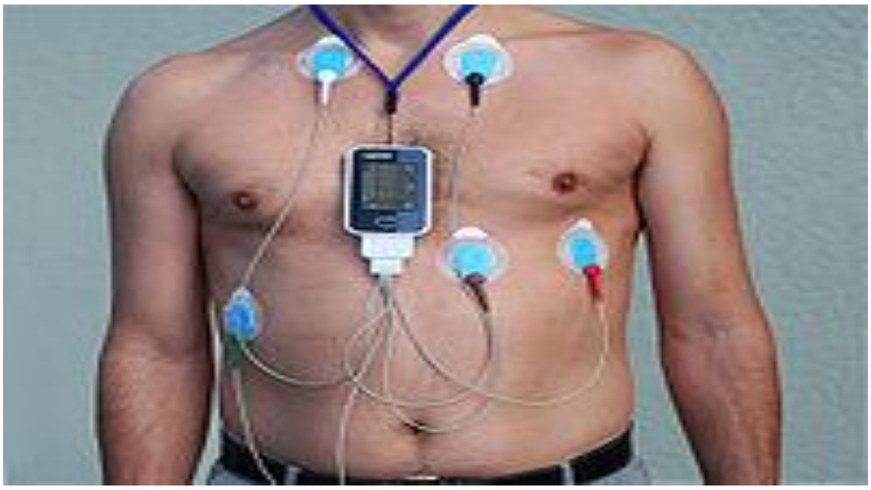

Figure 2.10: Holter monitor in use [40].

2.4.2.2 ECG Analysis Software

The recording of ECG signals usually lasts between 24 to 48 hours. However, the long term monitoring required encourages human errors during analysis. Therefore, an integrated automatic analyser which is available in the Holter software system automatically determines the various patterns of heart rate, heart rhythm and other parameters. Good signal quality is needed to determine an accurate automated analysis. The attachment of electrodes to the patient's body affects the quality of the recorded signal. In addition, strong limb movement also causes more noise to the recorded signal and the resulting signal is very difficult to process. Automated analysis is usually compiled in the Holter system and capable of giving information on heartbeat ECG morphology, beat interval measurement, heart rate variability, rhythm overview which may be corrected with the patient diary. Thus, the cardiologists are able to receive on analysis quickly and accurately. In addition, the system detects and analyses pacemakers. This process is useful for checking the correct function of pacemakers (automatic calibration) [41, 42]. Figure 2.11 shows a screenshot of the Holter ECG analyser.

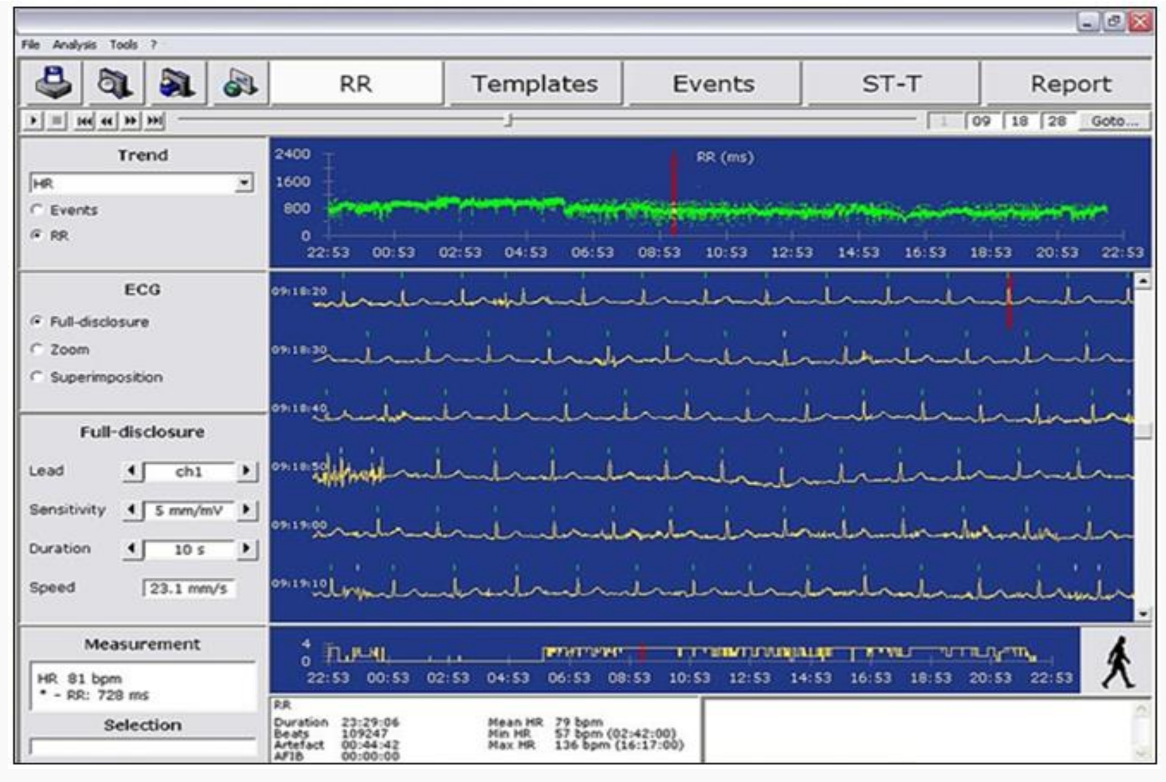

Figure 2.11: A screenshot of the Holter ECG [41].

A lot of information about the patient is available from the screenshot above. The ECG signal is recorded based on the peak R to R approach and it is taken from a Lead I channel. The duration for each frame is 10 seconds and the measurement of the heart rate is 81 beats per minute, which is normal. The duration of the monitoring process is about 24 hours and the mean heart rate is 79 beats per minute. The slowest heart rate is 57 beats per minute occurs about two and half hours after monitoring started, while the fastest heart rate of 136 beats per minute occurs 16 hours after monitoring started.

2.5 Atrial Fibrillation (AF)

AF is a leading cause of heart arrhythmia (irregular heartbeat). AF often does not show any obvious symptoms [43]. However, the present of AF can increase a patient's risk of stroke up to seven times compared to patients who do not suffer from AF. An examination of the patient's pulse is enough to detect the presence of AF. Clinically, the absence of P waves in ECG signals followed by an irregular heartrate confirms the diagnosis of AF. The absence of P wave becomes the best indicator of AF episode, however, in a lot of cases AF comes with rapid and irregular beating. Patients with AF occasionally feel chest pain, fainting, heart palpitation or short of breath [44, 45].

2.5.1 AF Diagnosis

The evaluation of AF involves various processes including diagnosis, research on the cause of the arrhythmia and classification of the arrhythmia. Some assessment also may be made of the patient’s health records, the patient's physical condition and ECG [46]. In specific cases, the patient's blood sample will be taken before being sent to the laboratory for further analysis [47]. If a patient is identified as having AF symptoms, the attack should be stopped immediately as it could be life-threatening. In these situations, most patients are placed on continuous cardio respiratory monitoring with ECG monitoring the progress of the patient's heart activity. Normally, the cardiologist will try to identify the root cause of the cardiac abnormality [48].

The ECG is used for the diagnosis of AF and detected by the absence of P waves or the demonstrable presence of totally irregular RR interval. This situation occurs because the electrical impulse activity in the atria ventricle is disorganized, so the rate at which AV node conductivity is totally irregular [46, 48]. Figure 2.12 illustrates the AF signal taken from Massachusetts Institute of Technology Beth Israel Hospital (MIT-BIH) database (afdb 04015). The figure shows the ECG signal without significant P wave and irregularity of the RR interval. The use of ambulatory Holter monitor is needed for the AF detection and recording. Figure 2.13 shows the normal ECG signal also taken from MIT-BIH database (nsrdb 16265). From both figures it can be illustrates the differences between AF and normal ECG signal. From the figures, normal signal has a regular rhythm and clearly shows the P, QRS and T peaks compares with AF signal, it has an irregular rhythm and unable to present the P, QRS and T peaks clearly. The AF signal also labelled as tachycardia type abnormality which the heart rate at the rest time more than 100 per minute.

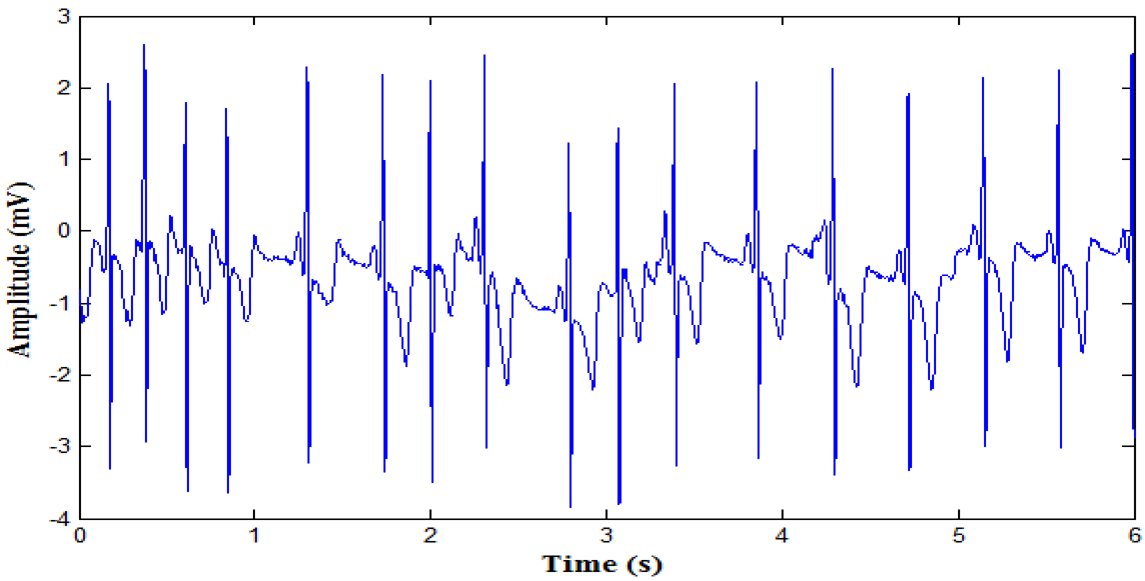

Figure 2.12: The AF ECG signal in the heart.

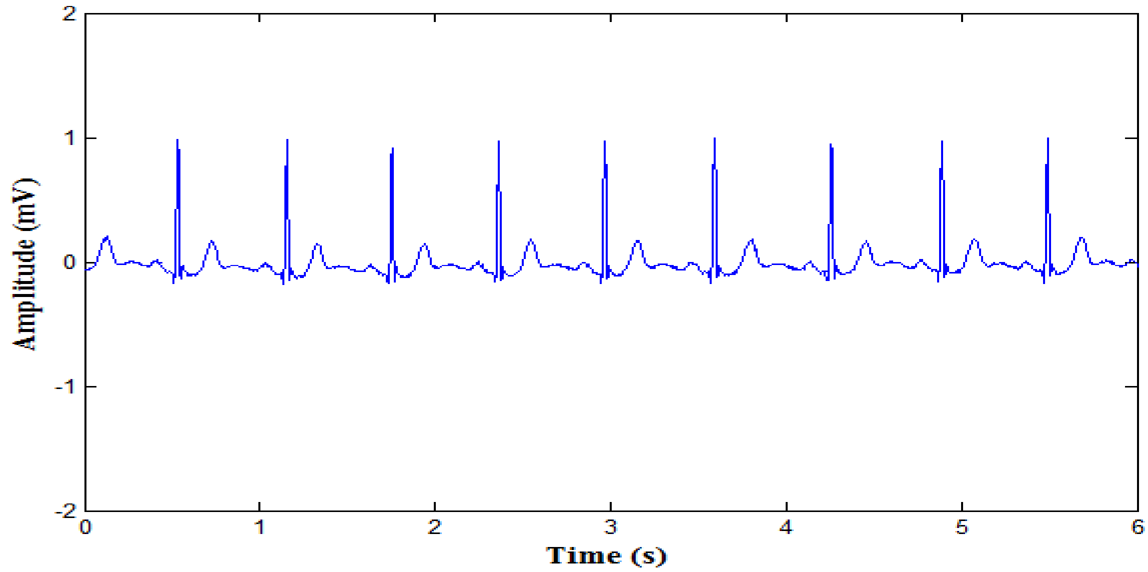

Figure 2.13: The normal ECG signal in the heart.

2.6 Conclusion

This chapter discussed cardiac rhythm abnormality, the ECG concept, the Holter monitor application for the recording of ECG activity and some information on AF abnormality. The Holter monitor acquires the ECG signal from patient's heart processes and analyses it to allow AF activity to be detected. Chapter 3 will review techniques used in ECG denoising. The filtered signal will be extract and the features will be tested in order to measure the significant and the suitability before being used as the indicator to the AF activity.

Chapter 3

ECG Analysis

3.1 Introduction

The filtering, the feature extraction and the pattern recognition; those stages are normally used in analysing the ECG signals. In this chapter, an overview of several techniques used by researches will be discussed in order to enhance the knowledge on ECG signal processing. A lot of techniques have been used for filtering the ECG signal. There are several types of noise contaminating in ECG signal such as BW, PLI, EMG and MA. In eliminating ECG noises, techniques such as active filter, adaptive filter and wavelet transform have been used. The process of information extraction from the filtered signal is subsequently carried out. Characteristics such as amplitude, duration and slope usually can be indicators of heart disorder. The last stage is to recognize the pattern of the signal. The extracted features parameter will be feed to the classifier in order to identify the group or the pattern of the signal.

3.2 ECG Database

The American Heart Association (AHA), the European Society of Cardiology (ESC) and the MIT-BIH database are some of the bodies which gathered arrhythmia signals in Physionet [49] database. Those databases are widely used in research based ECG signal and its applications. All databases are a standardized, quantitative, automated and taken directly from patients. In this research the normal and AF datasets are taken from MIT-BIH databases and used to measure the ability of the designed units.

3.3 ECG Filtering

The removal of noise contained in the ECG signal is an important early step in ECG signal processing. The noise in the signal should be minimized for a low SNR reading. The noise removal step should be done carefully since the next step process is rely on the current results. In general, there are a variety of noises contained in the ECG signal. In [50, 51], they have outlined four important noises that should be removed from the ECG signal. Various techniques have been used in reducing the noise from the ECG signal. Table 3.1 shows some summary of the contaminating noises in the ECG signal while Figure 3.1 shows the normal ECG signal and noises are taken from MIT-BIH database.

Table 3.1: Summary of contaminating noises in ECG signal.

Noise	Source	Description
BW	Measurement equipment.	0 to 0.5 Hz [10, 52].
PLI	Power line supply.	50 Hz or 60Hz, depending on the power supply of each country [50, 51].
EMG	Muscle.	Electric activity in muscle [8, 53].
MA	Body movement.	Muscle interaction in human body [10].

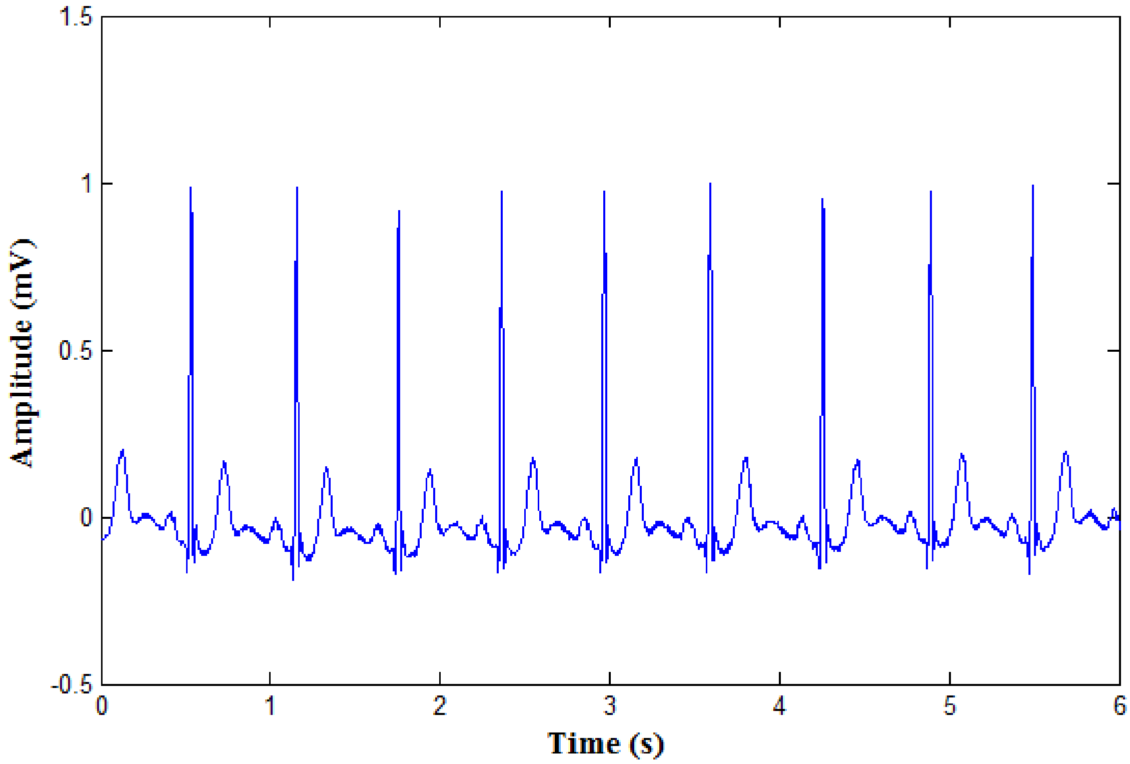

Figure 3.1(a): Normal ECG signal.

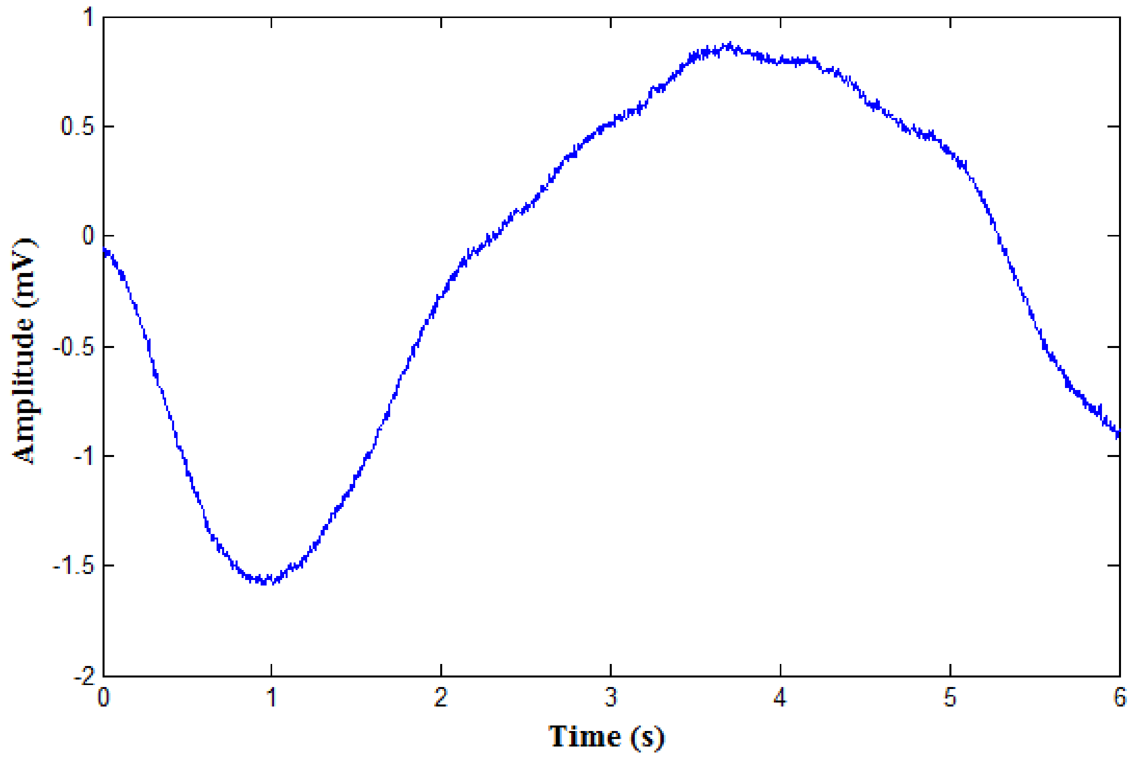

Figure 3.1(b): BW noise.

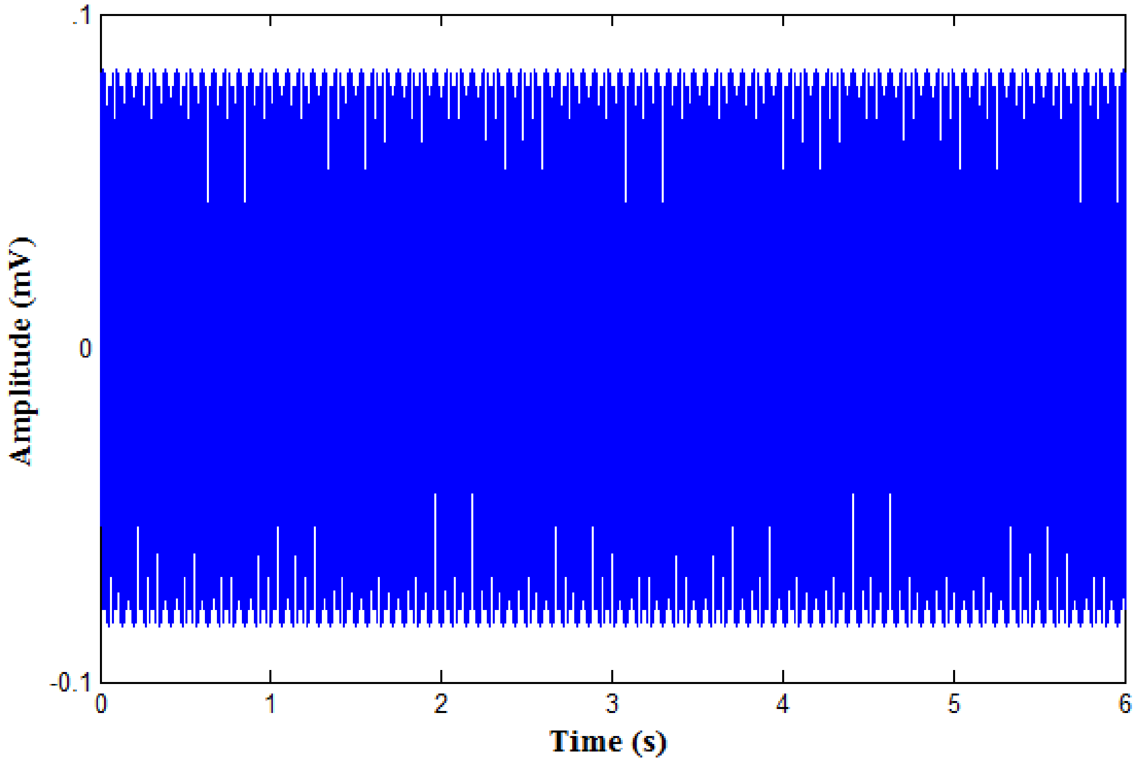

Figure 3.1(c): PLI noise.

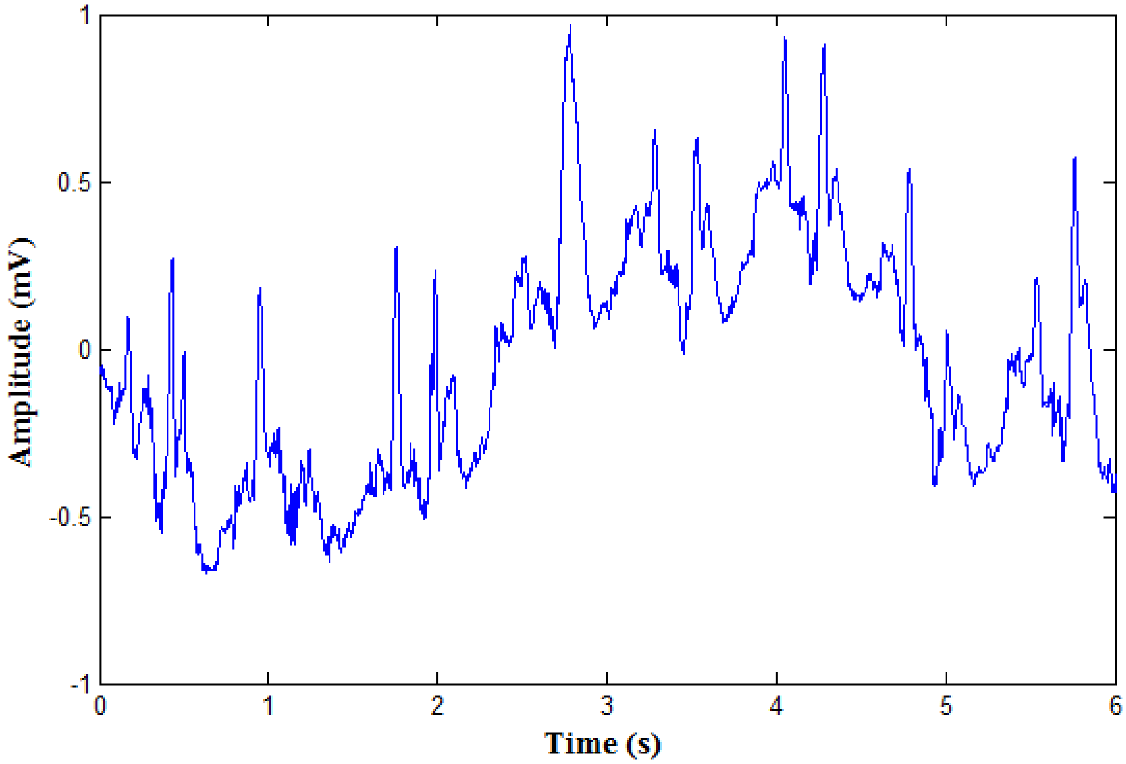

Figure 3.1(d): EMG noise.

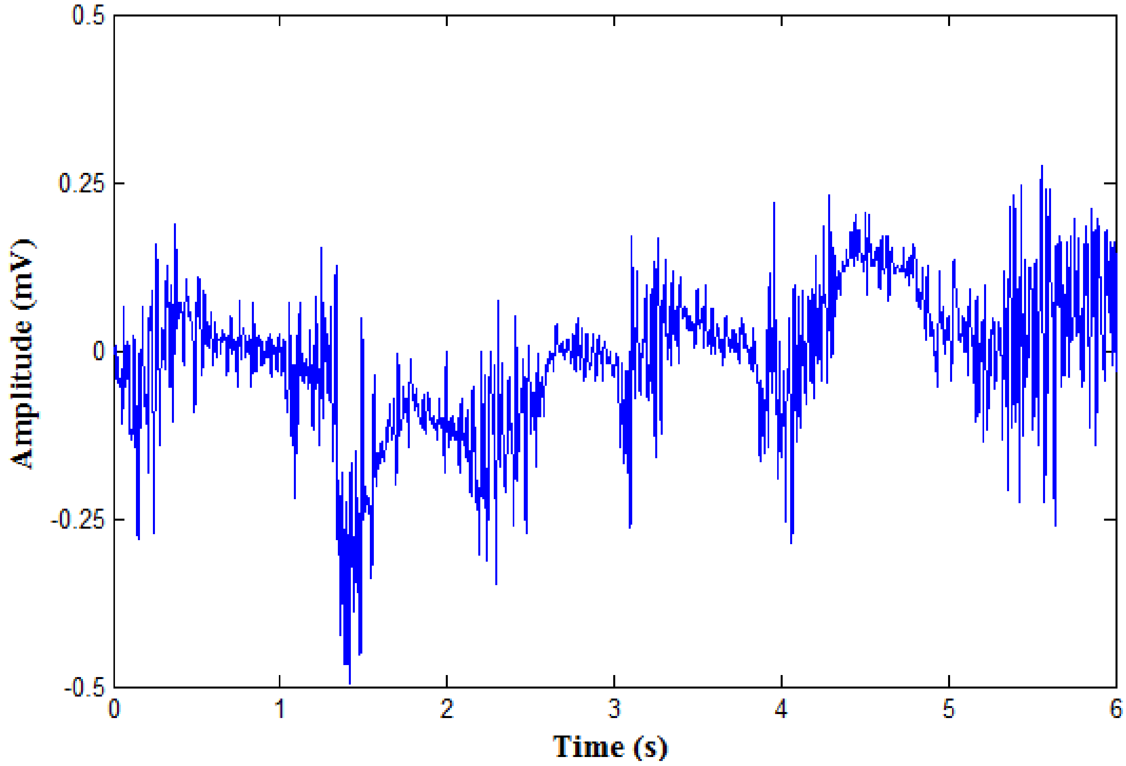

Figure 3.1(e): MA noise.

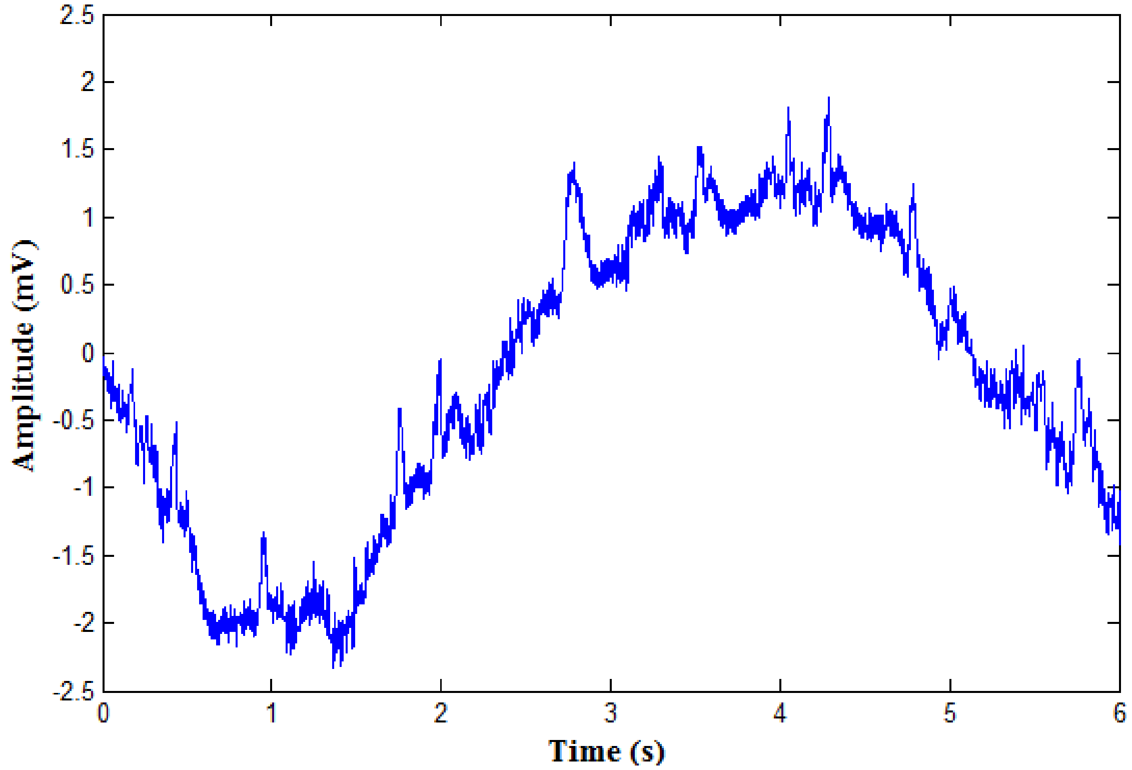

Figure 3.1(f): Corrupted normal ECG with BW, PLI, EMG and MA noises.

The BW is the noise caused by the ECG measuring equipment. Usually, the noise is in the range of 0 to 0.5 Hz [10, 52]. The PLI is the noise occurring in the power line source. Typically, this noise frequency is about 50 Hz or 60Hz depends on the power supply of each country [50, 51]. The EMG noise could occur by the electrodes placement on several parts of the body. As the electrode is placed in several different sections, the EMG noise that occurs around the respective electrode is different and uncorrelated [27, 54]. The EMG noise is also known as skin effect noise [8, 53].The MA noise, which is caused by patient movement is the most difficult noise to remove since its spectrum overlaps with the actual ECG signal [55, 56]. The MA noise produces a different reading on every single movement of the body. They suggested that the ECG signal is recorded while the patient is jogging, which allows a constant movement to occur [10]. However, in the most of cases the ECG readings are recorded during patients at rest and treated as free from MA noise.

3.4 Noise Reduction Methods

The noise reduction process is a preliminary step in the signal processing. The noise contaminating a signal should be minimized because processing signals with noise will result in less accurate results. Sometimes there is an overlap between the signal frequency and the noise signal [27, 36, 54, 57, 58]. Therefore, it is difficult to distinguish the information contained in the signal. If the noise removal process is not done cautiously then the information contained in the signal will be removed along with the noise. Nowadays, there are various techniques available for removing the noise present in the signal. There are many methods or techniques which are often used in removing the noise from ECG signal. However, this study only concentrated on the infinite impulse response (IIR)/finite impulse response (FIR) filter, the adaptive filter and the wavelet transform techniques.

3.4.1 IIR and FIR Filters

Noise filtering by using IIR and FIR filters have been by numbers of researcher. Some summaries of noises reduction of ECG signal by using IIR/ FIR shows in Table 3.2.

Table 3.2: Summary of ECG noise reduction using IIR/FIR.

Reference	Noise	Technique
Van Alste and Schilder [52]	BW/PLI	Notch filter.
Thakor and Zhu [10]	BW	Notch filter.
Min and Shi-Liu [59]	BW	Modified moving average filter.
Ling et al. [60]	BW	Combinations of high-pass filter with Savitzky Golay (SG) filter.
Kim et al. [61]	PLI	Notch filter.
Zhu et al. [62]	PLI	Discrete Fourier transform (DFT).
Ferdjallah and Barr [63]	PLI	DFT arrays and Constrained Least Mean Square (CLMS) adaptive filter.
Piskorowski [64]	PLI	Notch filter.
Panda and Pati [65]	EMG	Window approaches.
Jeyarani and Singh [66]	EMG	Low-pass filter.

The IIR/FIR filter is also widely used in reducing noise in the ECG signal before further processing is done. Van Alste and Schilder [52] use a notch filter in removing BW noise. However, the use of notch filters requires the BW noise frequency is identified before the notch filter is developed. Notch filter needs to be designed again if the BW noise contained in the ECG signal are changes. In other studies, Thakor and Zhu [10] also use a notch filter to reduce the effect of BW noise. Moving average filtering can also be used to reduce the effects of BW noise. Min and Shi-Liu [59] used a modified moving average filter to eliminate the BW noise. By taking into account the interval between the sampling data, the useful information from the ECG signal may be retained during the moving average calculation. Unfortunately the approach did not accommodate fast baseline changes. In another study, Ling et al. [60] stated that the use of a high-pass filter alone is unable to eliminate the effect of BW noise adequately. In order to overcome this problem, they have proposed a combination of a high pass filter with polynomial SG filter [60].The filter processed the low frequency signals while the SG polynomial filter smoothed the remaining signal. The filter needs to be re-designed for different BW noise contaminating ECG signals.

A notch filter has been used to reduce PLI. Van Alste and Schilder suggested the use of notch filters in removing PLI noise [52]. The use of notch filter is seen as an efficient way to reducing the PLI impact since a fixed 50/60 Hz interference is produced by the PLI. Zhu et al. [62] have proposed the use of DFT in eliminating PLI noise. They designed a narrow band frequency filter using a sliding DFT processor array. The approach is ineffective since 40 arrays of DFTs are needed to reduce the PLI noise. The removal of PLI was also attempted by Ferdjallah and Barr [63]. Firstly, a notch filter is used to detect any changes to the centre frequency variation. Then the poles and zeroes of the system are adjusted in reaching the optimum bandwidth, consequently the noise is removed. Both poles and zeroes adjusted for detecting the changes in the centre frequency of the optimal bandwidth. The CLMS algorithm is used to adapt both the poles and zeroes of the system. However, the work is not really compatible since PLI is a simple noise for the complicated technique but useful to be used for other noises. Piskorowski [64] proposed the use of notch filters to remove the PLI in ECG signal by reducing the transient response of the system. In Piskorowski's work, the PLI noise can be reduced as early as the ECG signal is processed. A non-zero initial condition must be identified in the first place before the transient response of the system is reduced by the notch filter. However, the approach is suitable for short signals only but not practical to be used for long signals since the PLI noise is constant.

The IIR/FIR filter also can be used in filtering the EMG noise. The FIR filter is generally implemented in a non-recursive way which guarantees a stable filter. Panda and Pati [65], used the window based FIR filtering which are rectangular, Hanning, Hamming and Blackman windows to do the noise filtering. Those windows are uncomplicated and capable to produce good results. The filtering process by using rectangular window based FIR has a sharp attenuation in the stop band and the filter has been stable during the pass band than others window. Jeyarani and Singh [66] used a low pass filter in order to remove the EMG noise of more than 100Hz. However, the electrical impulses represented by EMG noise are variable depending on the movement of the body. The development of a permanent filter is unable to filter the noise comprehensively. The problem will arise if the designed filter is not universal enough to accommodate all signals. Most of the FIR/IIR filters are unable to provide good MA noise reduction [10]. The problem occurs since spectrum of the signal and MA noise are overlapped. However, there are techniques available to filter the MA noise such as adaptive filter techniques and wavelets.

3.4.2 Adaptive Filter

The adaptive filter is a unique filter which adjusts its transfer function based on an optimizing algorithm [67]. Figure 3.2 show the block set design of an adaptive filter.

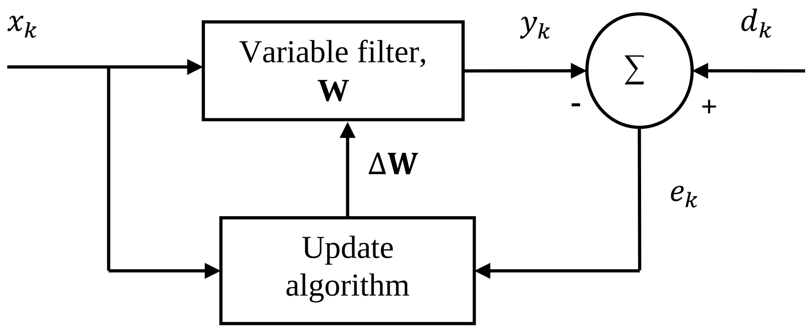

Figure 3.2: Adaptive filter block set.

The input signal of the system is x_k while d_k is the reference signal of the system. The input signal of this system will convolute with filter coefficient, $w$and then the result will be compared with the reference signal. The difference between the desired signal and the filter output is noted as error, e_k and the system will be used to update the filter coefficient. The process continues until the end of the signal. The $\Delta\mathbf{W}$ is the correction factor for filter coefficients. The least mean square (LMS) is an example of updating correction factor algorithm. Figure 3.2 shows the structure of a length L LMS update algorithm consist with system input x_k, input reference d_k, error of the system e_k and filter coefficient $\mathbf{W}_{k+1}$ updated according to [68, 69]:

$$\mathbf{W}_{k+1} = \mathbf{W}_k + \mu \boldsymbol{X}_k e_k \tag{3.1}$$

The updated filter coefficient is predicted one step ahead by summing current filter coefficient with the multiplication of μ, system input x_k and error of the system e_k. Parameter μ is the step size which selected to control the convergence rate of the system. Adaptive filters have been applied to signal processing [69], feedback cancellation [70], echo cancellation [71] and noise cancellation [72]. The summaries of noises reduction in ECG signal by using adaptive filter shows in Table 3.3.

Table 3.3: Summary of ECG noise reduction using adaptive filter.

Reference	Noise	Technique
Pandey [73]	BW	Stochastic gradient algorithm.
Paul and Mythili[74]	BW	Genetic algorithm (GA) and sign-data least mean square (SD-LMS).
Rahman et al. [75]	BW/PLI	Constrained stability least mean squares (CSLMS).
Ferdjallah and Barr [63]	PLI	Adaptive notch filter.
Thakor and Zhu [10]	PLI/EMG	Reference signal (signal from leg) and LMS.
Zhao and Ma [76]	PLI	EMD and adaptive filter.
Rahman et al. [5]	EMG/MA	Normalised sign regressor least mean square (NSRLMS).
Abbaspour et al. [77]	EMG	Adaptive neuro-fuzzy interference system (ANFIS).
Raya and Sison [72]	MA	LMS and RLS.

Adaptive filtering applications in noise cancellation are widely used and many modifications have been done to the original design by improving the system ability to perform better filtrations. Pandey [73] used an adaptive filter to remove the BW noise from ECG signals obtained from a Holter monitor. In his work, the primary signal was taken directly from an ECG Holter monitor while he added an absolute power spectrum of 3-channel accelerometer output as the reference signal. The stochastic gradient algorithm is used as the adaption method. The use of the LMS adaptive filter in the study gave encouraging result.

Paul and Mythili [74] used a combination of GA and SD-LMS algorithm to filter the BW noise. During the work, a SD-LMS adaptive filter was used to tune the GA to ensure that the BW noise in ECG signal is at a minimum. In the work, the ECG signals represented by 1 if a signal is greater than 0 and by -1 for a signal lower than 0. Although less complexity on calculation was made during the weight updating process but inaccurate result was obtained for the case of unbalanced signed signal. Rahman [75] used the constrained least mean squares (CSLMS) adaptive filter to remove the BW and PLI noises. The CSLMS is minimizing the squared Euclidean norm of the difference weight vector while the time-varying step-size of the CSLMS algorithm is inversely proportional to the squared norm of the difference. However, they only used CSLMS to remove the BW and PLI noises.

Ferdjallah and Barr [63] used adapted notch filters to eliminate the effect of PLI. The adaptive notch filter is used to find the changes of the frequency variation. The poles and zeroes of the system are adjusted in order to reach the optimum bandwidth and to remove the noise. The poles and zeroes are adapted for detecting the changes in the centre frequency of the optimal bandwidth. The technique became an alternative method to recognize the actual PLI rather than using the fixed 50/60 Hz PLI. Thakor and Zhu [10] used the reference signal (signal from the leg) to identify the real PLI. Both detection techniques used are capable of identifying the PLI but the filtering approaches used are no better than the normalised least mean square (NLMS) adaptive filter.

Zhao and Ma [76] proposed that the PLI is removed by using a series of EMD and the adaptive filter. The EMD technique is a data-driven technique used to decompose the ECG signal into a series of intrinsic mode functions (IMFs) [78]. An IMF represents an oscillatory mode as a part of a harmonic function. The IMF contains the same number of zero crossings and extrema and its envelopes are being symmetric with respect to zero. The ECG signal is filtered by using an adaptive filter based on the reference signal generated by the IMFs selected. In this research, the LMS adaptive filter was chosen to filter the IMFs. Again, the LMS adaptive filter is unable to better the NLMS adaptive filter result [69]. Unlike the wavelet technique, the EMD unable to promise the same number of IMF (subband) for both primary and reference signal.

Rahman et al. used the NSRLMS adaptive filter to reduce the EMG noise in ECG signals [5]. In the study, the signed input signal used may increase the performance of the NSRMLS filter. Here the error of the system was represented by 1 if the signals are greater than 0 and by -1 for signals lower than 0. The signed action on the error will result in an imbalance of data distribution if clustered directly to one group only. Abbaspour et al. [77] found that EMG noise removal from ECG signals is difficult because of overlap frequency content. Therefore, they proposed the use of an ANFIS and compared it with the realtime data. The implementation of this method is evaluated using several criteria including power spectrum density and coherence, signal to noise ratio (SNR), relative error and cross correlation. The use of a neural network requires a long training process to ensure the neural network is trained and capable to identify multiple types of EMG noises.

Thakor & Zhu [10] used an LMS adaptive filter for removing the EMG noise. This approach can be applied since the electrodes are placed in several different parts as illustrated in Figure 2.7. They used the unipolar 'Leads' in generating the primary and reference signal from human body. The placement of electrodes in several places may present the uncorrelated signals. They used the different voltage between the aVr and aVl, and signal at aVf electrode as the reference and primary signals, respectively. The approach used in this work has become a main reference to current research in identifying EMG noise in ECG signals. However, the recent use of the adaptive filter (NLMS) is able to provide results with even better noise removal than the LMS filter used in this work.

Raya and Sison [72] used an accelerometer to reduce the MA noise of ECG signals. The primary input has been collected from patient body and the accelerometer has been used as the input reference. As a result, the approach shows a good performance but filtering using LMS and RLS filters is unable to provide acceptable results. In Rahman et al.[5]used a NSRLMS algorithm to deal with the MA noise and enhance the results. However, the usage of adaptive filters requires a good reference signal. MA noise is difficult to detect since every muscle movement is different for each person. The use of adaptive filter in noise removal needs a good reference signal to perform the filtering process. Moreover, the properties of MA which overlap with ECG signals make the MA identification more difficult. The physical properties of the individual have the diversity of the possible movement which produces varying MA noises. As the result, the MA noise is hard to be observed, or to be used as a reference signal.

3.4.3 Wavelet Transform

Wavelets represent a mathematical approach that can serve as a tool to extract information from a variety of data types, not limited to data from image or audio signals only [79, 80]. In order to extract information from a given data, wavelet sets require that the data is fully analysed first. A reversible mathematical process is used to produce a complementary set of wavelets which will get the data without gaps or overlaps [81, 82].

The discrete wavelet transform (DWT) is a function of wavelet transform and widely used in denoising ECG signal. In numerical analysis and functional analysis, a DWT is any wavelet transform for which the wavelets are discretely sampled. As with other wavelet transforms, a key advantage it has over Fourier transforms is temporal resolution: it captures both frequency and location information (location in time).

The first DWT was invented by Hungarian mathematician Alfred Haar [83]. For an input represented by a list of 2^n numbers, the Haar wavelet transform may be considered to pair up input values, storing the difference and passing the sum. This process is repeated recursively, pairing up the sums to provide the next scale, which leads to 2^n-1 differences and a final sum. The most commonly used set of DWT was formulated by the Belgian mathematician Ingrid Daubechies in 1988 [84]. This formulation is based on the use of recurrence relations to generate progressively finer discrete samplings of an implicit mother wavelet function; each resolution is twice that of the previous scale. In her seminal paper, Daubechies derives a family of wavelets, the first of which is the Haar wavelet. Interest in this field has exploded since then, and many variations of Daubechies' original wavelets were developed.

The DWT of a signal x is calculated by passing it through a series of filters. First the samples are passed through a low pass filter with impulse response $g[n]$ resulting in a convolution of the two:

$$y[n] = x[n] * g[n] = \sum_{k=-\infty}^{\infty} x[k]g[n-k] \tag{3.2}$$

The signal is also decomposed simultaneously using a high-pass filter. The outputs giving the detail coefficients (from the high-pass filter) and approximation coefficients (from the low-pass). It is important that the two filters are related to each other. However, since half the frequencies of the signal have now been removed, half the samples can be discarded. The filter outputs are then subsampled by 2 with $g[n]$ denote as low-pass filter and h[n] denote as high-pass filter, as is Mallat's and the common notation [85].

$$y_{low}[n] = \sum_{k=-\infty}^{\infty} x[k]g[n-k] \tag{3.3}$$

$$y_{high}[n] = \sum_{k=-\infty}^{\infty} x[k]h[n-k] \tag{3.4}$$

This decomposition has halved the time resolution since only half of each filter output characterises the signal. However, each output has half the frequency band of the input so the frequency resolution has been doubled, with the subsampling operator ↓.

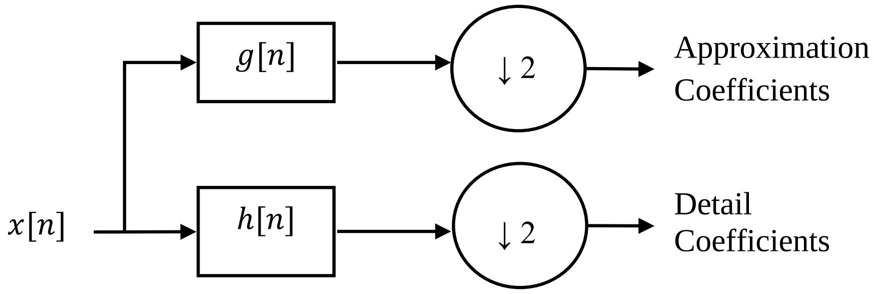

Figure 3.3: Block diagram of filter analysis.

The decomposition process is repeated to further increase the frequency resolution and the approximation coefficients, decomposed with low and high pass filters and then down-sampled. This is represented as a binary tree with nodes representing a sub-space with a different time-frequency localisation. The tree is known as a filter bank.

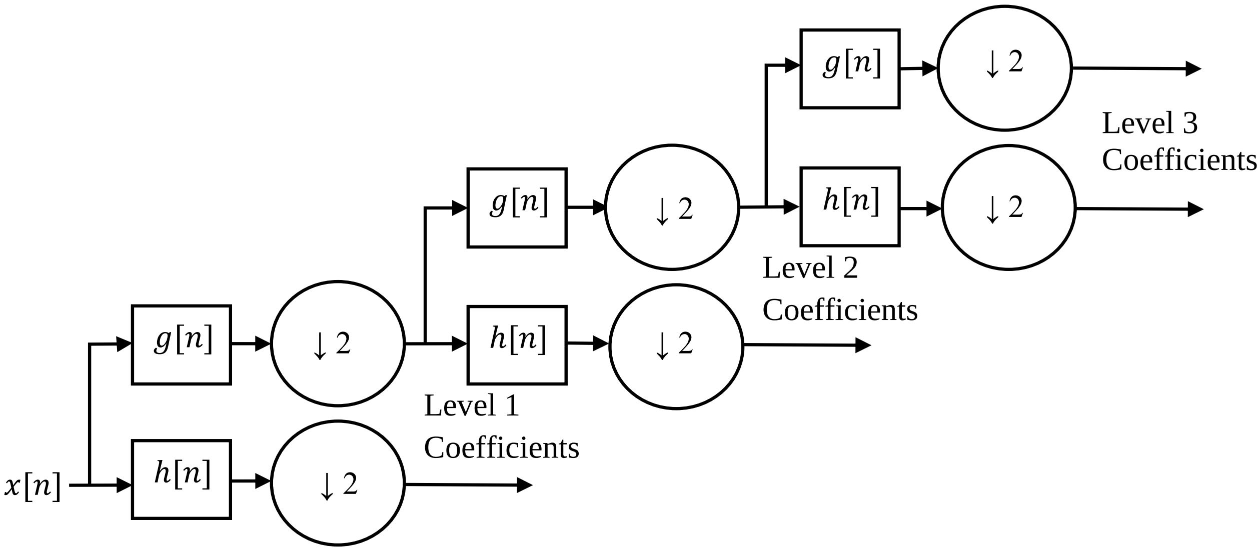

Figure 3.4: A 3 level filter bank.

At each level in the above diagram the signal is decomposed into low and high frequencies. Due to the decomposition process the input signal must be a multiple of 2^n where n is the number of levels. Numbers of mother wavelets used to decompose the signal such as Daubechies, Harr, biorthogonal, Mexican hat and others. However, in ECG signal processing, most of the researches are using the Daubechies as the mother wavelet since it is identical with the P, QRS and T complex [86, 87].

Several wavelet threshold methods can be used in removing the noise from signal based on two major threshold scheme which are hard thresholding and soft thresholding. The hard threshold can be illustrated as the process of setting to zero the elements whose absolute values are lower than the threshold. The soft threshold is an extension of hard threshold, first setting to zero the elements whose absolute values are lower than the threshold, and then shrinking the nonzero coefficients toward zero [88]. In signal denoising wavelet based threshold method often be used such as adaptive threshold selection using the principle of Stein's Unbiased Risk Estimate (rigrsure), fixed threshold methods $\sqrt{2log(x)}$, (sqtwolog), fixed threshold heuristic variant of the first option (heursure) and fixed threshold minimax (minimax) [89, 90].

The minimax method uses a selected fixed threshold that can produce minimax performance of the mean squared error compared to the ideal procedure. Therefore, this minimax principle can be used to design estimators for statistical applications. The minimax estimator is being used since it is able to obtain the minimum and maximum mean square error (MSE). The technique used in rigrsure is using a soft threshold estimator as threshold selection for the rules which are made on the basis of Stein's Unbiased Risk Estimate. The technique is able to estimate the risk and simultaneously minimize the risk in setting the threshold. The sqtwolog estimator applies a fixed-form threshold technique in order to deliver minimax results and has been multiplied with a small factor proportional to log (length (*signal*)). The heursure estimator is a combination between the sqtwolog and rigrsure estimators. Heursure depends on the value of the SNR, where very small SNR indicates the occurrence of the very noisy condition. If this situation is detected, a fixed form threshold is used to remove the noise [91-93].

Table 3.4: Summary of ECG noise reduction using wavelet.

Reference	**Noise**	**Technique**
Arvinti [94]	BW	Stationary wavelet transform (SWT) with Daubechies 2 as mother wavelet at level 8.
Zhe et al. [95]	BW	Wavelet, fast Fourier transforms (FFT) and Bayesian filter with Coiflet 5 mother wavelet.
Patil and Chavan [96]	PLI	Decomposition tree at level 5 using Daubechies, Symmlet and biorthogonal mother wavelet.
Weidong and Gotman [97]	EMG	Wavelet threshold denoising and independent component analysis (ICA).
Seung-Min et al. [98]	MA	Capacitive coupled with Daubechies 4 mother wavelet.
Strasser et al. [99]	MA	SWT.

Table 3.4 provides a summary of noise reduction methods using wavelet techniques. Arvinti et al. [94] in his study used a method based on stationary wavelet approximation in reducing the BW noise effect. In their study, the method used is non-supervised which is the main advantage compared to other techniques by allowing an automatic analysis of ECG. By using the proposed method, an accurate result is given in eliminating BW noise. Arvinti et al. [94] used the SWT approach based on Daubechies type 2 at level 8. The selection of Daubechies as the mother wavelet is capable to provide good results. In the work, Daubechies type 2 approaches used but the use of Daubechies type 4 were seen to be more

similar with the ECG signal shape. The similarity between mother wavelet and ECG signal allows maintaining the originality of signals during the noise filtering process. Zhe et al. [95] have been using a combination of wavelet denoising, a FFT bandpass filter and a Bayesian filter in filtering the BW and the results are compared with conventional ECG denoising approaches. In the study, they used Coiflet type 5 as the mother wavelet but this was no better than Daubechies mother wavelet. Here, the similarity between mother wavelet and ECG signal plays a big role to maintain the initial signal.

Patil and Chavan [96] found that wavelet is a good tool to analyse the non-stationary signals. The ECG signal corrupted with PLI and then denoised the signal by using a decomposition tree at level 5. They have done a comparison between the use of Daubechies, Symlet and Biorthogonal in reducing the impact of PLI. Although the fixed 50 Hz noise signal is used, results show the different performance by each mother wavelet. It was shown that the similarity between mother wavelet and ECG signal is capable to give good filtered signals. Weidong and Gotman [97] have introduced the use of wavelet threshold denoising and ICA techniques in getting rid of EMG noise in ECG signals. The ICA is a processing technique based on second order statistic that separate the independent components from main signals. The proposed extended ICA algorithm has been done and as a result, a higher order statistic calculation is not always necessary. In addition, the speed of the convergence is increased and able to be used in separating the subgaussian and supergaussian from the main sources. Compared with adaptive filters, the use of wavelet in reducing the effects of EMG do not need the noise to be identified as the reference signal in advance. In this study, the results given by the wavelet approach reduced the effects of EMG noise. However, the noises are still contaminating filtered signal. By applying the ICA technique to the filtered signals better results can be obtained. From the results, it is shown that the wavelet approach is unable to filter the EMG noise very well unless the wavelet is supported by other filtering techniques.

The capacitive coupled ECG is a new ECG measurement approach which detects the ECGs although others material are attached with body (i.e. cloth or electrode) [93].Capacitive coupled ECG is known as non-invasive measurement technology and using displacement current rather than conduction current for many conventional ECG measurement equipment. However, the capacitive coupled ECG is unable to satisfactorily remove MA noise. The MA noises have different frequency ranges although many studies indicate that MA noise occurs at signal frequency of less than 0.8Hz [10, 72]. Therefore, wavelet with the Daubechies type 4 as the mother wavelet is capable of reducing the noise. Although a small portion of the original ECG signal is eliminated together with the MA noise signal quality can still be maintained for long-term measurement.

Portable devices nowadays are capable to record the ECG activity. Normally, the device includes a transmitter that is capable of providing information of the patient. However, the devices are unable to prevent the MA noise from contaminating ECG signals. Various efforts had been made to address the problem. In order to solve the problem, Strasser et al. [99] used SWT to reduce the effects of MA noise in the ECG signal. The SWT offers an automatic multi-resolution thresholding scheme for the filtering process. The MA is the most difficult noise to remove because its spectrum overlaps with the actual ECG signal [10]. At the same time, the MA noise may contain both high and low frequency and stationary or non-stationary signals. The filtering process has to be done carefully to maintain the originality of the signal and to reduce the maximum amount of MA noise.

3.5 ECG Feature Extraction

Normally, ECG feature extraction is based on the characteristic of ECG complex and ECG waveform. The features extraction using characteristics of ECG signal are often characterized by amplitude, duration and slope of each peak in the ECG complex [2, 53]. In contrast, extraction by using the ECG waveform is usually performed by observation of the correlation coefficient, Fourier coefficient, form factor, wavelet coefficient and others [10, 100, 101]. For the analysis conducted to AF, the features extracted most are the RRI [40, 102, 103] and atrial activity (AA) [104, 105]. In addition, there are also studies done by combining both RRI and AA approaches [3, 106, 107].

3.5.1 Characteristic Based Feature

In ECG feature extraction, the detection of P, QRS and T complexes needs to be done before heart disorder can be detected. Table 3.5 illustrates the characteristic and technique used by researchers in detecting the characteristics of ECG peaks.

Table 3.5: Summary of ECG characteristic detection techniques.

Reference	Technique
Rincon and Fernandez [108]	Estimation and proportion of time duration.
Mukhopadhy et al. [109]	Hilbert transform.
Alhady et al. [53]	Multiple radial basis function (MRBF).
Mazomeous et al. [110]	Time domain morphology and gradient (TDMG).

Rincon and Fernandez [108] found that the R wave can be detected with high precision by using a wavelets approach. Once the R wave is found, then the other ECG features are extracted using a waveform segmentation approach. They described that the quality of PQS detection is highly dependent on the accuracy of the R wave. They use a wavelet-based algorithm to identify the wave R -the R to R interval can be determined after the R wave is detected accurately. The S wave represents the offset of the QRS complex corresponding to the depolarization ventricular. The range of the S wave location is detected after the R peak is discovered and mitigated by the addition of 6 units. The S wave estimated range is between 0.016 to 0.036 seconds after the R peak. The Q wave represents the beginning of the QRS complex. The Q peak is located within a period of 0.02 to 0.06 seconds before the peak R is found. The proportional calculation can be used to detect a wider QRS complex. The P wave represents the auricular depolarization of the heartbeat. Since this wave can be located near or far from the Q wave, so the proportion of the R to R interval is used to find the exact P point. The P to R interval duration is between 0.09 and 0.19 seconds depending on the R to R interval. In the proportional aspect, the limit is 14% to 22% of the R to R interval, respectively. However, the algorithm is valid for a specific area only and limited to minimum and maximum search.

Mukhopadhy et al. [109] suggested a detection technique of ECG features such as QRS duration, R peak amplitude, onset / offset / amplitude of the T peak, duration of S to T and Q to T. The technique used has been tested using data derived from Physikalisch Technische Bundesanstalt Diagnostic (PTB) database. In this study, an ECG signal was filtered to obtain a smooth signal before the Hilbert transform is used for derivatives to make sure the R peak region is easy to locate. The identified zero slopes at the beginning of the Q peak and at the ending of the S peak will be known as the QRS onset and the QRS offset, respectively. In order to detect the T peak, the same approach used to detect the R peak is also deployed. The T onset and T offset are detected by the approach used to detect the QRS onset and QRS offset, respectively. The amplitude of the R and T peaks, and the duration of QRS, QT and ST segmentation are measured using the average error. Algorithm performance is highly dependent on the selection of the threshold value.

Alhady et al. [53] also use some features in identifying the real peaks of P, QRS and T. The study identified numbers of features; amplitude and duration, pre-gradient and post-gradient and degree of each of the P, Q, R, S and T peaks. In this study the multiple radial basis function (MRBF) network is proposed to identify each of the P, Q, R, S and T peaks. The network is trained to identify by using five features as the input vector. A trained multiple radial basis function (MRBF) network identifies the peaks which are present in the ECG signal. Each peak is named as P_1, P_2, P_3, …., P_n until the end of the ECG signal is reached. From the extracted features for each peak the MRBF network decides that the peak is P, Q, R, S or T. Overall accuracy only occur with 86.53% accuracy and better prediction techniques need to be tested in order to provide high accuracy results.

Mazomenos et al. [110] used the time domain morphology and gradient (TDMG) based algorithm for extracting all fiducial time which are present in the PQRST complex. Then, the estimation on the characteristics were done and used to identify the temporal ECG parameters. The combination of extrema detection technique and slope information is used with adaptive threshold in order to achieve the extraction of time instances. At the beginning, the location of the R peak and QRS complex boundaries can be determined by observations on time scale. Then, the observation of the QRS complex can determine the peaks Q and S, as preceding and succeeding the QRS complex, respectively. The P and T peaks are estimated from the remaining fiducial points of the PQRST complex, at the left and right of the QRS complex, respectively. The approach used is based on Pan and Tompkins [32] work in estimating the boundary of each peak. However, the ECG signals must be filtered correctly before the boundary of each peak is estimated.

3.5.2 Waveform Based Feature

Table 3.6 shows a summary of approaches used to detect ECG signal by using waveform based feature.

Table 3.6: Summary of waveform based feature detection techniques.

Reference	Technique
Kumar et al. [111]	Curve mapping/matching.
Ge [112]	Linear approximate data transfer (LADT).
Sutar et al. [113]	Designed low cost cum computing device (LCAD).
Safie et al. [108]	Pulse active ratio (PAR) based PWM.

Kumar et al. [111] suggest an approach which is able to determine the amplitude of the P, QRS and T followed by period intervals (PR, RR, QRS, and QT). The features obtained are used to determine whether heart operation is a normal or not. Any changes to the heart's activity can be identified to facilitate cardiologists to recommend a total dose required. In their study, a curve mapping (CM) technique based curve slope method has been proposed to track the ECG signals. They also proposed the use of pattern matching between the healthy and diseased signals. Once these patterns are identified, they are used to apply the slope based point computation to recognise the various up and down sets. The CM technique is capable to match for regular ECG however, difficult to match the irregular ECG signal.

Ge [112], in the research used wavelet based filter (average filter and Mexican Hat mother wavelet) to reduce the noise effect in the ECG signals. Feature such as premature ventricular contraction (PVC) and NSR, taken from the MIT-BIH database, are extracted for a possible discrimination process. Then, the filtered signal is compressed by using the linear approximation data transfer (LADT) algorithm. Beats which have been identified are segmented by using a Hanning window with 200ms range before the QRS points (better known as the peak R) and 400ms after the QRS points. The Hanning window ensures that each end of the signal becomes zero and then decomposes the signal by using Daubechies mother wavelet. The technique extracts three main features from an ECG signal which are the variance, the energy and the consecutive ratio of the R to R peak. However, the peak estimation based on the boundaries of time is less suitable for irregular ECG signals.

In Sutar et al. [113] an intelligent diagnostic medical system was developed, using a LCAD to extract the ECG signal. Some significant features are extracted using the LCAD system. The use of time domain and frequency domain allows accurate detection of the QRS complex, and the ECG signal extraction is done correctly. The DWT is used to decompose the ECG signals for up to level 4. The R peak detection process uses a threshold value of 75% from the maximum value of the selected sample. The maximum absolute value of the sample will allow the R peak detection. The QRS complex is determined based on the location of the detected P peak. The Q and S peaks are below the baseline on the left and right of the reference R peak. The P peak detection is done by identifying the positive slope followed by the negative slope. The amplitude of the two slopes must be greater than 0.004mV/s. Based on the QRS complex, the T peak was determined based on probabilities. First, if the R to R interval is more than 0.7s, then the set of T starts and ends at 0.08s and 0.44s, respectively after the QRS complex. The second probability is if the PR interval is less than 0.7s, then the set of T starts at 0.04s after the end of the QRS complex and ends using the calculation ((0.7 * RR interval) - 0.06) after the end of the QRS complex.

Safie et al. [114] proposed a new feature extraction technique known as PAR implemented in the ECG signals for biometric authentication. The PAR development is based on the principle of PWM, which is widely used in other fields. A segmentation of the ECG signal is taken into account by taking a complete ECG complex, the P, QRS and T peaks as shown in Figure 3.5. A periodic triangular waveform segmentation which is superimposed with the ECG signal is used.

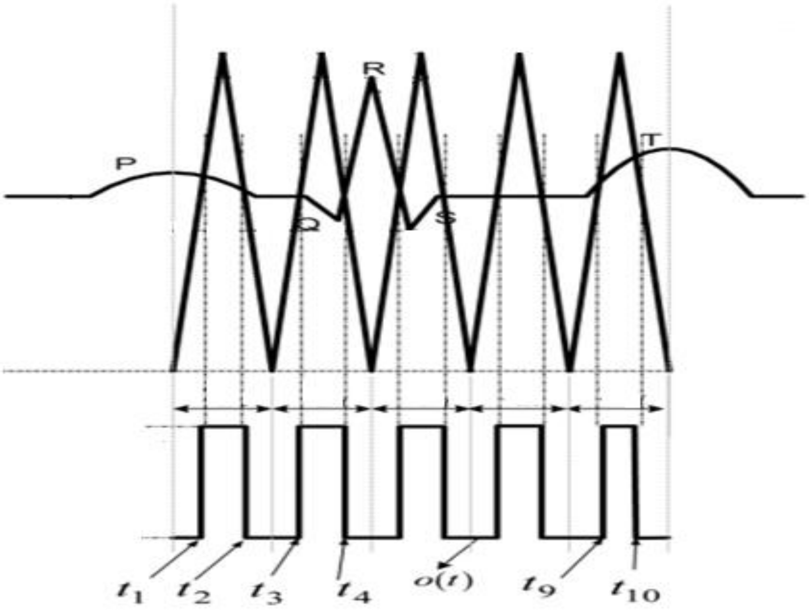

Figure 3.5: PAR pulse generation [114].

The features extracted are the pulse durations generated from the intersection points between the ECG complex and the periodic triangle waveform as shown in Figure 3.5. The first intersection point was selected from a positive slope and the last intersection point was selected from a negative slope. This technique was developed in order to extract time durations occurring from the intersection of the ECG signal with the periodic triangle waveform. Thus, time duration is longer for the horizontal part of the signal (i.e. S to T_{onset}), while the time duration is shorter at the peaks of the ECG signal. However, the PAR in using the triangular waveform leaves small parts of the ECG signal at the beginning and the ending of each complex. In addition, the PAR interest with the duration at the intersection points between the positive and negative slope at each triangular waveform.

3.5.3 AF Detection Algorithms

There are two main features allowing AF identification based on ECG signals: the electrical discharge from atria to the ventricles and the irregular electrical of AA [11]. The electrical discharges from the atria to the ventricles can cause irregular heart rate. AF is easy to be detect from an ECG signal with RRI and the absence of a P wave [2]. The AA can be analysed using either time or frequency domain approaches [2]. In [115] the signals were analysed based on the absence of P waves and using frequency spectrum analysis (FSA), which consists of the cancellation of ventricular activity (QRS complex and T wave), followed by the spectral calculation of the remaining atrial signal spectrum.

Table 3.7 shows the comparative results of AF classification which use the RRI, AA and a combination of RRI and AA methods. The comparative results of each technique is measured on the accuracy, sensitivity and specificity of predictions made. By assuming there are two class of datasets (A and B), the accuracy, sensitivity and specificity are calculates by:

$$Accuracy = \frac{number\ of\ true\ A + number\ of\ true\ B}{number\ of\ A + number\ of\ B} \tag{3.5}$$

$$Sensitivity = \frac{number\ of\ true\ A}{number\ of\ A} \tag{3.6}$$

$$Specificty = \frac{number\ of\ true\ B}{number\ of\ B} \tag{3.7}$$

Table 3.7: The comparative results of AF classification using various techniques.

Technique	**Result (%)**			
	Method	**Accuracy**	**Sensitivity**	**Specificity**
Colloca [102] et al.	RRI	97.63	96.35	98.91
Maji et al. [103]	RRI	96.00	96.00	96.00
Andersson et al. [116]	RRI	95.35	94.90	95.80
Escalona and Reina [40]	RRI	95.00	93.00	97.00
Ladavich and Ghoraani [117]	AA	94.75	99.28	90.21
Hayes and Teal [104]	RRI	93.62	94.76	92.48
Lee et al. [105]	AA	92.55	94.70	90.40
Lian et al. [118]	RRI	91.60	95.80	96.40
Babaezaideh et al. [3]	RRI/AA	91.37	87.27	95.47
Dash et al. [2]	RRI	90.50	90.00	91.00
Kostka and Tkacz [119]	RRI	88.50	90.00	87.00
Helfenbein et al. [107]	RRI/AA	84.00	71.00	97.00

In Hayes and Teal [104], a study was performed to check the feasibility of low-power ECG monitor to detect AF in real time. In the study, five beat and five rhythm detectors were constructed and the regression values of each were passed onto two further classifiers for AF detection. Power consumption was measured at 30mW giving 96 hours of continuous operation. The computation time for the signal sub-band filtering and heart beat interval calculations was measured at 2.1ms per 8ms intervals, and the heart beat classification at 10.2ms per classifier per beat detected. Low power consumption is needed in AF detection meaning that the low-power ECG monitor can only provide up to 96 hours of continuous operation even though AF episodes can last up to seven days.

The Dash et al. method combines three approaches for AF identification [2]. The first approach is to identify the variance of the RRI, which provides a good AF indicator. The second approach is the study of the QRS complex morphology to allow accurate calculation of RRI and, the final approach, is the use of the QRS spike features for AF identification since it is least influenced by muscle noise. In the research, the developed algorithm is able to detect the presence of AF by only analysing the RRI. However, problems can arise if the irregular signal occurs when the algorithm has already specified the coefficients.

Kostka & Tkacz [119] developed a system of biomedical signal classifiers, with a preliminary feature extraction stage, based on matched wavelets analysis and used neural networks and support vector machines as the classifiers. They tried to study some extraction algorithm rules in order to supply input vectors to the classifiers. The extracted features are gathered in Black Box parameters and used for testing purpose on 20 AF subjects and 20 control group subjects taken from the MIT-BIH database. The classification results showed that the use of selected significant features increased the generalization ability and gave better results for sensitivity and specificity measurement. However, the used Mallat mother wavelet is no better than the Daubechies mother wavelet since the Daubechies mother wavelet mimics the QRS wave better than the Mallat mother wavelet.

Escalona and Reina [40] in their research tried to detect abnormal heart rhythm by comparing the R to R peak interval with the difference between successive R to R peak intervals (ΔRR). In the research, a decision rule for identifying AF arrhythmic patterns has been derived from RR-intervals analysis. It was generated by using recorded ECG before, during and after the AF episodes. In this work, the time series were generated by measuring time differences (ΔRR) between the consecutive RR intervals. Similar to others approaches, this technique are placing emphasis on the R peak (duration) rather than other fiducial points.

Colloca et al. [102] investigated the dynamics of R to R peak interval series from NSR and AF episodes. The study focused on AF detection algorithms appropriate for a screening application which would allow for mass screening and address the under-estimation problem of AF. Again, RR analysis-based features were chosen. They used nine AF predictors in an SVM, allowing the predictive power of each published algorithm to be combined. Ten R-peak related features were taken from the ECG complex and the classification performance was assessed both univariate and when combined using a SVM. Out-of-sample test performance has been done by using MIT-BIH AFDB dataset. Although the approach is capable of producing high accuracy results, long window beats are needed.

A map of the R to R peak interval versus the change of the R to R peak interval has been plotted by Lian et al. [118]. The map was arranged in a grid with 25ms resolution in 2 axes and the non-empty cells are counted to classify the AF and non-AF episodes. The mapping is performed for each window and classification results are compared to the reference results. However, this method is unable to detect AF very well during the regular signal analysis and it also gives false alarms in non-AF occurrences during the irregularity signal analysis. Maji et al. in their study proposed a new technique based on phase rectified signal averaging (PRSA) in classifying the AF rhythm [103]. The performance of the approach is tested by using MIT-BIH arrhythmia dataset. In this study, R to R segment are processed by using PRSA principle, based on lining up few sections of the signal by centring at selected points called anchor point followed by a signal averaging.

A real-time detector for AF episodes is fabricated based on three parameters for characterizing the RR interval series, i.e., turning point ratio, root mean square of successive differences, and Shannon entropy. Andersson et al. in their study had developed hardware with ultra-low voltage operation which suitable for implantable loop recorders with ultra-low energy requirements [116]. Algorithmic and architectural optimizations are designed to minimize area and energy dissipation. The design is fabricated in 65-nm complementary metal-oxide semiconductor (CMOS) low-leakage high-threshold technology. Again the method has been tested using MIT-BIH AF dataset can capable to perform 94.90% and 95.80 for sensitivity and specificity, respectively.

Using the AA [11], the information is extracted on the amplitude of the P, R and T peaks and several time durations are associated with each ECG complex. Usually, the P-waves are not always present in AF signals and are replaced by fibrillatory waves. The AA can be analysed using time domain and frequency domain methods. The time domain will detect the absence of a P-wave whilst analysis using frequency domain will cancel the ventricular activity (QRS complex and T wave). Fourier analysis is used to balance the remaining signal. Lee et al. [105] introduced a novel method for the automatic detection of AF using time-varying coherence functions (TVCF). In the research, TVCF is estimated by the multiplication of two time-varying transfer functions (TVTFs). The two TVTFs are obtained using two adjacent data segments with one data segment as the input signal and the other data segment as the output to produce the first TVTF; the second TVTF is produced by reversing the input and output signals. We found that the resultant TVCF between two adjacent NSR segments shows high coherence values (near 1) throughout the entire frequency range. Detection results vary depending on the number of beats used during the classification process. In general, longer beats can produce more accurate predictions and vice versa.

Babaeizadeh et al. developed a real-time AF monitoring algorithm to eliminate false-positive AF alarms [3]. The algorithm uses RRI as the indicator and it is modelled by a Markov model to calculate the RR Markov score. This score reflects the relative likelihood of observation of RRI in AF episodes versus the observation outside the AF episodes. However, the episodes of AF are sometimes misclassified as non-AF and vice versa. Furthermore, the P wave detection is difficult in the presence of high frequency noise. The AF classification is achieved by adding the AA analysis; the PR interval variability and P wave morphology similarity to the Markov model.

Helfenbein et al. stated that RR interval variation can no longer be the main feature for AF detection [107]. The power spectrum and autocorrelation of the atrial signal provide good discrimination. They used Philips DXL algorithm which detected the AF in the presence of paced rhythms and provides interpretations for both rhythms. The algorithm uses QRST subtraction with frequency domain analysis of the residual. For classification, a decision tree classifier used power spectrum as the features as well as irregularity of non-paced beats. On a testing set of 1,057 paced ECGs with 194 AF cases, the algorithm had sensitivity of 71% and specificity of 97%. From the result, it was shown that the generalization process was not performing well during training phase since the gap between sensitivity and specificity results was too large.

Ladavich and Ghoraani applied Expectation-Maximization algorithm to train and create a multivariate Gaussian Mixture Model (GMM) of the feature space [117]. In their research, they applied the model for identifying P-wave absence (PWA) and, in turn, AF. This novel atrial activity based method detects the absence of NSR P-waves from the surface ECG. The proposed model extracts nine features from P-waves during SR and develops a statistical model to describe the distribution of the features. The algorithm was tested on 20 records in the MIT-BIH dataset. The classification process combined with seven beats and shows 99.28% on sensitivity and 90.21% on specificity.

3.6 ECG Pattern Recognition using Neural Network

Artificial neural network (ANN) is a branch of artificial intelligence as it based on brain function. Based on the principles of brain, the artificial neural network designed to resemble a brain operation such as structure building, learning techniques and operating techniques [120]. Figure 3.7 shows diagram of the nonlinear neuron model.

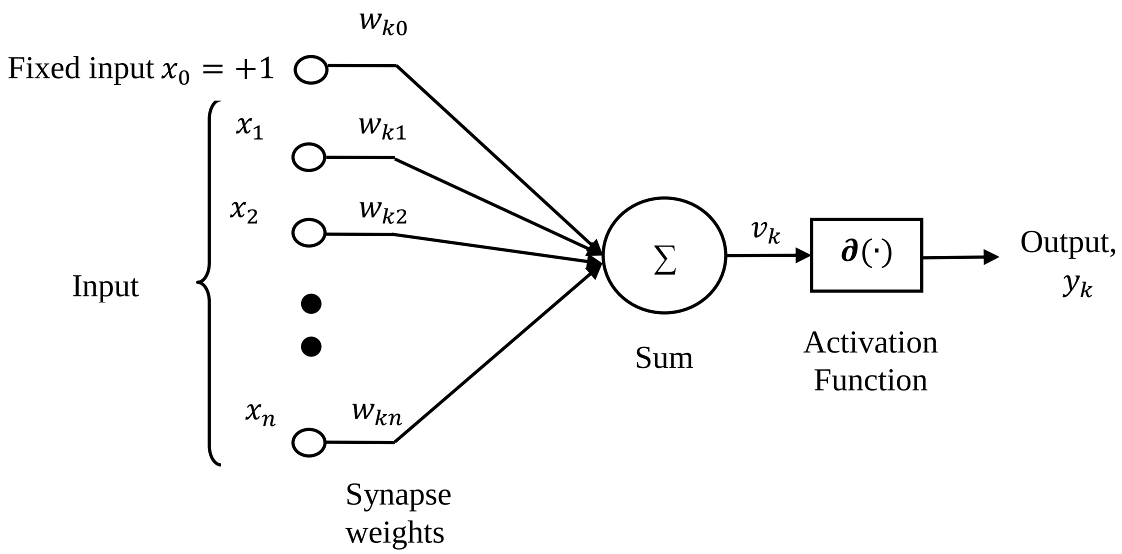

Figure 3.6: Nonlinear neuron model [121].

Based on the Figure 3.6 essential components of a neuron formation is a set of synapses or network connection, a sum and an activation function. Each synapse of neuron is given a weighting value. By assuming the neuron has k number of synapses, consequently it has k input. $(x_1, x_2, .., x_k)$ are the input at each synapse while the $[w_1, w_2, .., w_{kn}]$ are the weight at each synapse and $\boldsymbol{\partial}(\cdot)$ is the activation function of the model. Input x_j at the input synapses connected to the neuron will be multiplied by the value of the k^{th} synapse weights $[w_k]$ influence the weight value for the processing of the synapses to the output of the neuron. A sum process adds all the multiplied signals or input and bias, and the result are sent to the activation function. The mathematical modelling of neurons based on Figure 3.6 can be defined based by the following two equations:

$$v_k = \sum_{j=1}^{n} w_{kj} x_j + w_{k0} x_0 \tag{3.8}$$

and

$$y_k = \boldsymbol{\partial}(v_k) \tag{3.9}$$

In (3.8) and (3.9), v_k is the summing output, x_j is the input signal of the k^{th} data or synapse, w_k is the weights to the k^{th} synapse of neuron and $\boldsymbol{\partial}(\cdot)$ is the activation function, and y_k is the output product. There are several types of activation functions often used; namely, the fixed limiter function, the piecewise linear function, the sigmoid function and the linear function [121].

3.6.1 Hybrid Multilayer Perceptron (HMLP)

There have been several modified versions based on conventional MLP networks, such as the addition of a linear connection directly from the input layer to the output layer to form a new network known as HMLP network. Mashor [12] showed that HMLP networks can improve the accuracy of results compared to conventional MLP networks. The ability of ANNs to make good predictions is highly dependent on the training algorithms used and the design of the structure [122]. The direct linear connection between the input and the output layers has been applied in an effort to improve the efficiency and generalization of conventional nonlinear neural networks [118, 120-121], resulting in the HMLP network.

Naturally, improved training algorithms were also sought to deal further improves performance.

An MLP neural network is a highly nonlinear functional structure that can be trained to implement a desired input-output mapping [123, 124]. They also stated that using a nonlinear network, such as MLP to model a linear system will not produce an accurate prediction. In order to do that, HMLP network does cope well with linear systems owing to the direct input to output connections, represented by the dashed line in Figure 3.7. The figure consists of a set of an input layer, a single hidden layer and an output layer. The MLP network with one hidden layer is enough to give good prediction results as shown by Funashashi [125] and Cybenko [126]. Therefore, further discussion in this thesis only involves neural networks with one hidden layer.

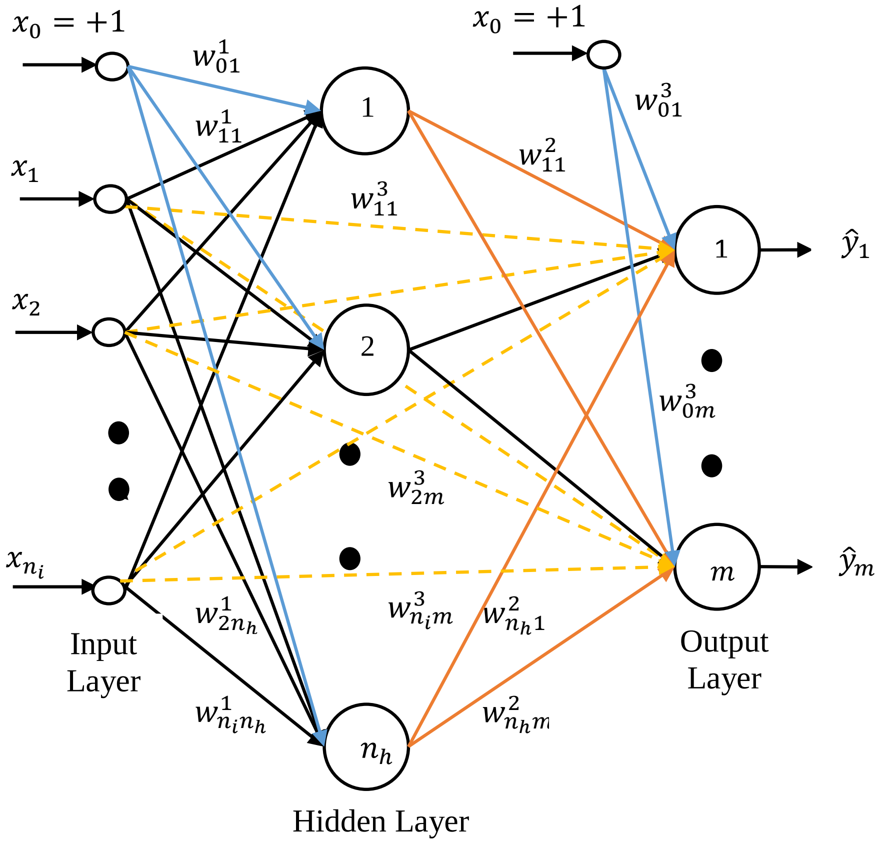

Figure 3.7: A schematic diagram of a HMLP network with one hidden layer.

The output of the network is given by:

$$\hat{y}_k(t) = \sum_{j=1}^{n_h} w_{jk}^2 \, \partial\left(\sum_{i=1}^{n_i} w_{ij}^1 x_i^0(t) + w_{k0}^1 x_0^1\right) + \sum_{i=1}^{n_i} w_{ik}^3 x_i^0(t) \tag{3.10}$$

$for\ 1 \leq j \leq n_h$ and $1 \leq k \leq m$

where w_{ik}^3 represents the weight of the additional linear connection between the input and output layers, n_i and n_h are the number of input nodes hidden nodes, respectively. $\boldsymbol{\partial}(\cdot)$ is the activation function with the sigmoid activation function chosen to activate the HMLP network. The weights w_{ij}^1, w_{jk}^2, and w_{ik}^3 are unknown variables and they need to converge to optimum values in order to minimize the prediction error defined as:

$$e_k(t) = y_k(t) - \hat{y}_k(t) \tag{3.11}$$

with $y_k(t)$ being the actual output from the system while $\hat{y}_k(t)$ is the predicted output.

3.6.2 Training Process

The learning period is an important process in a neural network. The process ensures that the neural network is able to meet its intended design functionality. There are two types of learning paradigms often applied: supervised learning and non-supervised learning [121]. Datasets will be divided into two parts: training dataset and testing dataset which will be used in the training and the testing phases respectively [12, 127]. By using supervised learning, the learning process is able to form a set of functions based on the training data. The training dataset contains a pair of input and output parameters. The supervised learning task is to predict the values of the function for each input data input based on the observation of the training datasets (pairs of input and target output). Supervised learning can produce a global model that will map the input to the desired output. However, in other cases it will implement mapping conducted as a set of local models as nearest neighbours' algorithm (nearest neighbourhood).

On the other hand, unsupervised learning methods require established training models to do the estimation. The learning process is different from supervised learning because the process has no output target. In unsupervised learning, a set of input data will be collected and it is assumed that the input data is a set of random variables. A density model will be developed based on the datasets and unsupervised learning will be based on past experience. In other words, the learning process does not have any targets to guide it and relies only on experience from the past [128]. Unsupervised learning is very useful for data compression. All compression algorithms depend on the probability distribution of each input dataset.

3.7 Conclusion

This chapter reviewed the entire process of determining the abnormality of AF from an ECG signal. The ECG signal processing engaged with the noise filtering stage, the feature extraction process and classification works in order to determine the AF. Significant research has been conducted in removing noise contaminants in ECG signal. Many approaches have been put forward in order to extract features from clean ECG signals and a number of classification techniques have been developed for classifying the clean ECG signal by using the extracted features. In Chapter 4, novel noise reduction unit which consists: i) bandstop notch filter to eliminate PLI noise, ii) LMS based adaptive filter in removing EMG noise and iii) wavelet based filters in reducing BW and MA noise.

Chapter 4

Novel ECG Noise Reduction Unit

4.1 Introduction

In the previous chapter, researches on noise filtering techniques, feature extraction processes and classification based ECG signals have been reviewed. In this chapter, a novel noise reduction unit is presented in order to reduce the effect of BW, PLI, EMG and MA noises that contaminate the ECG signal. The unit incorporates three approaches. In the first, a bandstop notch filter is used in eliminating the PLI noise. The second component uses an IPNLMS adaptive filter which is shown to provide good filtering results in removing the EMG effect. The third component involves a combination of STHL wavelet based filters have been applied in the unit to reduce denoise the effect of BW and MA noise. Comparative studies have been done to measure the capability of IPNLMS adaptive filter and STHL filter. These show that those filtering techniques outperform other techniques with significant results. All the designed filters have been tested by using datasets taken from MIT-BIH database for both signals and noises.

4.2 Noise Reduction Unit

The notch filter is capable to provide significant results and used again to complete the noise reduction unit. Figure 4.1 shows the noise reduction unit structure.

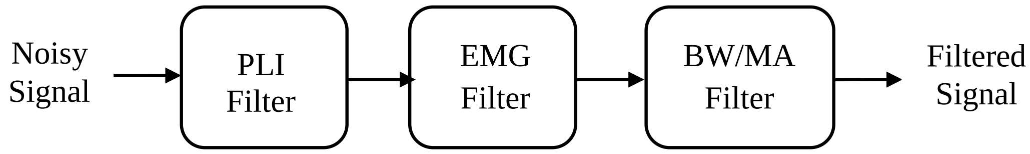

Figure 4.1: The novel noise reduction unit with different filters of each noise.

As indicated in Figure 4.1, the noisy ECG signal is input to the noise reduction unit. Figure 4.1 shows the denosing process of the noisy signal by using three different filters. Each noise uses an individual filter to reduce the noise effects.

4.2.1 Bandstop Notch Filter in Eliminating PLI Noise

The first filter to be used in the novel noise reduction unit is bandstop notch filter which is designed to eliminate the 50/60 Hz PLI in ECG signals. The elimination process is accomplished by using the bandstop notch filter since the EMG noise is characterized by a unit gain at all frequencies except the sinusoidal frequencies at the zero gain. The notch filter is setup with two different settings for countries which used 50 Hz in the power lines and for countries which used 60 Hz for power lines. In this study, IIR bandstop notch filter has been designed using Filter Design and Analysis Tool (fdatool) which is at 50 Hz. The signal with 50 Hz is rejected while other frequency of the signal is passed. In the process, the PLI noise signal which is 50 Hz is rejected from ECG signal. Detail on IIR notch filter design is discussed in section 4.3.1.

4.2.2 LMS based Adaptive Filter in Removing EMG Noise

The second filter to be presented in the novel noise reduction unit is an LMS based adaptive filter to be used in removing the EMG noise in ECG signals. The LMS adaptive filter was discussed in detail in subchapter 3.4.2. However, the LMS adaptive filter inadequate to process stationary and non-stationary signal simultaneously. Beginning with the NLMS for both stationary and non-stationary signal a new improved algorithm is developed.

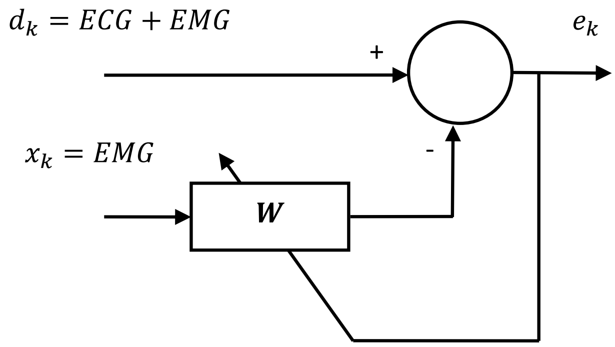

Figure 4.2: Adaptive filter structure.

The NLMS adaptive filter is used to normalize the step size parameter in the adaptive filter that was discussed in Section 3.4.2. As a result, an improvement of the stability and convergence rate of the filter output compared to the basic LMS adaptive filter [69]. The filter coefficient updates related to the NLMS adaptive filter algorithm with L length is given by:

$$\boldsymbol{W}_{k+1} = \boldsymbol{W}_k + \frac{\mu x_k e_k}{{x_k}^T x_k} \tag{4.1}$$

where $\boldsymbol{W}_k$ is the filter coefficient, $\boldsymbol{W}_{k+1}$ is the updated filter coefficient, ${x_k}^T x_k$ is the normalized factor, e_k is the error of the system and μ is the fixed step size used to control maladjustment.

Although the NLMS adaptive filter have been used in many ECG studies and is capable to process both static and dynamic signal but the speed of convergence is not guaranteed [129]. The proportionate normalised least mean square (PNLMS) adaptive filter has the capability to converge faster than the NLMS algorithm. PNLMS adaptive filter is widely used in echo cancellation field but not used in processing the medical signal such as ECG. In PNLMS adaptive filter, each gain is approximately proportional at each position to the current tap filter coefficient. The filter coefficient of the PNLMS adaptive filter is updated with the extra step-size update $\boldsymbol{Q}_k$ [129] as follows:

$$\boldsymbol{W}_{k+1} = \boldsymbol{W}_k + \frac{\mu \boldsymbol{Q}_k x_k e_k}{{x_k}^T \boldsymbol{Q}_k x_k} \quad (4.2)$$

where the diagonal matrix of the gain is [129]:

$$\boldsymbol{Q}_k = diag[q_0, \cdots, q_{L-1}] \quad (4.3)$$

and the gain can be computed as [129]:

$$q_l = \frac{\gamma_l}{\sum_{i=0}^{L-1} \gamma_i}, \qquad 0 \le l \le L-1 \quad (4.4)$$

with the impulse response as [129]:

$$\gamma_l = max\{\rho * max[\delta_p, |w_0|, \dots., |w_{L-1}|]|w_l|\} \quad (4.5)$$

where parameters ρ and δ_p have typical values of 5/L and 0.01, respectively, and δ_p is a small positive number used to avoid overflow [130]. The ρ is selected so as to avoid γ becoming very small, while the constant δ_p is important at the beginning when all coefficients are 0. The initial convergence slows down when ρ and δ_p is too large.

During the implementation of PNLMS adaptive filter in echo cancellation, the performance of the PNLMS was seen by Benesty and Gay [130] to be no better than NLMS adaptive filter when the impulse response is scattered. In order to improve the situation, they [130] proposed an improved version of PNLMS, IPNLMS adaptive filter to overcome the disadvantages inherent in the PNLMS. The IPNLMS adaptive filter employs a combination of proportionate (PNLMS) and non-proportionate (NLMS) in the updating the filter coefficients.

The weight updating algorithm and diagonal matrix which relates to IPNLMS is same as in (4.4) and (4.5), respectively. However, the estimated gain for IPNLMS, given by [130], is:

$$q_l = \frac{1-\alpha}{2L} + (1+\alpha)\frac{|w_l|}{2|\boldsymbol{W}|}, \quad 0 \le l \le L-1 \tag{4.6}$$

The updated filter coefficients are controlled by a factor of α. Note that when $\alpha = -1$ then the second term in (4.6) becomes zero and thus behaves as a conventional NLMS adaptive filter. The IPNLMS will functions as PNLMS adaptive filter whenαin first term in (4.6) is unity.

Deng and Doroslovacki [131] capable to overcome the slow convergence of PNLMS adaptive filter in their study. An additional μ-law is applied during updating the filter coefficient of PNLMS (micro proportionate normalised least mean square, (MPNLMS)). The MPLNMS adaptive filter provides better performance than the conventional PNLMS adaptive filter. Deng and Doroslovacki [131] stated by lowering the computational burden on PNLMS adaptive filter may reduce the computational complexity which inherent from the PNLMS. The process is increased the convergent speed and a faster outcome could be performed.

The same procedure as in (4.2) and (4.3) are used by MPNLMS in updating the filter coefficient and diagonal matrix, respectively. A μ-law has been added to filter coefficient of the PNLMS adaptive filter with:

$$F(|w_l|) = \frac{\ln(1+v|w_l|)}{\ln(1+v)}, |w_l| \le 1, \quad 0 \le l \le L-1 \tag{4.7}$$

the impulse response of PNLMS in (4.6) is changed to:

$$\gamma_l = max\{\rho * max[\delta_p, F(|w_0|), \dots., F(|w_{L-1}|), F(|w_l|)]\} \tag{4.8}$$

The gain is estimated based on (4.6). The constant 1 used in (4.7) is to avoid negative infinity at the initial stage when $|w_l| = 0$. The denominator $\ln(1+v)$ normalizes the $F(|w_l|)$ to be in the range of 0 to 1. $v = 1/\varepsilon$ with variable ε is a small positive number chosen based on the EMG noise level. The ε is chosen based on the SNR of the signal used. In this study, the NLMS, PNLMS, IPNLMS and MPNLMS are used to denoise the EMG noise from the ECG signal.

4.2.3 Wavelet based Filter in Reducing BW and MA Noise

The third filter to be applied in the novel noise reduction unit is wavelet based filters to be used in reducing the BW and MA noises in ECG signals. This filtering process is represented by Figure 4.3. In this study a combination of two wavelets based filter is used to denoise the BW and MA noises which comprises two stages. Figure 4.3 shows the way of BW and MA noises are reduced, with $x(n)$ is the corrupted ECG signal with BW and MA noises and $y(n)$ the filtered signal.

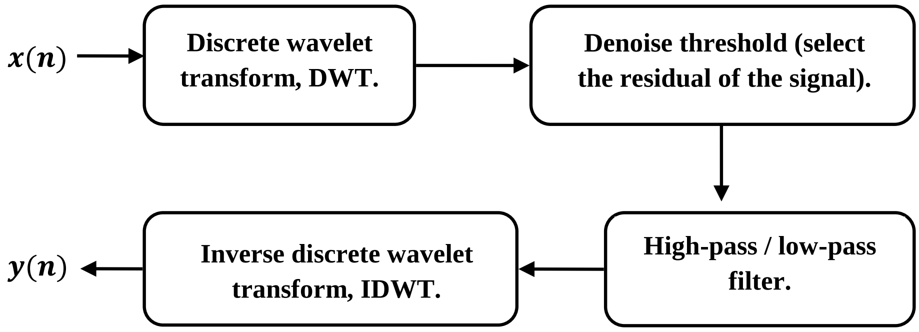

Figure 4.3: Block diagram for the filtering process of BW and MA noises.

The filter is designed to be able to remove both low and high noise frequency from the ECG signal. At the first stage, the wavelet denoising techniques with several threshold methods (sqtwolog, heursure, rigrsure, minimax) as discussed in section 3.4.3 and are employed to remove the high frequency noise. In this stage, the high frequency MA noise signal is reduced from the ECG signal. After the high frequency is removed, the second stage is taken place to reduce low frequency noise signal from BW and MA by using high-pass/low-pass filter. For both stages, the Daubechies type 4 (Db4) has been chosen as the mother wavelet and for the decomposition process, the high/low pass has been made up to level 7. The filtered signal, $y(n)$ is provides after the wavelet transform signal is inversed from the frequency domain to the time domain signal.

4.3 Experimental Results

In this section, the denoising results of the PLI, EMG, BW and MA from the normal ECG signal are presented. The developed filters as discussed in subchapters 4.2.1, 4.2.2 and 4.2.3 have been used in reducing the effects of those noises. In measuring the capability of the filters, three different ECG signal condition taken from MIT-BIH database are used as comparative study with normal (nsrdb 16265) and AF (afdb 04015) ECG signals. The SNR reading of the filtered signal is used to show the filter performance. SNR can be calculate by:

$$SNR_{dB} = 10\ log_{10} \frac{Average\ Power\ of\ ECG\ signal}{Average\ Power\ of\ Noise} \tag{4.9}$$

4.3.1 PLI Elimination

The notch filter for eliminating is setup by using fdatool toolbox. The notching response type is selected and IIR design method with a single notch filter is chose. Frequency sample of the ECG signal is 500 per second and frequency notch is set at 50 Hz by assuming the power supply is 50 Hz. The SNR reading of the signals corrupted by PLI noise is measured and compared to the signals which been filtered by the bandstop notch filter. The results, tabulated in Table 4.1, show the performance of the bandstop notch filter in order to eliminate the PLI noise in the ECG signal. Each signal has been added with 50 Hz (assuming the power line is 50 Hz) of PLI and the notch filter has been designed to remove the noise.

Table 4.1: PLI removal from normal and AF signal.

	SNR Reading, (dB)	
	Normal	**AF**
Corrupted Signal	5.15	6.91
After Filtering	12.16	15.06

The results tabulated in Table 4.1 shows significant improvements between the corrupted and filtered signal for the normal and AF signals. The bandstop notch filter is capable to reject the 50 Hz of PLI noise. The signals itself have a range of frequency however, the 50 Hz of PLI noise made the eliminating process easily be done and resulting some significant results.

Figures 4.4 and 4.5 show the signal performance before and after the filtering process for each condition. Better signals have been obtained after the signals were filtered by a notch filter. The comparison between the corrupted signals and the filtered signals by the notch filter is shown in the figures. Figures 4.4 and 4.5 show the performance of the notch filter; (a) corrupted signal and (b) signal after PLI removal. The 50 Hz of PLI contaminating in the signals can readily be removed by a notch filter. Since the PLI is known in advance, the notch filter is designed based on the specification of the PLI noise. From the results, it shows that the notch filter is capable to reduce the PLI effect from normal and AF signals. A notch at 50 Hz is designed since the PLI is fix at 50 Hz frequency. Most of the PLI effects are removed by the filter since the frequency of ECG signal (normal and AF) and PLI frequency totally different and not overlapped. Normal ECG signal always doing 80 beats per minute which are 1.2 Hz while AF which is tachycardia condition at rest are 120 beats per minute, which are around 2 Hz. The main idea in designing the notch filter at 50 Hz is to cut-off the 50 Hz signal and release the rest signal behind as the filtered signal.

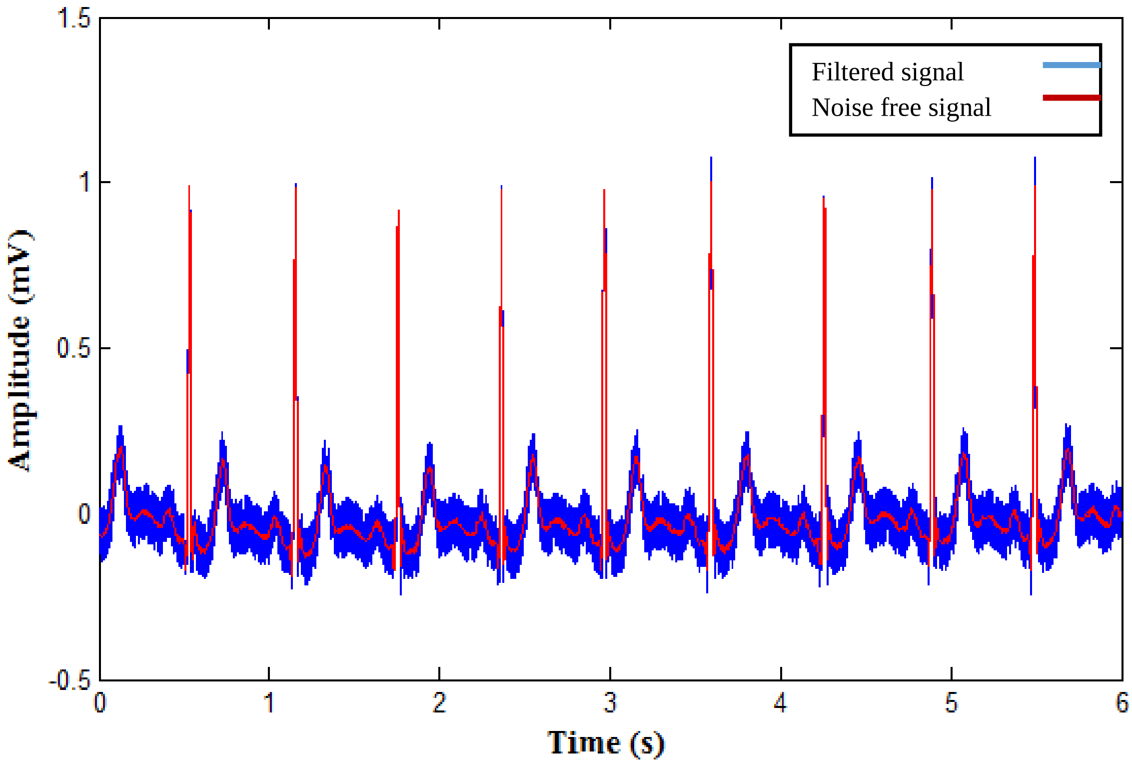

Figure 4.4(a): Normal signal with PLI noise.

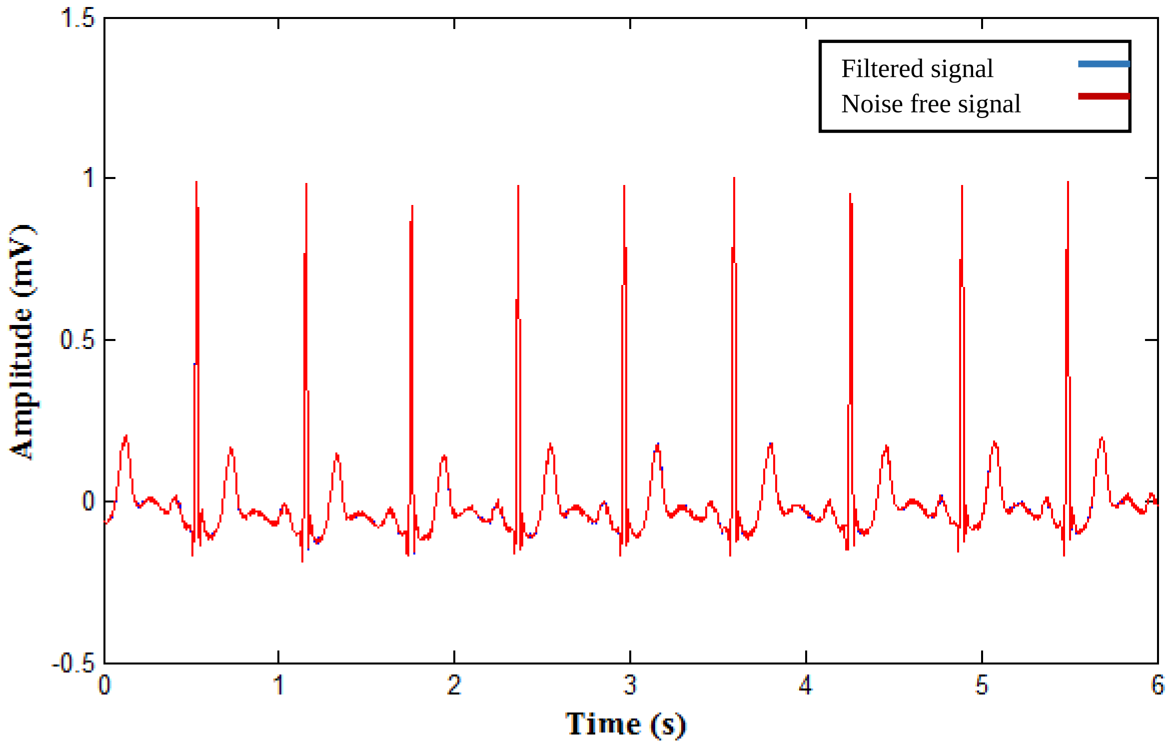

Figure 4.4(b): Result after PLI noise removal from normal signal.

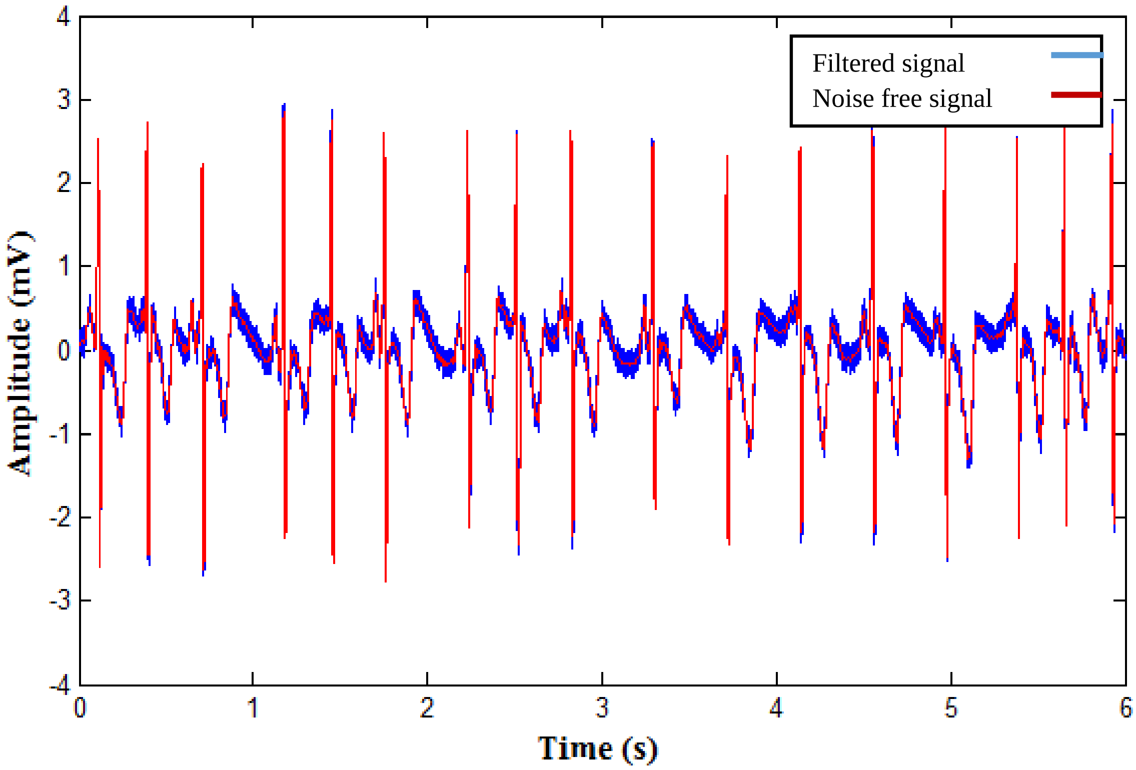

Figure 4.5(a): AF signal with PLI noise.

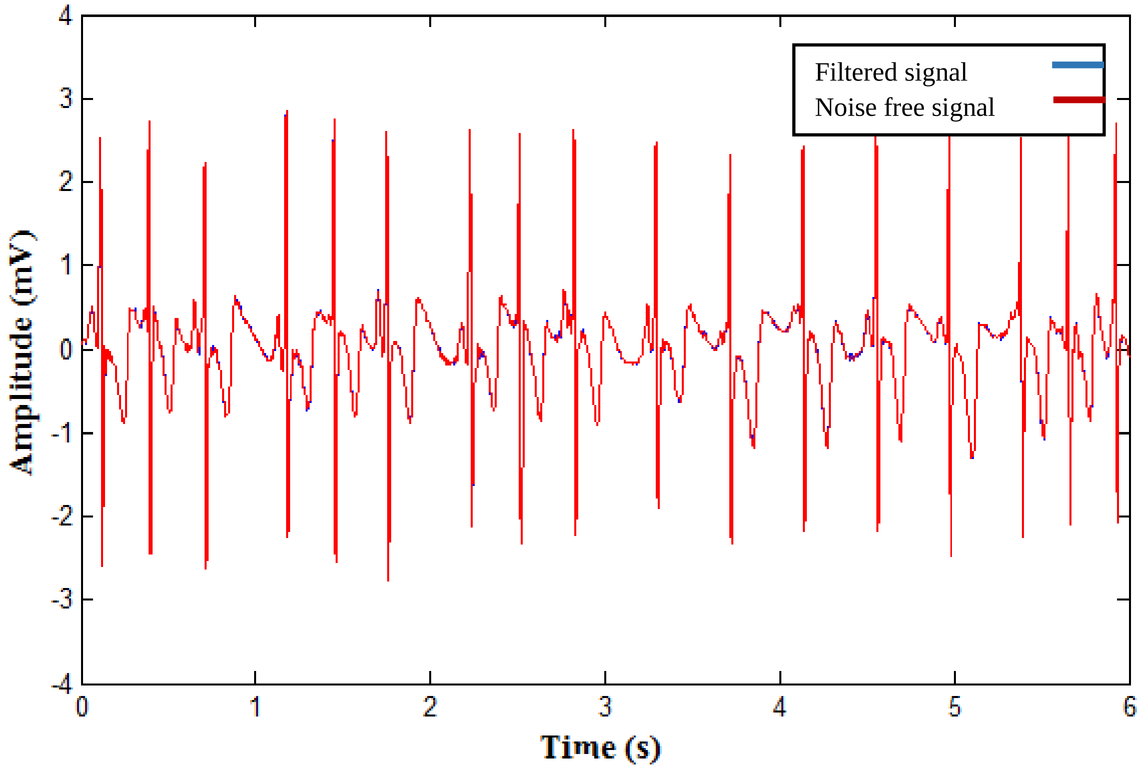

Figure 4.5(b): Result after PLI noise removal from AF signal.

4.3.2 EMG Removal

Several LMS based adaptive filters were used to filter on subjects with normal, AF and LVE signals. The approach involved the denoising of EMG noise using the NLMS, PNLMS, IPNLMS and MPNLMS adaptive filters as described in section 4.2.2. In this study, the fixed step size, $\mu = 0.01$ is used with initial 100 taps are selected of each adaptive filter (NLMS, PNLMS, IPNLMS and MPNLMS) in order to find the simplest filter structure which capable to obtain the smallest MSE results. Figure 4.7 and 4.8 shows the adaptive filters performance for each signal. For normal signal, the most complex structure is given by NMLS adaptive filter with 23 taps while AF signal only need 8 taps to comply as the simplest structure with MPNLMS give the largest calculation complexity. Figure 4.6 and 4.7 shows the adaptive filter (NLMS, PNLMS, IPNLMS and MPNLMS) performance for each signal. In order to optimum the performance of the adaptive filter (NLMS, PNLMS, IPNLMS and MPNLMS), its designed with 23 taps for normal signal and 8 taps for AF signal, respectively.

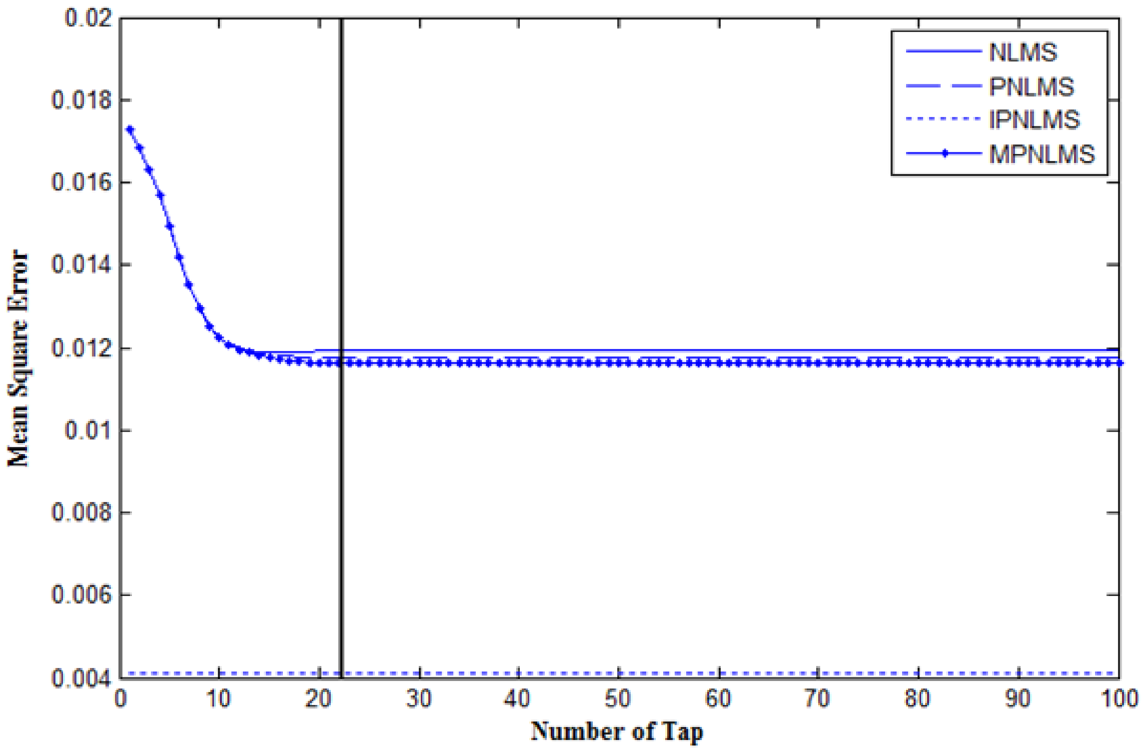

Figure 4.6: The MSE performances for normal signal.

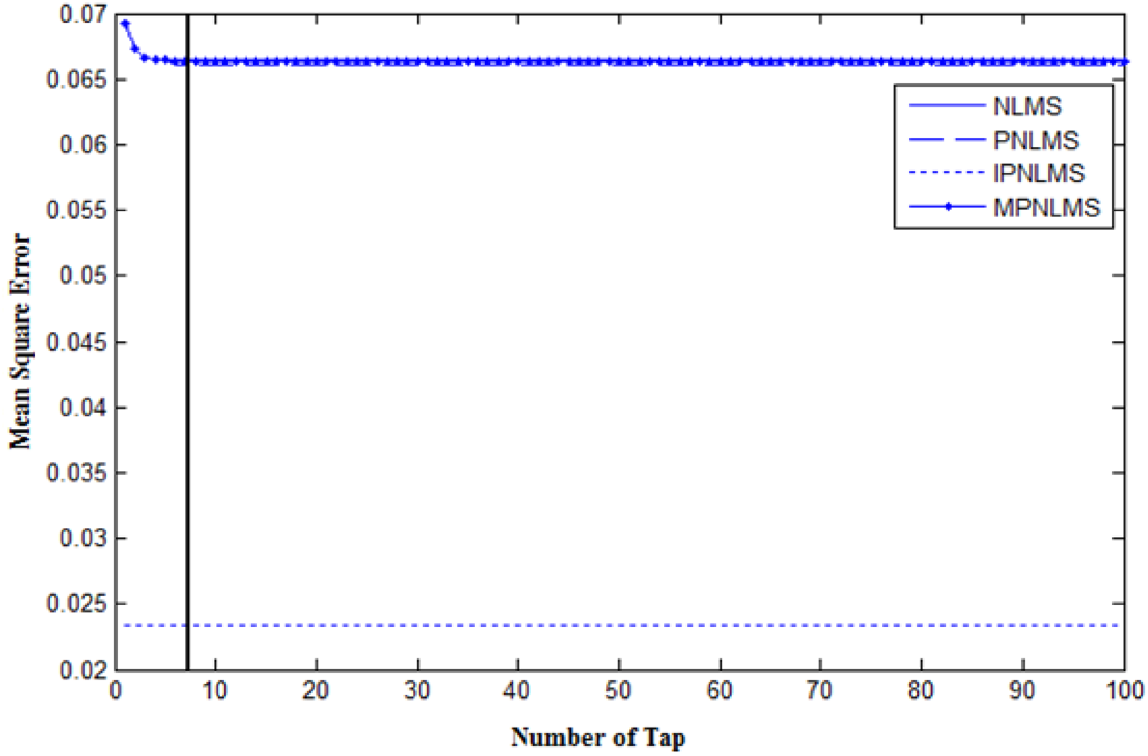

Figure 4.7: The MSE performances for AF signal.

Each adaptive filter (NLMS, PNLMS, IPNMLS and MPNLMS) have their own advantages and disadvantages. For NLMS adaptive filter, the filter capable to converge faster than other adaptive filters but the MSE is larger than other filters. Table 4.2 shows the EMG noise elimination performance of each filter. The best overall performance in reducing EMG noise was obtained by using the IPNLMS algorithm as the adaptive filter.

Table 4.2: EMG removal from normal and AF signal.

	SNR Reading, (dB)	
	Normal	**AF**
Corrupted Signal	12.95	7.47
Filtering Technique	**Normal**	**AF**
IPNLMS	**15.04**	**9.86**
PNLMS	14.87	9.12
MPNLMS	13.67	9.11
NLMS	13.67	8.63

Table 4.2 shows that all denoising techniques (NLMS, PNLMS, IPNLMS and MPNLMS) yield better results compared to the corrupted signals. Hence, IPNLMS produced good results compared to others filter in reducing EMG noise from those normal and AF signals. The PNLMS adaptive filter also provided better results than MPNLMS but no better than the IPNLMS adaptive filter. The NLMS adaptive filter is also able to reduce the effect of EMG noise but modified versions of the NLMS adaptive filters (PNLMS, IPNLMS and MPNLMS) are able to process the signal in a better way. In Figures 4.8 and 4.9 the outputs of the NLMS, PNLMS, IPNLMS and MPNLMS adaptive filters are compared for signals from normal and AF signal against the corresponding noise free signals in each case. All (a) figure shows the filtering result by using NLMS, (b) shows the filtering results by using PNLMS, (c) shows the filtering results by using IPNLMS and (d) shows the filtering results by using MPNLMS adaptive filters.

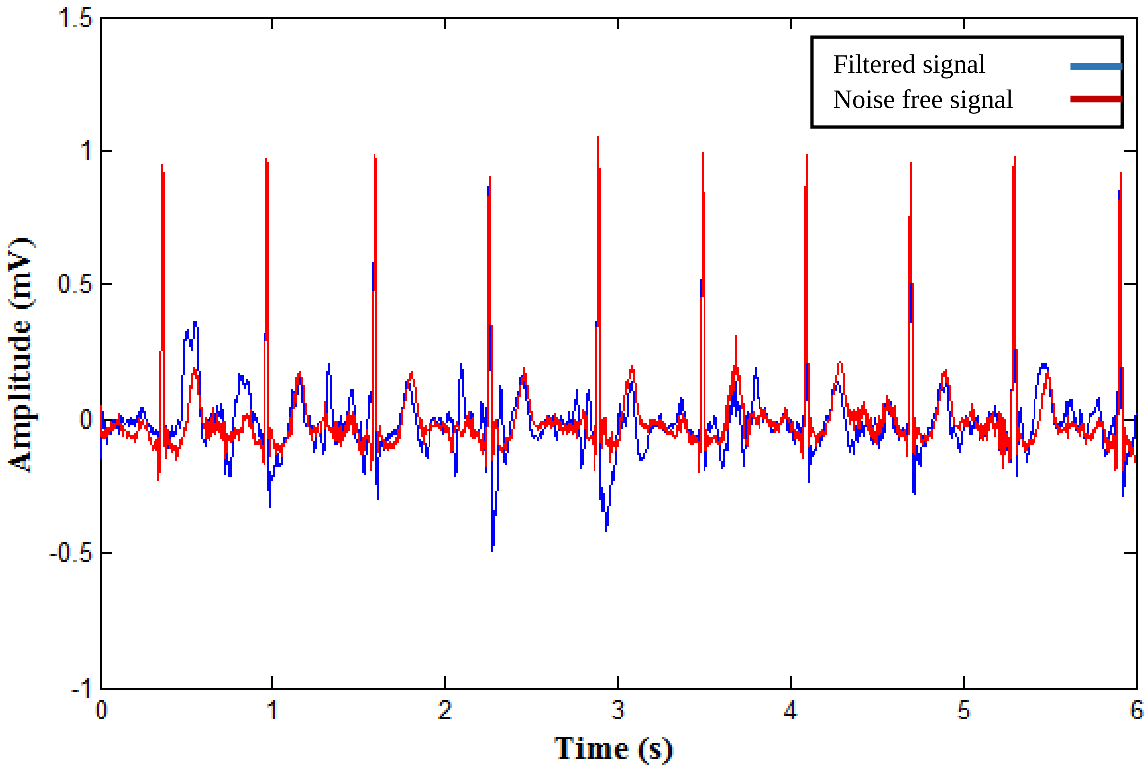

Figure 4.8(a): Result of EMG noise removal from normal signal filtered by NLMS.

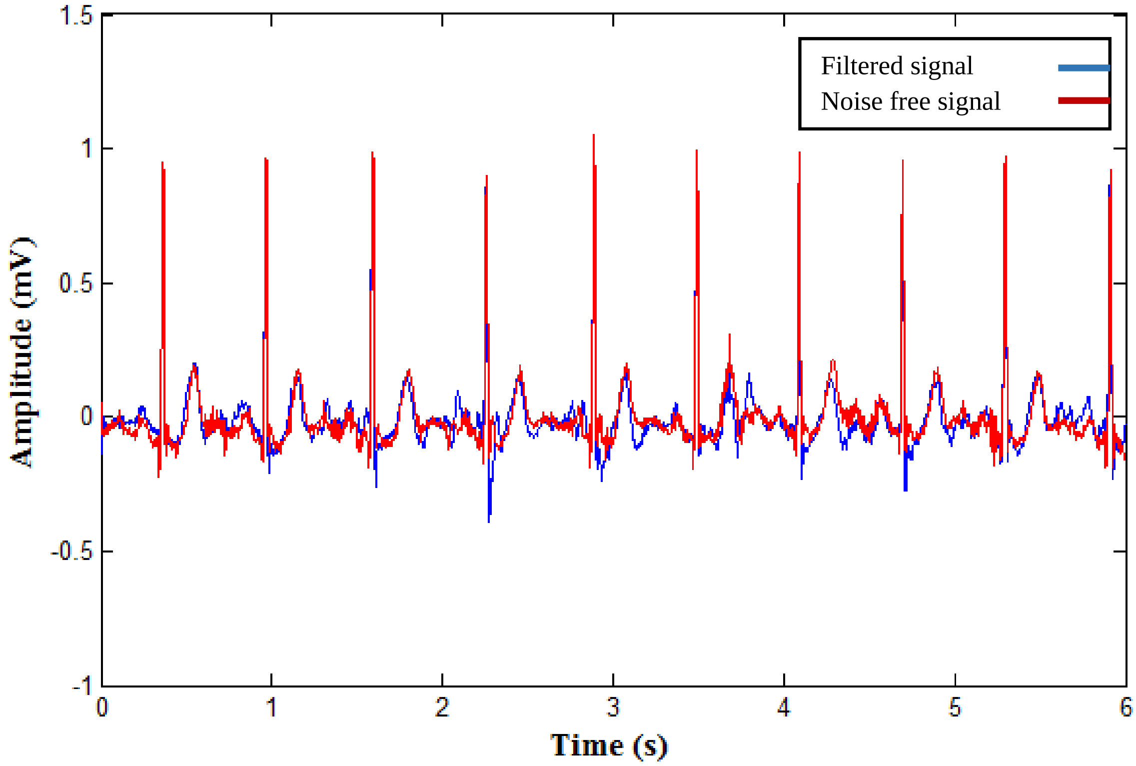

Figure 4.8(b): Result of EMG noise removal from normal signal filtered by PNLMS.

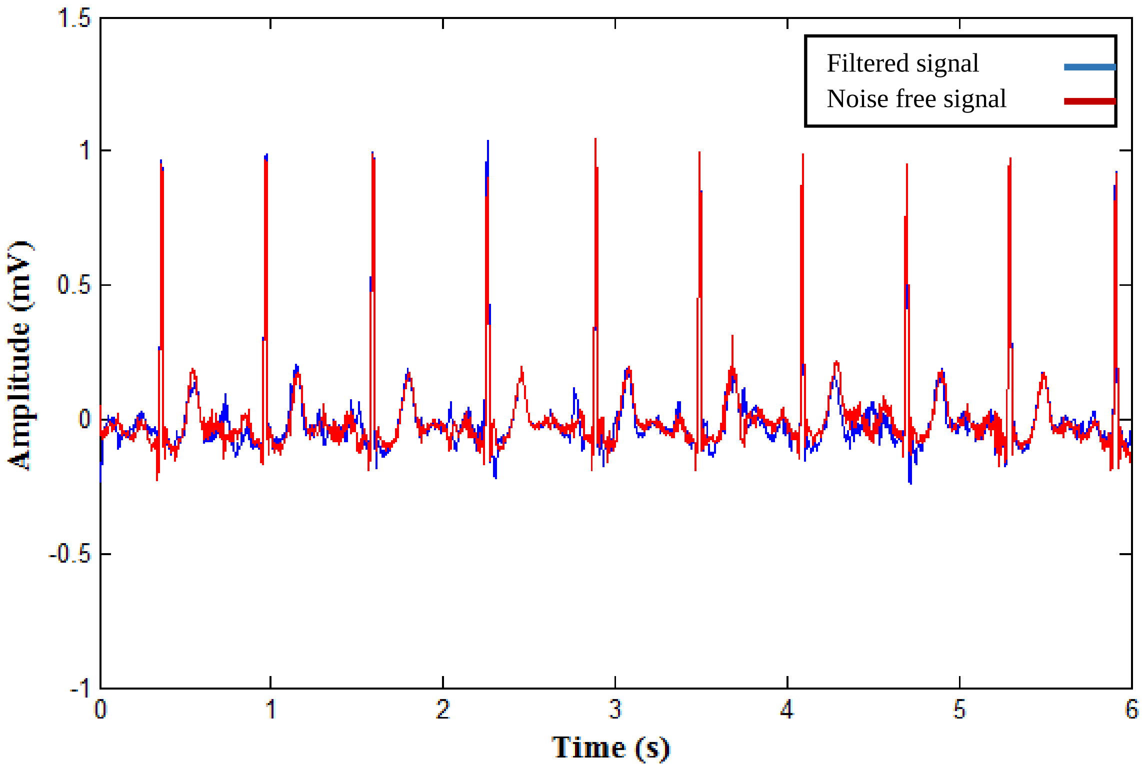

Figure 4.8(c): Result of EMG noise removal from normal signal filtered by IPNLMS.

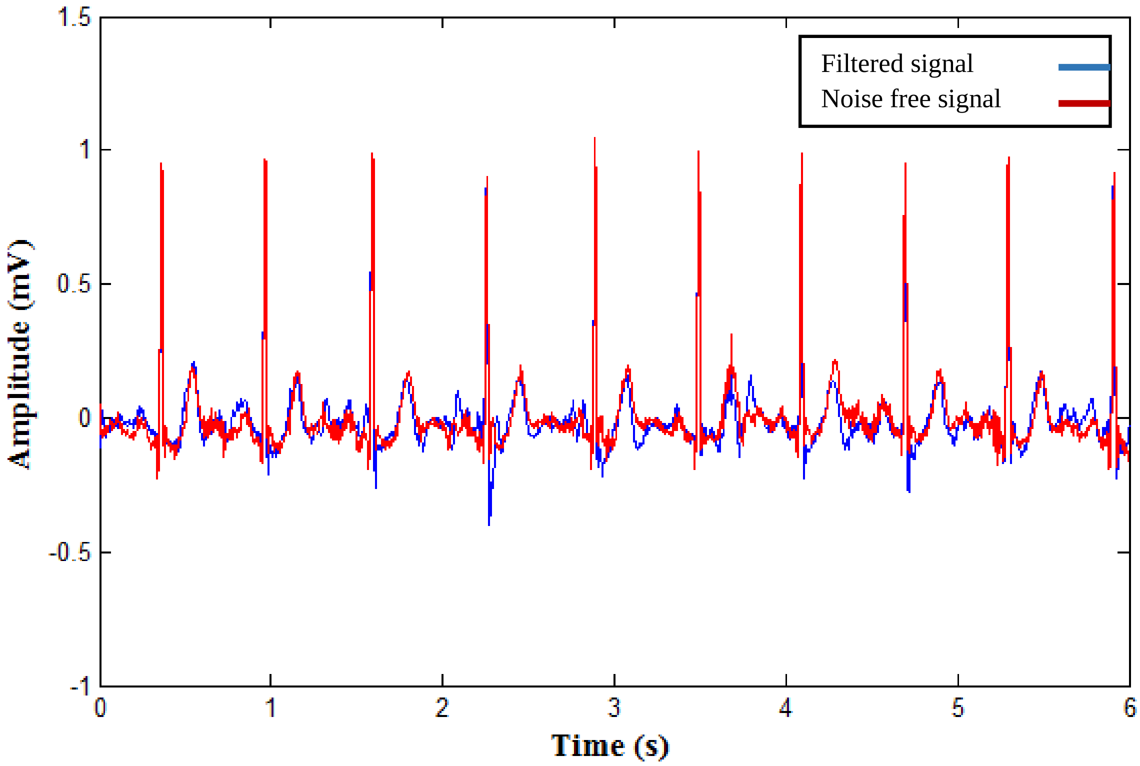

Figure 4.8(d): Result of EMG noise removal from normal signal filtered by MPNLMS.

Figure 4.8 shows the results for the noise removal process from subjects with normal ECG signals. The ability of the four different adaptive filters to reduce the effects of the EMG noise has been tested. Table 4.2 shows that the IPNLMS adaptive filter is the best overall filter. From the results, it shows that the all adaptive filters (NLMS, PNLMS, IPNLMS and MPNLMS) capable to provide better results than corrupted signal. The signals are recorded by two different accelerator which perceiving ECG signal with EMG noise at an accelerator and EMG noise alone at another accelerator. The normal signal have the same pattern of complex. The distance between R to R peaks almost regular. The characteristic of the complex ECG itself make the adaption of the adaptive filter becomes easier and capable to provide better filtering results. The result shows IPNMLS shows the best results among other since the pattern of the ECG complex itself may results the IPNLMS adaptation process doing better than others filter.

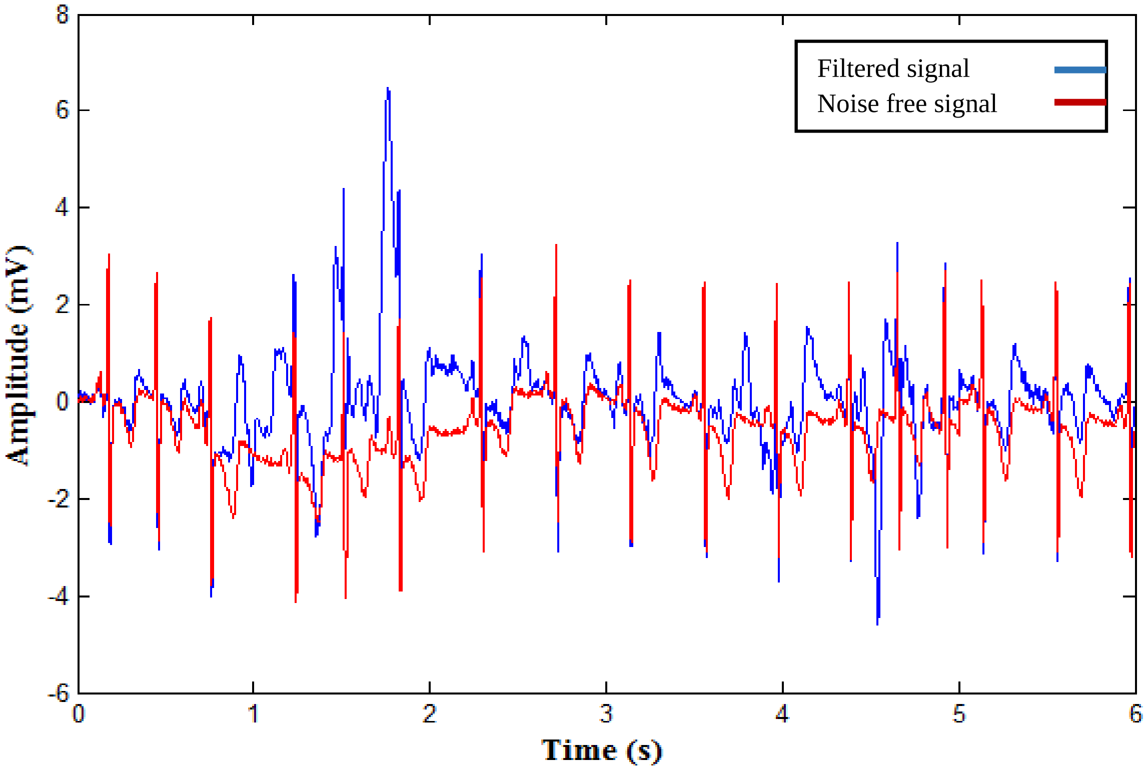

Figure 4.9(a): Result of EMG noise removal from AF signal filtered by NLMS.

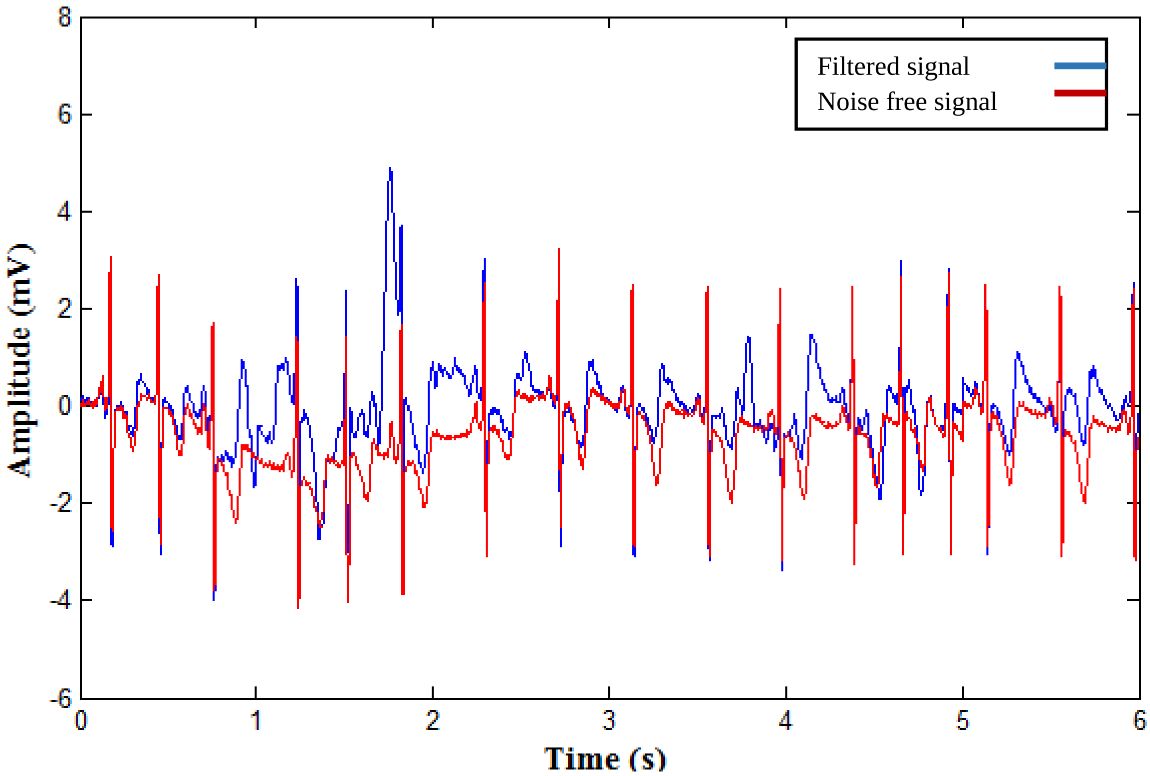

Figure 4.9(b): Result of EMG noise removal from AF signal filtered by PNLMS.

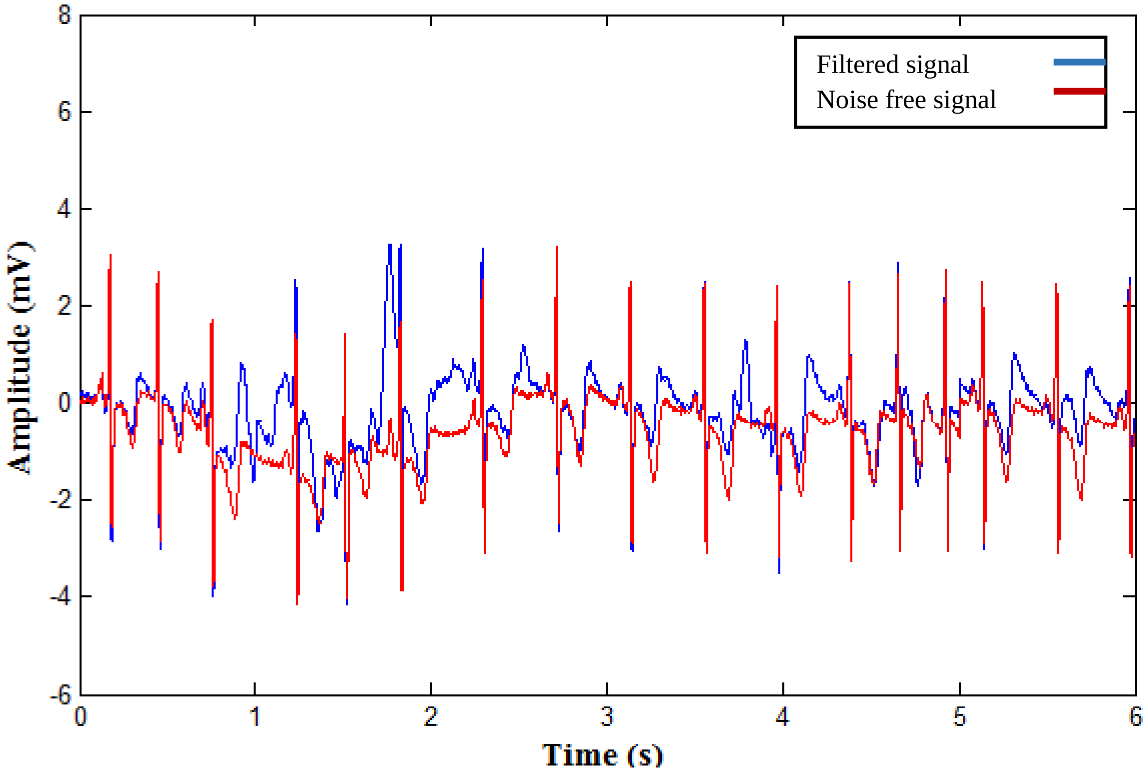

Figure 4.9(c): Result of EMG noise removal from AF signal filtered by IPNLMS.

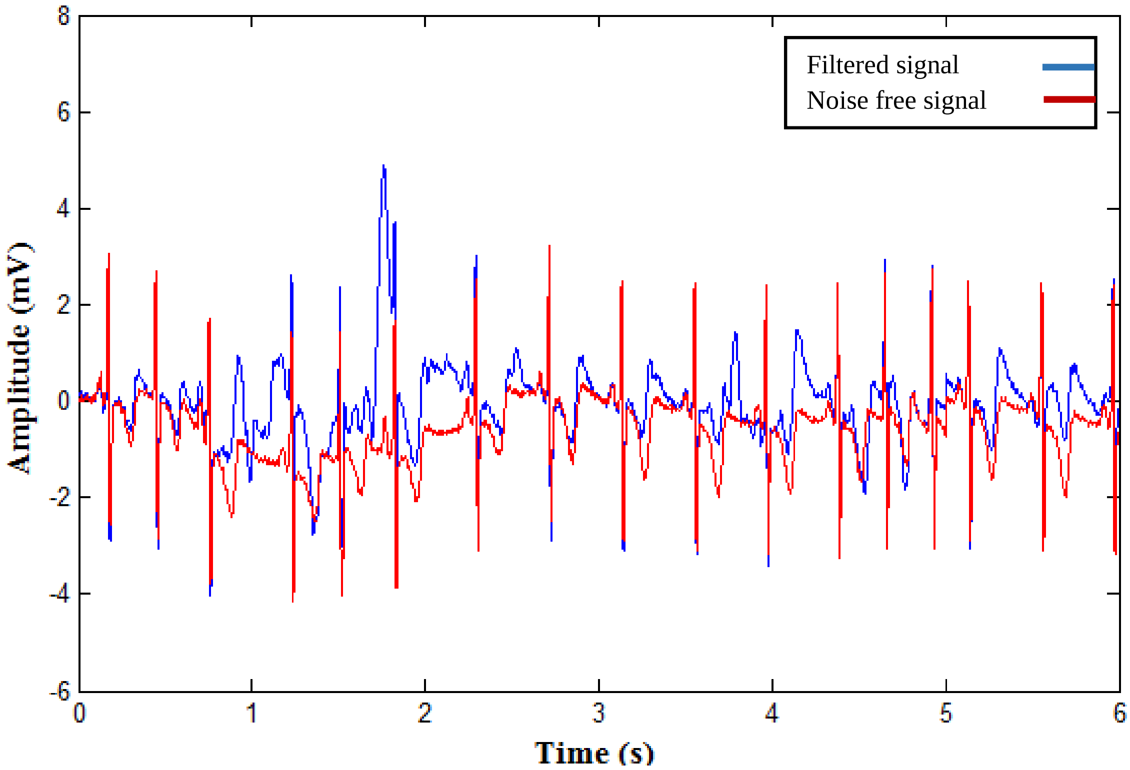

Figure 4.9(d): Result of EMG noise removal from AF signal filtered by MPNLMS.

Figure 4.9 shows the results for the EMG noise removal from subjects with AF signal. Once again the ability of the four different adaptive filters to reduce the effects of the EMG noise has been tested. Based on Table 4.2 again, the IPNLMS is doing better filtering process than other adaptive filters (NLMS, PNLMS, IPNLMS and MPNLMS). The same recorded process were done by recording ECG (AF) signal and EMG signal at an accelerator and EMG signal alone at another accelerator. Compare with normal signal, the AF signal do not have equal pattern of ECG complex and the R to R peaks are irregular. The characteristic of the AF signal make the adaptive process of adaptive filters more difficult than normal signal. The result shows that IPNMLS again gives the better results than others adaptive filters.

Based on Figure 4.8 and 4.9 it can be seen that the addition of proportional gain (PNLMS) is insufficient to obtain the optimum results. The merger of PNLMS and NLMS, producing IPNLMS is capable of improving the filter performance. This combination is necessary to overcome the scattered response signal faced by PNLMS. Other improvement has been made in improving the PNLMS performance by adding the μ-law during weight updating process, producing the MPNLMS. However, the MPNLMS is no better than IPNLMS to tackle the scatter current impulse response problem. The IPNLMS adaptive filter which provides the best results, it is used to be compared with other techniques.

Table 4.3: The comparative study on denoising the EMG noise from ECG signals.

	SNR Reading, (dB)	
	Normal	**AF**
Corrupted Signal	12.95	7.01
Filtering Technique	**Normal**	**AF**
IPNLMS	**15.04**	**9.86**
DWT	9.37	13.25
EMD	8.19	12.95
NSRLMS	11.14	7.97
CSLMS	13.86	9.75

The results given by the DWT and EMD approaches are shown in Table 4.3. Compared with adaptive filters technique, DWT and EMD approaches do not need any pattern/model as the reference. The EMG noise is an uncorrelated noise, it can be recorded and removed moved since the frequency and spectrum of the EMG itself is not overlapped with the ECG signal. The results tabulated in Table 4.3 indicate that the DWT and EMD are only slightly superior to the IPNLMS on AF subjects but the IPNLMS provide significantly superior results for normal signal. The results shows that IPNLMS adaptive filter have the advantage and their disadvantage. The IPNLMS capable to provided better results for same and regular pattern of ECG but DWT and EMD provides better performance for irregular pattern. Notes that the results given by the NSRLMS and CSLMS adaptive filters are also included. No better than IPNLMS, the adaptation process done by IPNLMS filter shows better results than NSRLMS and CSLMS. The IPNLMS capable to adapt the EMG noise and results more EMG noises contaminating in the ECG signal might be reduce.

4.3.3 BW and MA Denoising

The denoising process uses the wavelet based denoise threshold methods (Sqtwolog, Rigrsure, Heursure and Minimax) as discussed in section 3.4.3 and high-pass/low-pass filter. Since the MA noise occurring in the ECG signal was unpredictable, the combination of denoise threshold at first stage and followed by the high-pass/low-pass filter is used to cancel both high and low frequency noise which including the MA and BW noises. The results of all methods used are shown in Tables 4.4 for normal and AF signals. From Table 4.4, on average, both sets of signals show the best results when using the STHL technique compared to the other methods. The results show that the combination of wavelet based denoising threshold techniques with the high-pass/low-pass filters yields a better outcome compared to filtering by using threshold methods alone. Based on Table 4.4, the denoising techniques (ST, RT, HT and MT) also yield better results compared to the corrupted signals. However, better results are obtained by filtering the outcomes of ST, RT, HT and MT using high-pass/low-pass filter. The results show good improvement compared to the corrupted signals and the results using just the denoise threshold.

Table 4.4: BW and MA removal from normal and AF signals.

Technique	SNR Reading, (dB)	
	Normal	**AF**
Corrupted Signal	5.12	0.25
Filtering Technique	**Normal**	**AF**
Sqtwolog Threshold & High/Low Pass (STHL)	**18.75**	**10.22**
Rigrsure Threshold & High/Low Pass (RTHL)	17.57	8.93
HeursureThreshold & High/Low Pass (HTHL)	17.56	8.93
Minimax Threshold & High/Low Pass (MTHL)	16.98	9.64
Sqtwolog Threshold (ST)	8.12	1.17
Rigrsure Threshold (RT)	7.85	0.51
HeursureThreshold (HT)	7.83	0.52
Minimax Threshold (MT)	6.98	0.91

The denoising techniques alone unable to obtain good performance since it is cannot remove the low frequency noise (from BW and MA) from the ECG signals. In order to overcome this problem, the proposed approach, serial combination of denoise threshold and high-pass/low-pass filter have been used since it attempts to remove both low and high frequency noise. The MA noise is an unpredictable signal so it is difficult to provide a pattern or model of the noise. In order to filter the noise, wavelet based denoise technique among the best technique to do the filtration of ECG signal with Daubechies as the mother wavelet since it is mimic to the ECG complex. Figures 4.10 and 4.11 show the results filtering process of the ST and STHL proposed technique in removing both high and low frequency noises, respectively as the technique capable to obtain better performance than others.

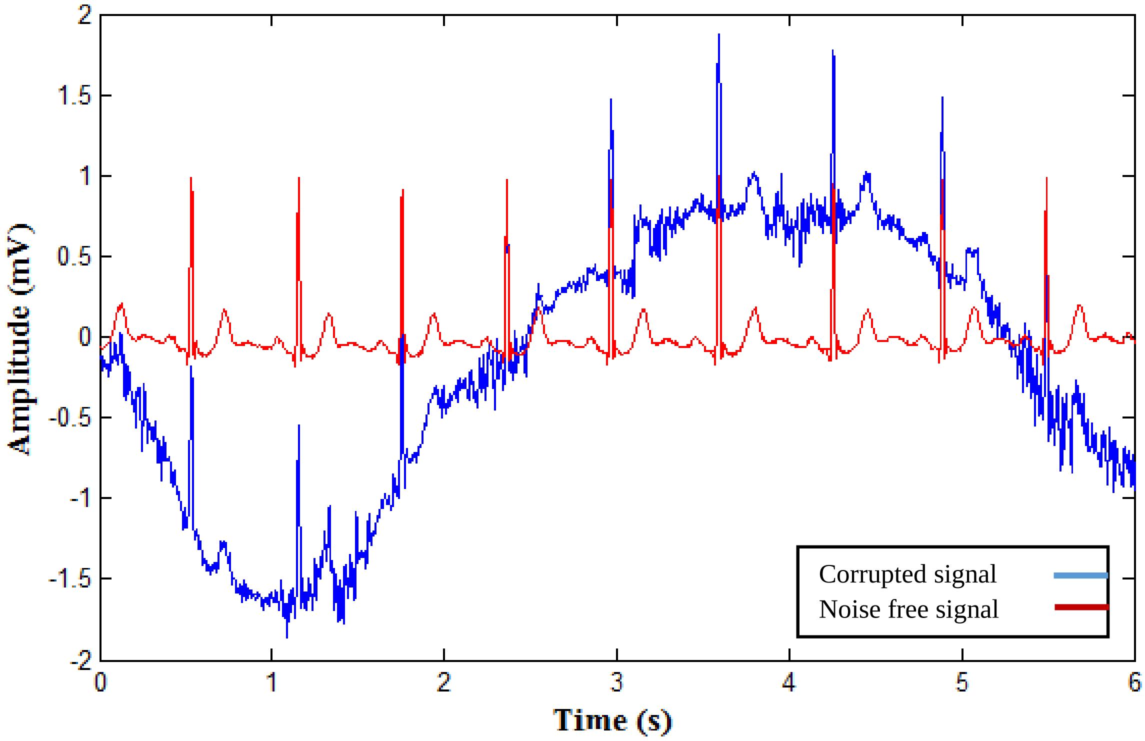

Figure 4.10(a): Normal signal with BW and MA noises.

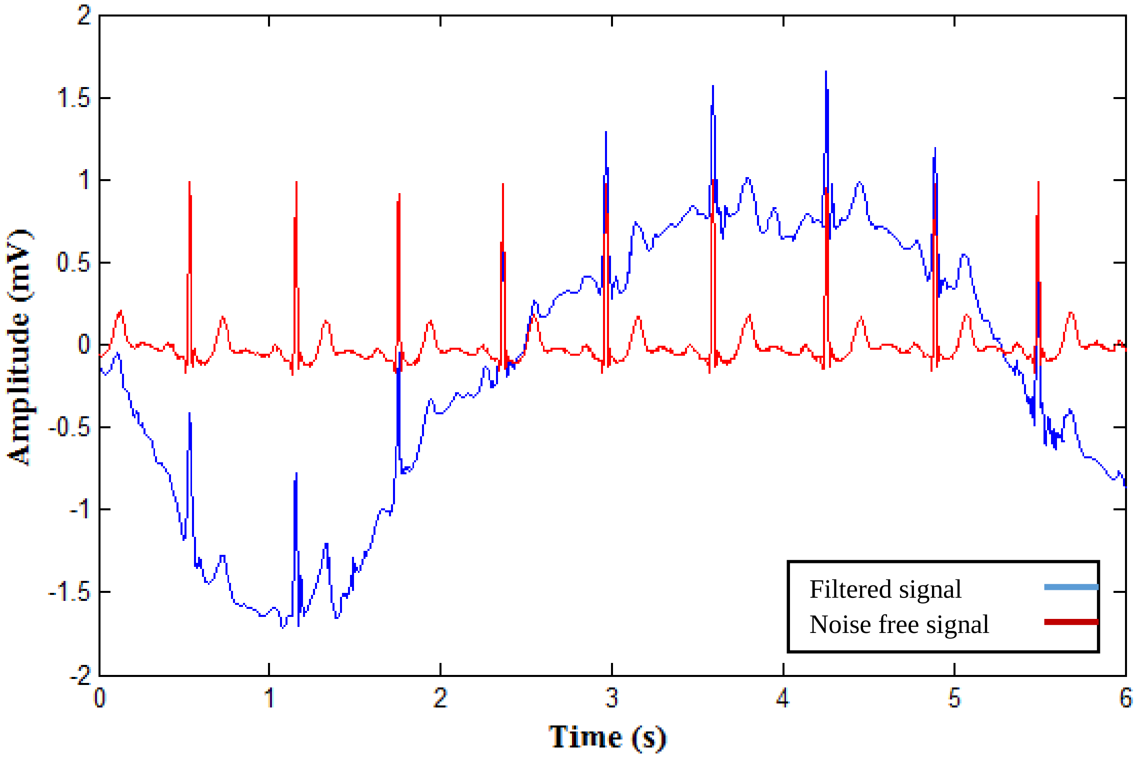

Figure 4.10(b): Result of MA noise removal from normal signal after ST is applied.

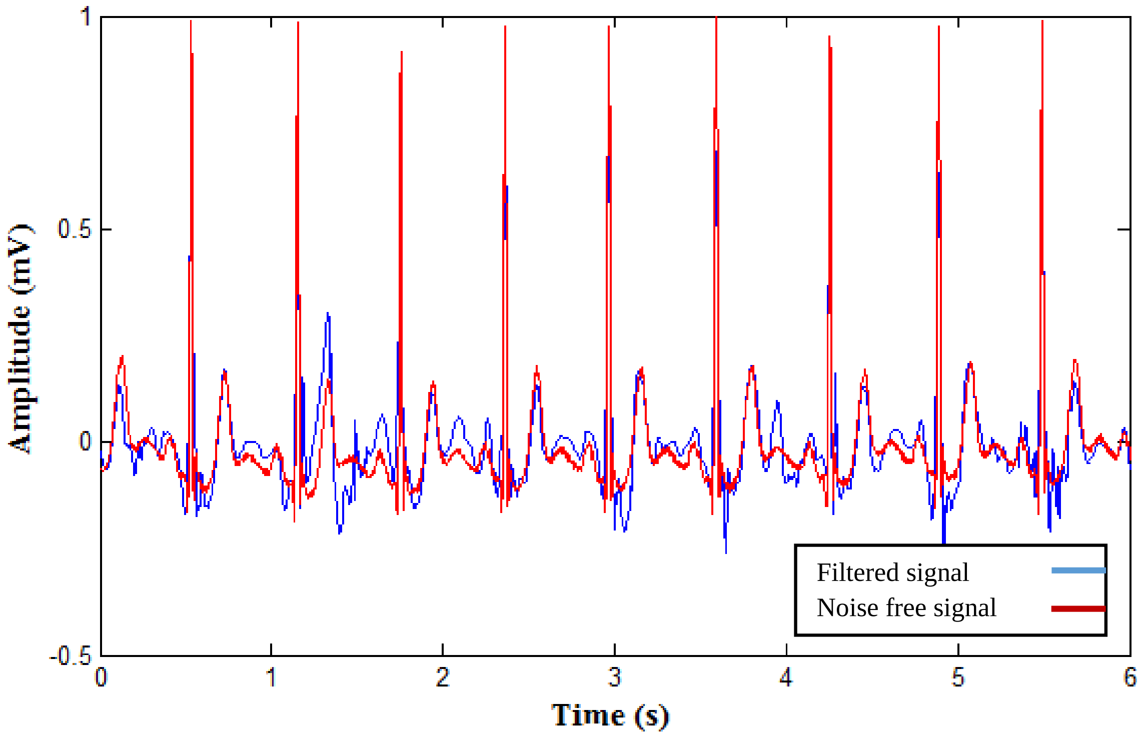

Figure 4.10(c): Result of MA and BW noises removal from normal signal after STHL is used.

Figure 4.10 shows the comparison between the noise removal techniques and its performance. Figure 4.10(a) shows the signal containing low and high frequency noise. The ST denoising technique is applied to the signal and it has significantly removed the high frequency noise, leaving the low frequency noise and original ECG signal as shown in Figure 4.10(b). Figure 4.10(c) shows the result of STHL denoising technique in removing both low and high frequency noise, leaving the ECG signal behind. However, the ECG signal is not totally clean because there is still some noise in the signal with most of the important information of the signal yet to be processed. The BW noise is a low frequency signal while MA is an unpredictable noise which contained both low and high frequency signal. The signal becomes worse since the spectrum and frequency of the noise is overlapped with ECG signal. Figure 4.10(b) and 4.10(c) shows the filtering processes to reduce the effect of BW and MA noises in ECG signal. However, Figure 4.10(c) shows the ECG signal still contaminated with noises, whilst to avoid information from ECG signal is removed along with noise signal.

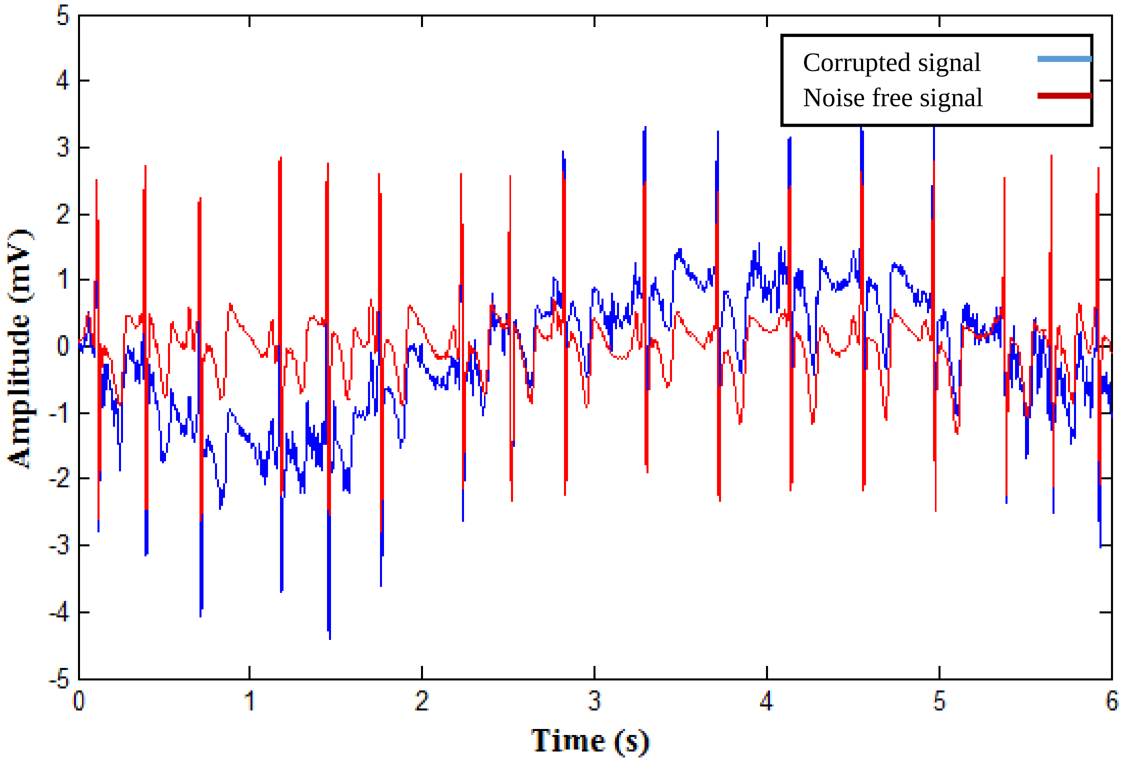

Figure 4.11(a): AF signal with BW and MA noises.

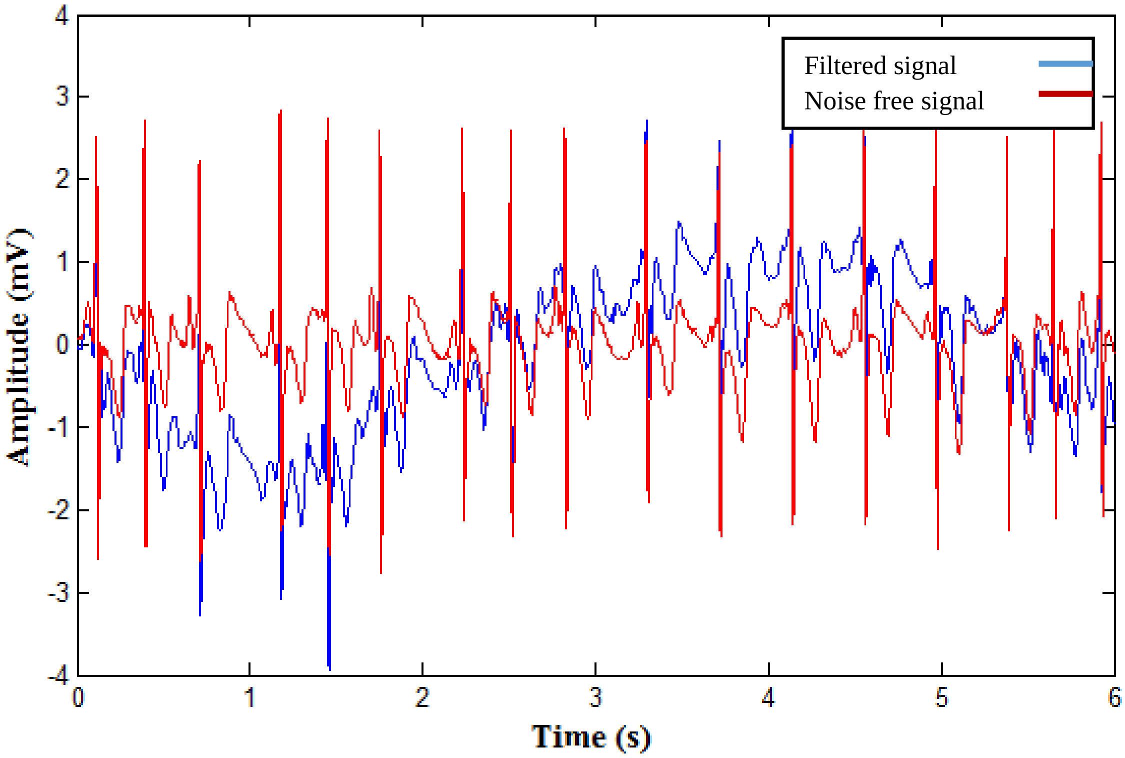

Figure 4.11(b): Result of MA noise removal from AF signal after ST is applied.

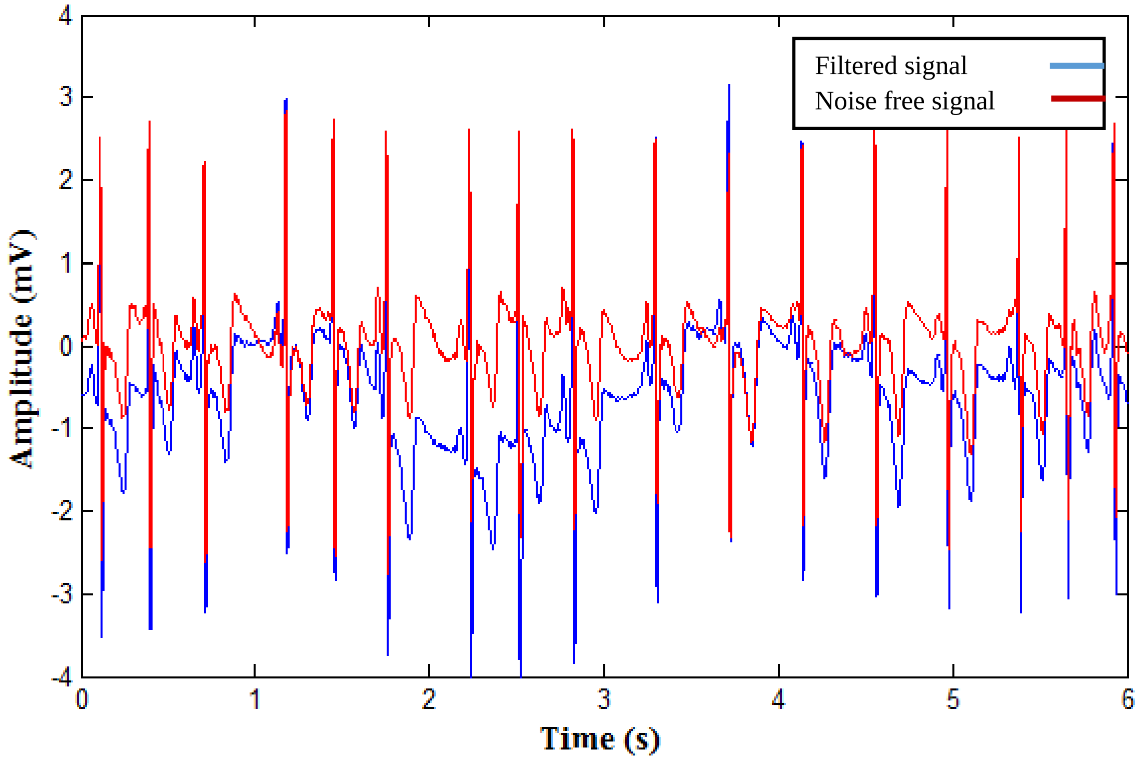

Figure 4.11(c): Result of MA and BW noises removal from AF signal after STHL is used.

A similar experiment to that shown in Figure 4.10 was repeated with different ECG signals as shown in Figures 4.11 for subject with AF. The corruption by BW and MA made the ECG signal become as shows in Figure 4.11(a). Figure 4.11(b) shows the result after ST denoise threshold takes place and remove the high frequency noise from the ECG signal. By using the STHL denoise approach, both the high and low frequency signal are ridded off form the ECG signal as shows in Figure 4.11(c). Most of the important information is still present although some noise still corrupts the signal since the spectrum of the noise overlapped with the ECG signal. Again, both low frequency and high frequency noise from BW and MA signals. Figure 4.11(b) shows the high frequency noise has been rid-off from the ECG signal. Figure 4.11(c) shows the filtered ECG signal but still contaminated with noises, in order to maintain the original signal. However, most of important information could be collected from the signal such as the duration and the amplitude of the P, QRS and T peaks.

Table 4.5: The comparative study on denoising the BW and MA noises from ECG signals.

	SNR Reading, (dB)	
	Normal	**AF**
Corrupted Signal	6.58	2.73
Filtering Technique	**Normal**	**AF**
STHL	**12.75**	**8.29**
EMD	10.83	6.51
DWT	9.86	7.54
NSRLMS	10.85	7.71
CSLMS	9.98	7.91

Table 4.5 tabulated the comparative study between STHL denoising technique and other techniques such as EMD, DWT and adaptive filters (NSRLMS and CSLMS). The STHL denoise technique which provides the best filtering results among other wavelet denosing technique is used to be compared with other techniques. From Table 4.5, it shows the STHL is superior to overcome three others approach in denoising the signals. The EMD technique capable to provide better result but no better than STHL technique. The DWT technique is good to reduce the low frequency effect but unable to reduce the high frequency noise effect effectively from ECG signal. For both NSRLMS and CSLMS adaptive filters, the performance are based on the effective noises are recorded since the unpredictable movement of human body may result the recording of the noises are not doing well. The performance of NSRLMS and CSLMS are measured on how far the adaptive filters could adapted with the noises. Table 4.5 shows the adaptive filters no better than STHL technique, and also no better than DWT and EMD technique. In overall, all techniques capable to denoise the corrupted signals in with better SNR results compared to the corrupted signal. The removal technique performed by adaptive filters easily could reduce the noise effects since it is concentrates on time domain with respects to the accuracy of the accelerometer. The STHL, DWT and EMD performed the denoising process in the transform domain. Denoising process by using frequency domain is more preferable in denoising the MA and BW noise since directly denoise rather than need to identify the reference of adaptive filter at the first place before doing the filtration.

4.4 Discussion

In the ECG noise reduction unit, the bandstop notch filter has been designed in order to eliminate the PLI. Some previous study stated that the notch filter is widely used and capable to perform significant result in PLI elimination. The bandstop notch filter is designed by notching at 50 Hz, which remove the signal with 50 Hz from the ECG signal. The filter will be block the 50 Hz signal while release the rest of the signal behind. The LMS based adaptive filters are used and shown to be capable of producing superior results in removing EMG noise from the ECG signal. The NLMS, PNLMS, IPNLMS and MPNLSM adaptive filters are used in the ECG filtering process. The outputs show the capability of the proposed method to reduce the effect of EMG noise and leave behind the important information from the original signal. From the result, the IPNLMS adaptive filter gives the best performance than other adaptive filter and in some comparative study, the IPNLMS adaptive filter capable to overcome others filter used. The outputs show the capability of the proposed method to reduce the effect of EMG noise and leave behind the important information from the original signal. The modified adaptive filters (PNLMS, IPNLMS and MPNLMS) which are used extensively in the communication fields were shown to be capable of mitigating the effects of ECG signals that are contaminated with EMG noise.

The noise reduction unit also consist with combination of wavelet denoise threshold and wavelet high-pass/low-pass filter (STHL, RTHL, HTHL and MTHL) which are capable to produce better results compared to wavelet denoising threshold methods applied on their own (ST, RT, HT and MT). The experimental results also show the capability of the proposed method to denoise both the low frequency and high frequency noise leaving behind the important information of the original signal. In the study, the STHL technique has been identified to be able to produce best performance than other filter. A comparative study have been done to inspect the STHL filter performance. By comparing with other selected filters, the STHL filter has outperformed other filter and gives significant results.

4.5 Conclusion

This chapter presented a novel ECG noise reduction unit in denosing the contaminating noises in ECG signal. In this study, four types of noises; the BW, PLI, EMG and MA noises in the ECG signal have been identified and numbers of filter are used and designed in order to remove those noises. In the novel ECG noise reduction unit, the bandstop notch filter has been designed to eliminate the PLI. The IPNLMS adaptive filter has been selected to remove the EMG noise and wavelet based STHL technique has been identified to be able to reduce the effect of BW and MA. In the noise reduction unit, all filtering process is done individually and no the interconnection between each filter. However, the process is linked together and discusses in Chapter 6, which is the development of a new approach of the ECG analysis system. In the next chapter, a novel pattern recognition unit is developed which consist of feature extraction process and classification process. A novel feature extraction has been introduced in providing more significant feature and a development of a novel classification network proven to obtain high accuracy performances.

Chapter 5

Novel Pattern Recognition Unit

5.1 Introduction

In the previous chapter, the noise reduction unit has been used in reducing the contaminating noise in the ECG signal. Techniques used were shown to provide significant improvement. In this chapter, the feature extraction and classification processes are been formed as pattern recognition unit in recognising the best feature, and use it as the indicator to perform the classification process. In this study, a novel RPD is used to obtain the feature extraction of the normal (Normal Sinus Rhythm, number: 16272, 16483, 16539, 16786, 17453 and 18177) and AF (Atrial Fibrillation, number: 04048, 04746, 04908, 04936, 05091, 06453, 06995, 07162, 07879 and 07910) ECG signal which taken from MIT-BIH database. In this study, ECG signals from 16 subjects The RPD is a new approach in extracting the amplitude of the signal. Instead the used of the RRI as the morphology is isolating the signal to beat by beat, the PTI has been introduced. The use of PTI morphology enables to compensate the lack of RRI in processing the signal from moving subject. Moreover, the results given by PTI could be used to double check the RRI performance.

The classification process is taking place after the significant feature is extracted to be the input vector. In this thesis, HMLP network is used as the classifier for measuring the suitability of the RRI's and PTI's extracted features to be used as the input vector. In performing the classification, improvement on HMLP network in subchapter 3.6.1 has been done and significant improvement of accuracy results is shown. By doing a multi-stage classification using the HMLP network (MCHMLP) may improve the performance of the conventional HMLP network. An improvement also is done to the current MCHMLP network. The CHMLP is developed by rearrange the sequence of second classification done by MCHMLP network. Better results are shown to prove the ability of CHMLP network in doing the classification process. Several samples are taken from the machine learning repository UCI [14] (Pima Indians Diabetes, Iris, Glass, Wine, Lung Cancer, Ionosphere and Hayes-Roth) are used to test the ability of the MCHMLP and CHMLP in doing the classification.

5.2 Pattern Recognition Unit

In this study, an approach used for ECG signal detection is presented by using the RRI morphology in extracting the feature and use them as input vector for the classification process. Instead of using the RRI morphology, this study also suggests the extraction of feature from the PTI to be used in complementing to lack of RRI. Some improvements of the conventional classification technique, the HMLP network are developed in order to perform high accuracy results. Figure 5.1 shows summary the pattern recognition unit.

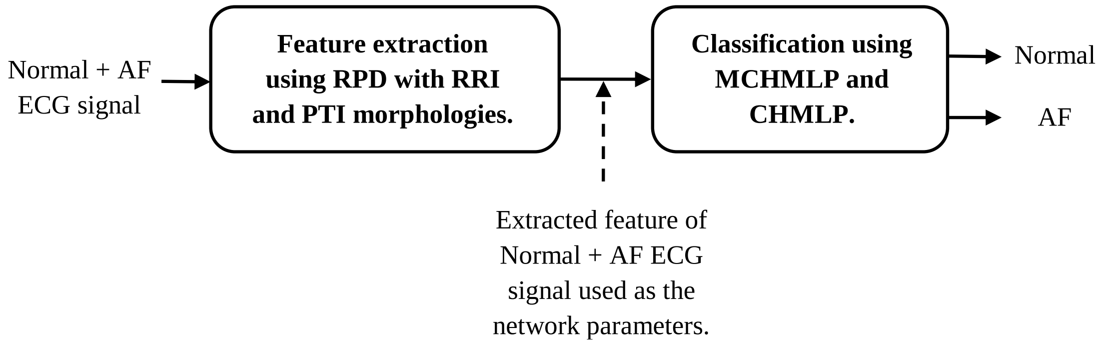

Figure 5.1: The pattern recognition unit; (a) extraction feature process by using RRI and PTI morphology and (b) classification process using MCHMLP and CHMLP networks.

Figure 5.1 shows the pattern recognition unit, which comprises of feature extraction process and classification process. The feature extraction process is done by using RPD technique with both the RRI and PTI morphologies. The intersection points between each ECG complex and RPD are used as the input vector to the MCHMLP and CHMLP. The characteristic of the input vector are being the indicator to classify the signal, either belong to normal group or AF family.

5.2.1 Rectangular Pulse Domain (RPD) Feature Extraction Process

Figure 5.2 shows the flowchart of the RPD development. In this study, an approach used for AF detection is presented by using RRI morphology. A novel pulse domain technique, the RPD technique is developed and performed to extract required features. The new method uses rectangular pulses to obtain the amplitude of the intersection points (between the pulses and the ECG signal).

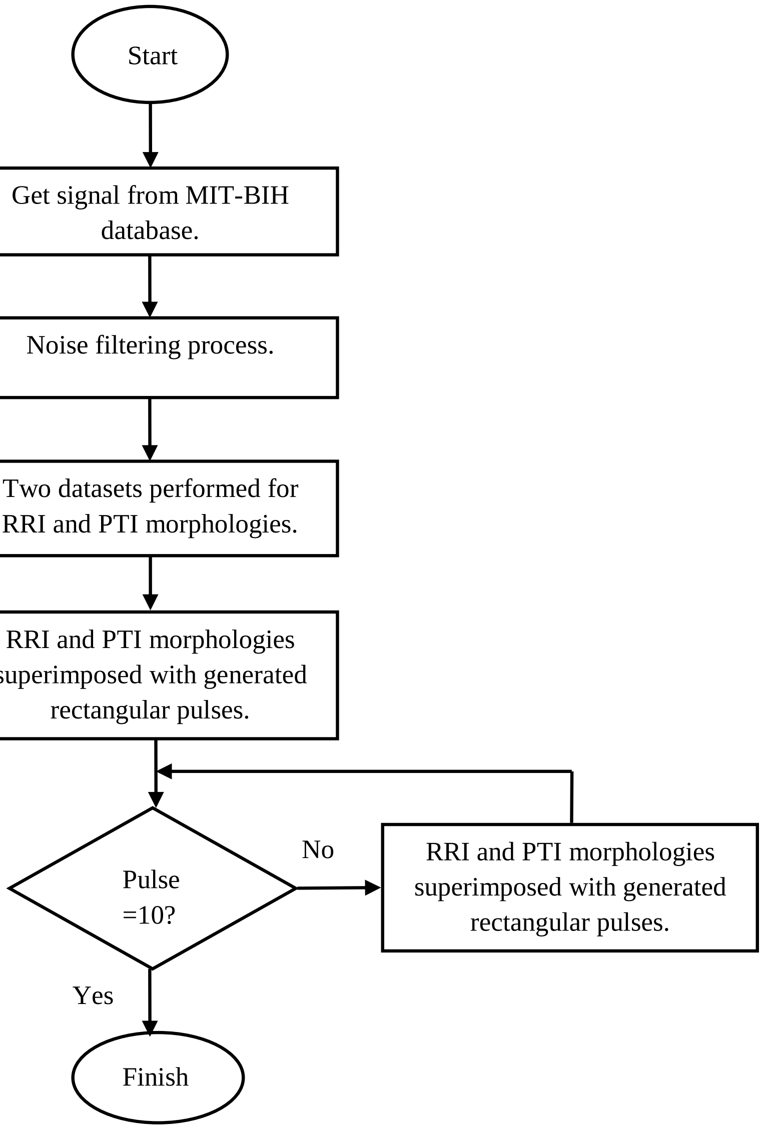

Figure 5.2: The flowchart of the RPD based feature extraction process.

This study is extended with the use of the PTI morphology in the approach to test the PTI as a means of detecting AF. The problem occurs when different activities were done such as stairs climbing or quick run, heart rate are varies based on the size of patient/people and varies speed the activities. Most heart rate readings are taken when the subject is at rest or walking on a treadmill with constant velocity which can be controlled. However, readings of the heart rate for nonstationary patient also capable to be analysis by removing the interval between complexes. This process will leave only complexes with duration from peak P to peak T. Instead the RRI, the region of PTI is taken at the highest point of the P peak to the highest point of the following P peak. Figure 5.2 shows the extraction process of PTI complexes.

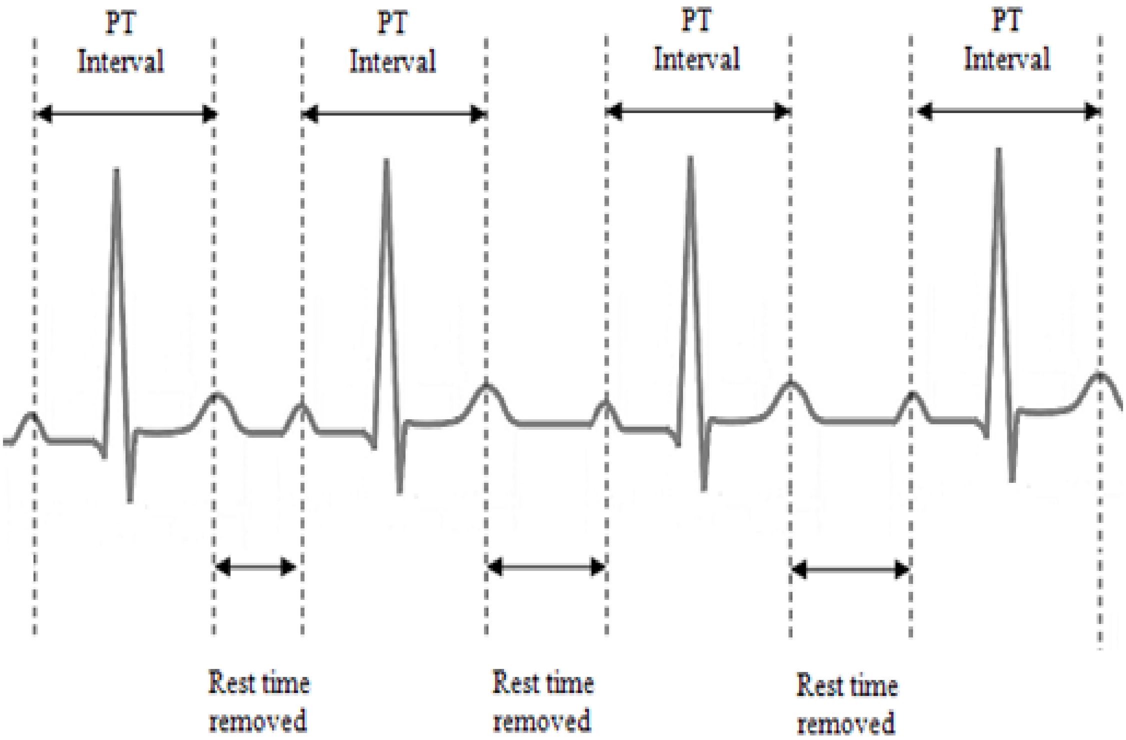

Figure 5.3: Extraction of irregularity of PTI and rest time removal.

Figure 5.3 shows the flowchart of the RPD based feature extraction process. In the RPD technique, the process begins by reading signals from MIT-BIH database. Next, the contaminating noise in the signals is reduced. The filtered signal is separated into beat-by-beat according to RRI morphology and PTI morphology, which generates two different datasets. Both the RRI and PTI morphology datasets, each beat is superimposed with numbers of rectangular pulses. This study considers the beat superimposed with one to ten rectangular pulses. The amplitude of the intersection point between the beat and rectangular pulse/pulses are taken to be the input vector to the classifier.

In this study, the ECG signals were taken from the MIT-BIH database are filtered in order to reduce noise effects. Two datasets (each one containing all the signals) were then formed from the signals one for RRI and one for PTI morphologies. Rectangular pulses are generated and superimposed on the RRI and PTI morphologies complexes. The amplitudes of each intersection point between the ECG and the pulses were used to form the input vectors for the neural network. The extracted feature at the intersection points between the complex ECG signal and the four rectangular pulses. Therefore, eight intersection points are taken as the input vector to be classifying by the HMLP network. Figures 5.4(a) and 5.4(b) shows the intersections of an AF complex with the rectangular pulses, while the intersections of a normal complex with rectangular pulses are shown in Figures 5.4(c) and 5.4(d).

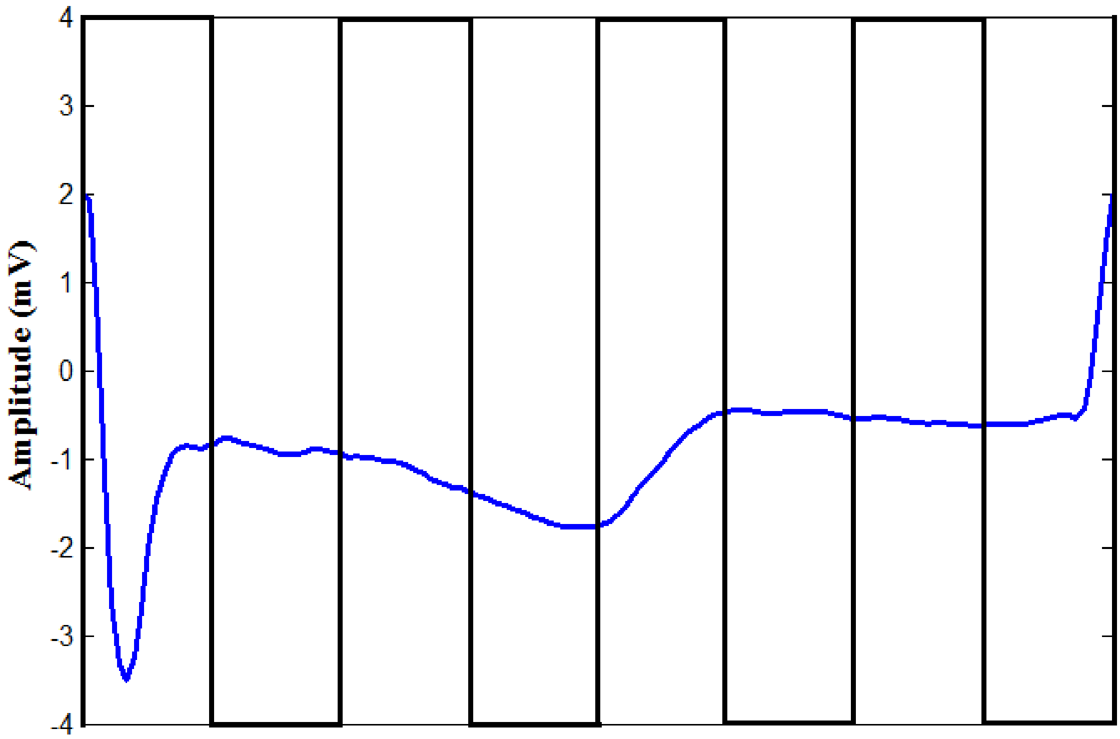

Figure 5.4(a): ECG Feature extraction based on RRI (AF signal).

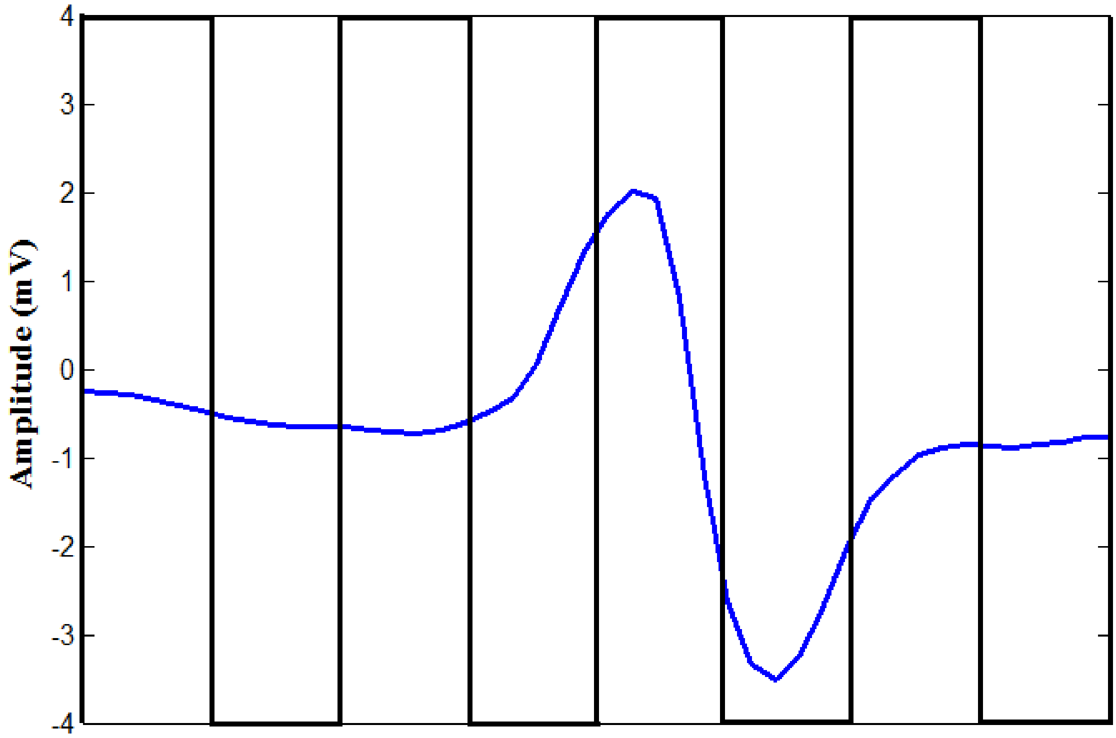

Figure 5.4(b): ECG Feature extraction based on PTI (AF signal).

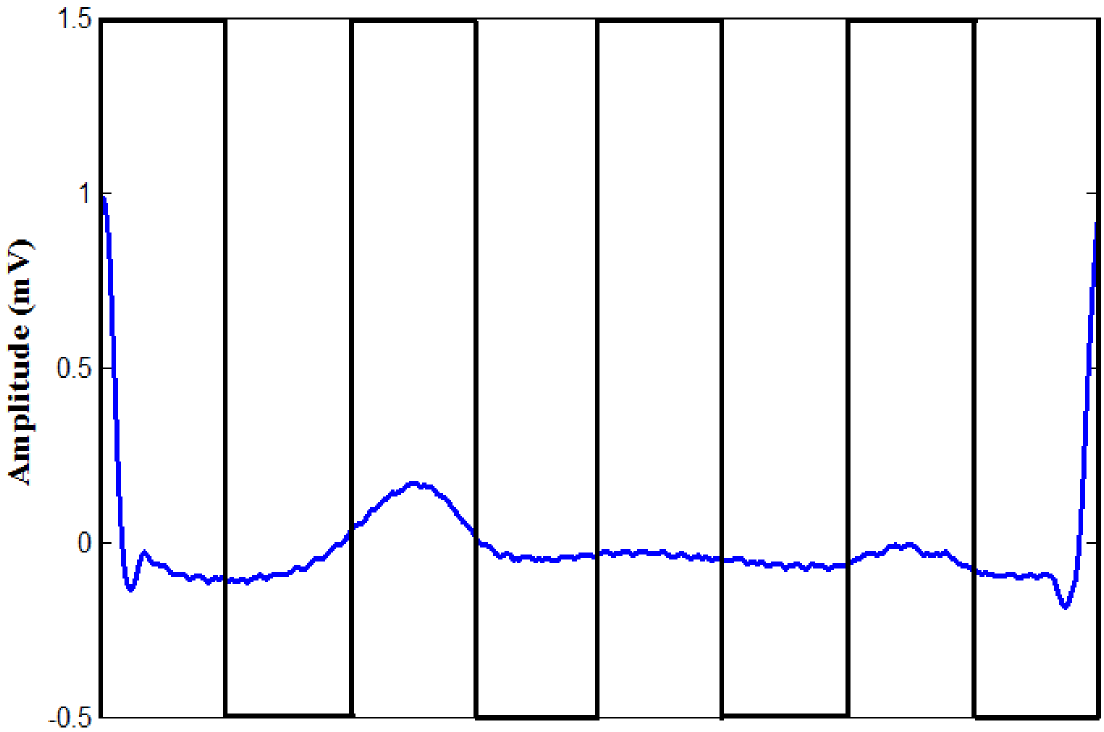

Figure 5.4(c): Feature extraction based on RRI (Normal signal).

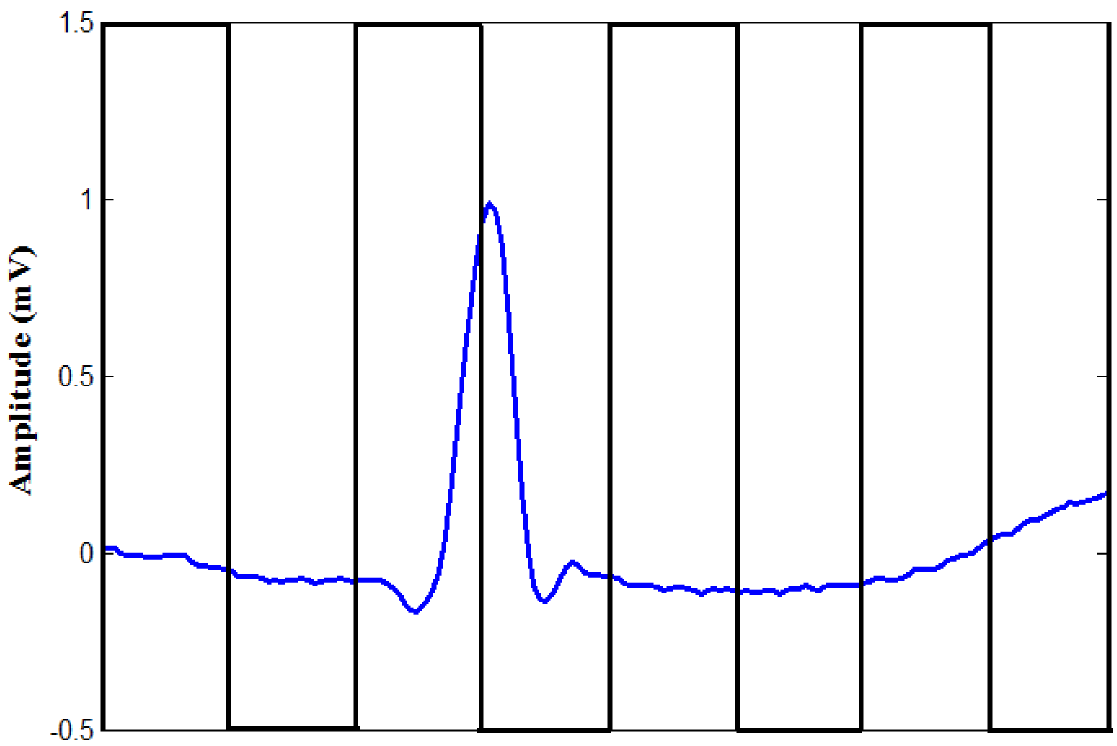

Figure 5.4(d): Feature extraction based on PTI (Normal signal).

In the case of no P peak, the peak will be replaced by the fibrillatory wave as done by [46]. For the case of inverted T peak, the lowest point of the inverted T peak is selected as the ends of PTI morphology. Clearly, the use of just a few pulses would not generate enough features to achieve good classification. On the other hand, extracting too many features could be an unnecessary. A test is carried out to identify the optimum number of rectangular pulses for the highest possible accuracy as shown in Table 5.1 and 5.2. The accuracy of the HMLP classification is calculated as Equation 3.5.

Table 5.1: The HMLP classification performance by using extracted features from RRI morphology as the input vector.

Number of Hidden Node	**Number of Rectangular Pulse / Accuracy Result (%)**									
	1	2	3	4	5	6	7	8	9	10
1	90.20	91.30	92.86	94.20	93.12	93.58	99.96	93.15	92.56	92.30
2	91.65	91.89	93.05	94.95	93.56	93.60	93.05	93.05	92.70	92.55
3	91.98	93.30	93.56	**95.94**	93.56	93.89	93.25	93.05	93.01	92.70
4	92.36	93.30	93.56	**95.94**	93.56	93.89	93.25	93.05	93.01	92.71

Table 5.2: The HMLP classification performance by using extracted features from PTI morphology as the input vector.

Number of Hidden Node	**Number of Rectangular Pulse / Accuracy Result (%)**									
	1	2	3	4	5	6	7	8	9	10
1	91.18	93.01	93.69	95.20	94.69	94.69	93.98	92.96	92.56	92.25
2	92.65	93.26	94.05	**95.53**	94.98	94.85	94.21	93.01	92.78	92.48
3	93.01	93.26	94.56	**95.53**	94.98	94.85	94.56	93.46	92.78	92.70

Table 5.1 and Table 5.2 shows the performance of HMLP network in doing the classification by using RRI and PTI morphology, respectively. From the tables it is seen the use of four rectangular pulses (eight intersections) is sufficient to produce the best classification. The HMLP is capable of providing 95.94% and 95.53% of accuracy for RRI and PTI, respectively. The highest accuracy performance on RRI and PTI morphologies were given by using 5 hidden nodes for RRI and 3 hidden nodes for PTI. Classification results are remain at 95.94% for RRI and 95.53% for PTI even the number of hidden node is increase. At this moment the HMLP network has reached its optimum level. The HMLP network needs sufficient dataset to provide high accuracy results but, a large dataset made the network become more complex and the network unable to classify well.

5.2.2 Neural Network Classification

In this study, an improvement version of the HMLP network is introduced, which is repeating the classification process at the second stage. The novel classification technique is known as MCHMLP. The proposed method is affected by adding another HMLP network to the output layer of the conventional HMLP network. These networks are in cascade so that the output of the first network is the input of the second network. Figure 5.5 shows the block diagram of the proposed method.

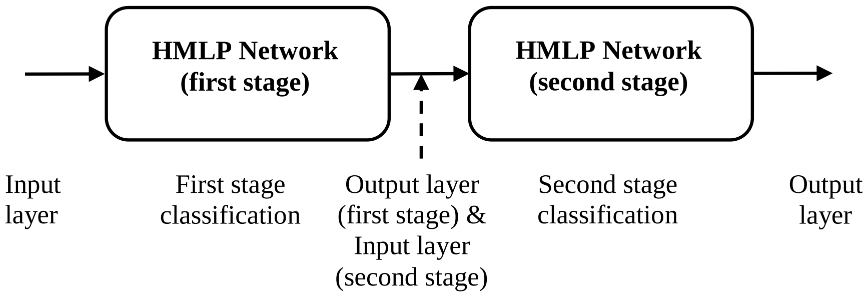

Figure 5.5: Block diagram of the proposed network architecture.

By refer to the block diagram, the first HMLP network is fed with training input vectors, which consist of several parameters representing the input vector features. These features correspond to the various attributes used for the classification in each case. The network is trained in order to find the best performance of the classification process. It is considered that the best possible performance has been attained when the error of the network has reached a small value and remains constant even though the number of nodes increases. At this moment, it is considered that the network has obtained the highest level of convergence and reaching its optimum structure. Then, the output of the first HMLP network becomes as the input vector and fed to the second HMLP network. The same procedure will be performing as done in the first HMLP network to obtain the highest level of convergence and the optimum structure.

Another improvement held in this study is by cascading two HMLP networks in series known as Cascade-HMLP (CHMLP) network. The CHMLP network is the improvement of the MCHMLP network. A new feeding arrangement to the second stage network makes a different between the MCHMLP network and the improvement network, the CHMLP. The improvement of the CHMLP network is shown in Figure 5.6.

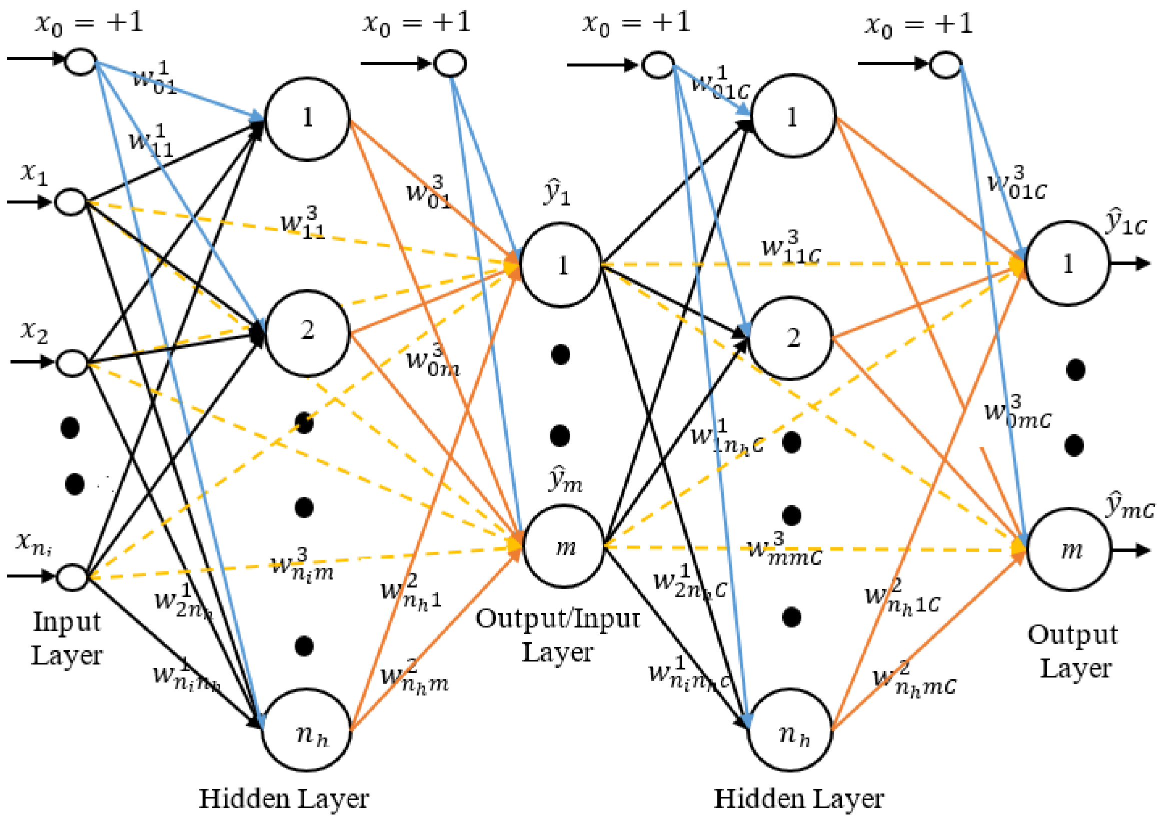

Figure 5.6: A schematic diagram of CHMLP network with one hidden layer.

In the MCHMLP network structure, the second HMLP network is fed with the input only after the first HMLP reaching its optimum structure. With the new arrangement, the CHMLP network performs the second classification process afterwards the first classification is done at each iteration and stop after obtaining the highest level of convergence and reaching its optimum structure at the second HMLP network. Equation 5.1 is the modified version of the conventional HMLP network output. Respect to the output of the HMLP network in Equation 3.8, the output is feeding to the second HMLP network as the input data. The cascading network is working in a similar way to the first HMLP network. The final output of the CHMLP network, $\hat{y}_{kC}$ is shown as by respecting the output of HMLP network in:

$$\hat{y}_{kC}(t) = \sum_{j=1}^{n_h} w_{jkC}^2 F_C\left(\sum_{i=1}^{n_i} w_{ijC}^1 \hat{y}_k(t) + w_{k0C}^1 x_{0C}^1\right) + \sum_{i=1}^{n_i} w_{ikC}^3 \hat{y}_k(t) \tag{5.1}$$

$$for\ 1 \le j \le n_h, 1 \le k \le m$$

where w_{ikC}^3 denotes the weights of the additional linear connection between the input and output for the second network but to the output layer for cascaded/second HMLP network. $n_h$is the number of hidden nodes while m is the number of outputs of the network. The weightsw_{ijC}^1, w_{jkC}^2 and w_{ikC}^3 need to converge to optimum values in order to minimize the prediction error. F_C is the activation function, and a sigmoid function has been chosen for the HMLP network. Since the structure of the conventional HMLP network and the proposed CHMLP network are similar apart from the input vector.

The objective of applying the multi-stage classification is to redo the classification that happens at the first stage network and provide the second stage network an opportunity to improve the overall result. Both the MCHMLP and CHMLP networks are operated with multi staging classification process. Each neural network has its own convergence limitations based on the structure of the network, type of training algorithm used and the size of the data available for training. If the accuracy of the network keeps giving the same results even when the number of iterations is increased, this means the network is near or at its highest convergence point. So, by using the output of the first stage as input for the second network we could improve on the convergence limitations of first HMLP network. The second stage network will re-classify the wrong classification held at the first stage network. Two improvement version of HMLP (MCHMLP and CHMLP) networks were tested its ability to identify patterns in the seven problems taken from machine learning repository UCI [14]. The selected datasets include a variety of different sizes and patterns as summarized in Table 5.3.

Table 5.3: Dataset descriptions.

Datasets	**Size of datasets**	**Number of features**	**Number of classes**
Pima Indian	768	8	2
Iris	150	4	3
Glass	214	9	6
Wine	178	13	3
Lung Cancer	32	30	3
Ionosphere	351	34	2
Hayes-Roth	132	4	3

5.2.3 Improvement on HMLP Network Performance

First of all, the MCHMLP and CHMLP networks need to be tested their ability before used to detect AF activity. For all UCI datasets as tabulated in Table 5.3, each dataset is randomly divided into two subsets of 80% as a training sample and 20% as test sample to form a predictive test. This procedure is repeated until the smallest constant standard deviation is obtained. This study limits the number of hidden nodes to 10 for each classifier (CHMLP, MCHMLP, HMLP, MLP and RBF networks) and a maximum of 10 iterations for K-Mean. However, there are classifiers that are able to reach the point of convergence with less than 10 hidden nodes or iterations. Table 5.4 shows the classification performance of the CHMLP, the MCHMLP and other classifier for Pima Indian, Iris, Glass, Wine, Lung Cancer, Ionosphere and Hayes-Roth datasets. The performance of the classification techniques are measured by the accuracy of the prediction techniques which calculated as Equation 3.8 and the MSE. The MSE is calculated by:

$$MSE = \left(\sum_{k=1}^{n}\left(y_k - \hat{y}_k^2\right)\right)/n \qquad (5.2)$$

with y_k is the predicted output while $\hat{y}_k$ is the actual output. n is the number of data used.

Table 5.4: Classification performance of the CHMLP, MCHMLP and other classifiers on several datasets.

Dataset	Classification Technique, Accuracy (%) / MSE					
	CHMLP	**MCHMLP**	**HMLP**	**MLP**	**RBF**	**K-Mean**
Pima Indian	**77.92 / 4.12**	*77.50 / 9.36*	74.10 / 15.84	70.78 / 28.52	70.57 / 26.94	73.92 / 8.82
Iris	**98.83 / 1.19**	*98.83 / 3.88*	98.83 / 4.16	96.67 / 5.11	85.64 / 28.84	91.98 / 8.70
Glass	**90.45 / 3.69**	*90.01 / 6.40*	89.96 / 8,41	72.10 / 32.49	69.54 / 28.62	71.19 / 16.97
Wine	**99.77 / 0.67**	*99.77 / 1.15*	99.77 / 3.42	70.87 / 42.38	67.87 / 26.63	96.12 / 5.34
Lung Cancer	**92.31 / 10.96**	*89.92 / 12.39*	88.76 / 13.67	50.00 / 28.94	65.70 / 39.31	70.57 / 26.73
Ionosphere	**95.02 / 2.19**	*94.27 / 3.57*	93.68 / 4.67	85.71 / 13.10	87.60 / 29.70	92.57 / 6.00
Hayes Roth	**83.65 / 18.58**	*81.35 / 9.67*	80.82 / 15.68	68.24 / 16.56	70.03 / 31.58	79.57 / 15.92

As tabulated in Table 5.4, the CHMLP network produces the highest testing accuracy for all the datasets and lowest MSE for all datasets with the exception on the Hayes Roth dataset where the MSE is slightly higher than obtained by HMLP. In the case of the Iris and Wine datasets, the accuracy performance is similar for the CHMLP, MCHMLP and HMLP networks. However, the MSE is significantly lower for the case of CHMLP network. In the case of Pima Indian Diabetes and Hayes Roth datasets, the CHMLP network unable to produce high accuracy results due to the problem with the large overlap between two groups in the datasets. The datasets are divided into different groups and parts of the data are subset of each group and create a difficulty to be classified since it is highly overlapped. As the conclusion, the CHMLP network is shown to be able to obtain the best classification results and better than others network. The result shows the CHMLP network has the capability to generalize the datasets in training phase and performs good results in testing phase.

For MLP, RBF and K-Mean classification, results for all datasets are no better than HMLP, MCHMLP and CHMLP networks. The performance of these three classification are based on type of data and tabulation of data itself. For Pima Indian Diabetes, K-Mean produce better result and follows with MLP and RBF. However, for the Iris and Glass datasets, MLP gives better results and follow with K-Mean and RBF. Nevertheless, the MCHMLP also outperforms all the other networks (except the Cascade-HMLP network) in obtaining the highest overall accuracy for every dataset used. Sometime, the accuracy of MCHMLP and HMLP networks are equals but, the performance of standard deviation made the different between the networks. The problem occurs during the use of Pima Indian Diabetes and Hayes Roth. The high overlap databases during the classification process reduce the performance of the classifier. Although the MCHMLP results has been outperform by the Cascade-HMLP network, but the performance of the MCHMLP network is not far behind. The MCHMLP network is providing high accuracy classification with small standard deviation results. The MCHMLP network also capable to generalize the datasets in training phase, whilst performs good results in testing phase.

Nevertheless, the MCHMLP network also outperform all the other classification technique (except for CHMLP) in obtaining the highest accuracy for every dataset. For several time, the accuracy performance for MCHMLP and HMLP are equals but, the performance on MSE made the different between the networks. The problem occurs during classification of Pima Indian Diabetes and Hayes Roth. The high overlap databases during the classification process reduce the performance of the classifier. Although the performance of MCHMLP no better than CHMLP network but the results is not far behind. The MCHMLP capable to provide high accuracy results and low MSE performance for each datasets. The MCHMLP network also capable to generalize the datasets during training, whilst performs good results in the testing phase. As the both Cascade-HMLP and MCHMLP networks are proven capable to generalize the datasets and provide high accuracy, then the extracted features of the normal and AF signal are fed to the networks. Table 5.5 shows the classification result given by the CHMLP and MCHMLP networks based on RPD feature extraction technique and use both the RRI and PTI morphologies.

5.3 Atrial Fibrillation Classification

Some experiments involving feature extraction and classification will be obtained. The RPD feature extraction is use to extract feature from the ECG signal. The extracted features are obtained by using both RRI and proposed PTI morphologies. In other hands, the classification is done by the improvement version of the HMLP network, the MCHML and CHMLP networks.

5.3.1 RPD Feature Extraction

Normal and AF signals are taken from the MIT-BIH database and extracted using RPD. Then, the amplitude of the intersection of the rectangular pulses and the signal are fed to the classifiers for classification process. Results from the HMLP network are compared with ten other classifiers. Table 5.5 which are in order of decreasing accuracy shows the results of the AF classification using several techniques. The RRI method appears as the most important indicator for AF identification. The RRI method becomes the important indicator for AF identification. Several researchers also applied the AA technique as the features. The accuracy, sensitivity and specificity are calculated based on Equation 3.5, 3.6 and 3.7.

Table 5.5: The comparative result of AF classification using various technique.

Technique	Result (%)			
	Morphology	Accuracy	Sensitivity	Specificity
CHMLP	**RRI**	**95.94**	**97.46**	**94.42**
CHMLP	**PTI**	**95.53**	**97.56**	**93.50**
MCHMLP	RRI	93.64	91.20	96.08
MCHMLP	PTI	91.89	89.20	94.58
HMLP	RRI	91.60	95.80	96.40
HMLP	PTI	91.55	97.64	85.55
MLP	RRI	89.92	90.26	89.58
RBF	RRI	89.17	88.45	89.89
K-Mean	RRI	88.62	88.52	88.72
K-Mean	PTI	86.45	88.20	84.70
MLP	PTI	82.18	84.34	80.02
RBF	PTI	80.32	79.84	80.80

The results show the CHMLP network is competence to produce the highest classification accuracy using the RPD based RRI morphology feature extraction. The CHMLP network is able to classify the AF dataset with 98.00%, 97.52% and 98.84% accuracy, sensitivity and specificity, respectively. The MCHMLP network comes second with 96.12%, 95.66% and 96.58% accuracy, sensitivity and specificity, respectively. The HMLP network enables to give good results with 95.94%, 97.45% and 94.42% for accuracy, sensitivity and specificity, respectively. The small margins which the CHMLP network outperforms the rest of the classification methods, in terms of accuracy, vary from 2% to 15%. The results show the HMLP based structure capable to do the classification process accurately. The good result also reflected by the suitability between the feature parameter and classifiers used during the classifying process. The RRI morphology is allowed the classification of AF activity takes place whether the P peak is detected or not. As mentioned in the literature, the RRI morphology becomes an important information contributor in the classification of AF. The rest classifier (MLP, RBF and K-Mean) also gives better accuracy result but unable to outperform the classification performance of CHMLP, MCHMLP and HMLP networks.

The PTI morphology also capable to give high accuracy AF classification as the results illustrated in Table 5.5. The PTI morphology appears to be the best approach if no information is provided as to the condition under which the ECG signal is obtained. The CHMLP network is able to classify the AF dataset with 96.15%, 94.75% and 97.54% accuracy, sensitivity and specificity, respectively. The MCHMLP network also produced good results with 96.04%, 95.64% and 96.44% while HMLP network with 95.52%, 97.56% and 93.48% for the corresponding outputs. Clearly, a good combination of feature extraction and classifier facilitate PTI as a significant contributor to AF classification. The analysis of ECG signals with the extracted features taken from the PTI could be used to prevent the problems ECG signal analysis since most of the signals are taken during rest time rather than performing activities. The K-Mean, MLP and RBF also shows good classification results by using PTI morphology as the feature extraction technique. However, this classification technique unable to outperform the results given by CHMLP, MCHMLP and HMLP networks. The results show that the PTI morphology can offers a reliable input vector. The results tabulated in Table 5.5 shows the generalization of all the datasets based on the PTI morphology for classification.

5.4 Discussion

In the ECG pattern recognition unit, the rectangular pulse domain (RPD) has been used to extract the information from filtered ECG signal. The ECG complexes are formed in RRI and PTI morphologies. Rectangular pulses are generated and superimposed on the RRI and PTI morphologies complexes. The amplitudes of each intersection point between the ECG and the pulses were used to form the input vectors for the neural network. From the study, four rectangular are gain seven input vector to the classier which proved by HMLP neural network classifier. By using four rectangular it will gain seven intersections which is just enough to perform high accuracy prediction. Too many intersections may let the classier become more complex but insufficient input vector let the network unable to generalize.

From the HMLP classifier results, it has reach their optimum performance with 95.94% based on RRI morphology and 95.53% based on PTI morphology. In this study, an improvement version of the HMLP network is introduced, which is repeating the classification process at the second stage, known as MCHMLP. The proposed method is affected by adding another HMLP network to the output layer of the conventional HMLP network. These networks are in cascade so that the output of the first network is the input of the second network. Another improvement held in this study by cascading two HMLP networks in series known as Cascade-HMLP (CHMLP) network. The CHMLP network is the improvement of the MCHMLP network. A new feeding arrangement to the second stage network makes a different between the MCHMLP network and the improvement network, the CHMLP. The improvement of CHMLP and MCHMLP networks are shown by Table 5.4 which CHMLP and MCHMLP networks shows significant improvement comparing with others classifier.

The ability of CHMLP and MCHMLP in doing classification are be continues to classify the AF activities. Table 5.5 shows the performance CHMLP and MCHMLP network in doing AF classification by using feature extracted by using RPD technique. Both RRI and PTI morphologies are used as the input vector to the networks. From the results, it shows the CHMLP and MCHMLP outperforms others classifier in classify the AF activities. The network gain significant performance than original network (HMLP) with around 4% for CHMLP and 2% for MCHMLP, respectively based on RRI morphologies. Both networks are capable to produce significant improvement based on PTI morphologies. Based on PTI morphology performance, 2% and 0.5% improvement have been provided by CHMLP and MCHMLP networks, respectively.

5.5 Conclusion

This chapter presented novel pattern recognition in detecting the AF signal activity and developed some improved of the HMLP classification network. From this study, a novel PRD feature extraction technique has been used to feed the feature to the HMLP network. As the results, the HMLP network has granted better performance of AF detection. Both the RRI and the suggested PTI morphologies are used for extracting the feature. This study also reveals the used of the PTI morphology is also successfully and accurately to be used for detecting AF when information on how the ECG was obtained is not available. The improvement of HMLP network, which are the CHMLP and MCHMLP networks are designed to implement multi-stage classification by using the output of the earlier stage results. Datasets from UCI machine learning repository database such as the Pima Indian

Diabetes, Iris, Glass, Wine, Lung Cancer, Ionosphere and Hayes-Roth have been used as benchmark data. A study has been done on the various classifiers and the same datasets are used in this study. The CHMLP and MCHMLP networks capabilities are compared with other classifiers to measure the ability of the network to produce a better outcome. Results show that overall the CHMLP and MCHMLP networks outperforms all other classifiers (HMLP, MLP, RBF and K-Mean) with better performances both on accuracy and MSE. Nevertheless, PTI morphology appears to be the best approach if no information is provided as to the condition under which the ECG signal is obtained. In Chapter 6, the system is developed and further discussions on the system are available.

Chapter 6

ECG Analysis System

6.1 Introduction

In previous chapter, the feature extraction and classification processes are been formed as novel pattern recognition unit in recognising the best feature, and use it as the indicator to perform the classification process. In last chapter, the study produces a new PRD feature extracting method in extracting feature form ECG signal and novel development of MCHMLP and CHMLP networks for classification process to be obtained. In this chapter, both the novel noise reduction unit (Chapter 4) and the novel pattern recognition unit (Chapter 5) are combined together to develop a new approach of ECG analysis system in detecting the AF activity. The system starts by processing the ECG signal until the classification results either the signal is an AF or not is shown.

6.2 ECG Analysis System

The new approach of the ECG analysis system is developed to process the raw ECG signal which directly taken from the patient. Figure 6.1 shows the whole system been designed and works.

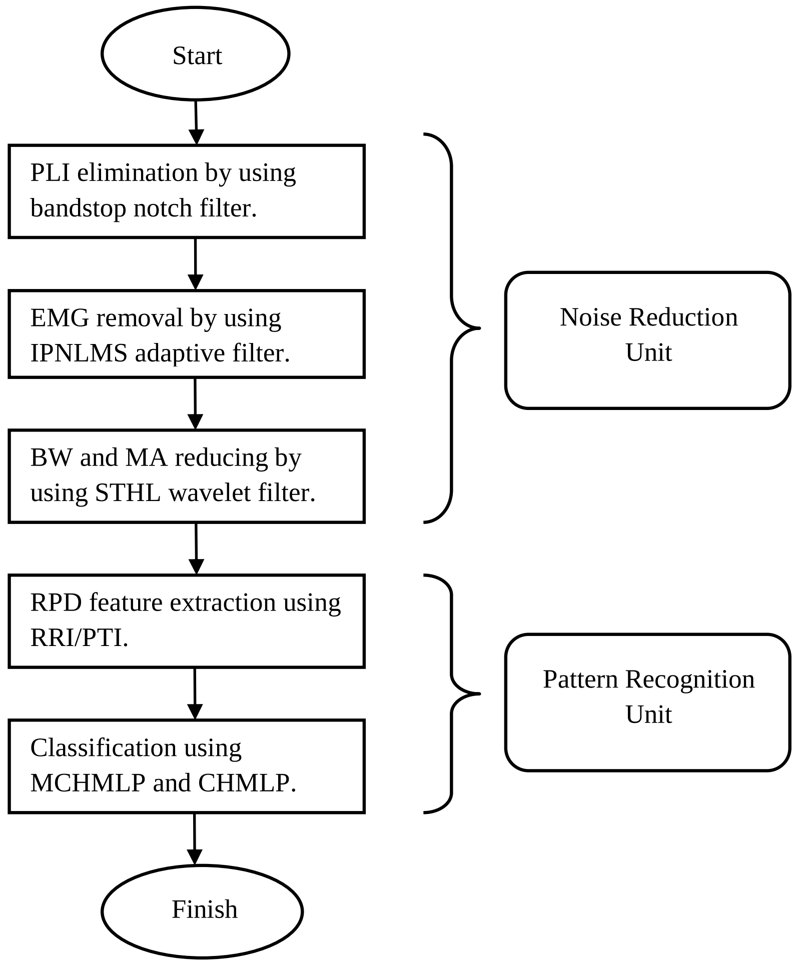

Figure 6.1: The flowcharts of the ECG analysis system.

The system consists of two main units, which are the noise reduction unit and the pattern recognition unit. Each unit has its own responsibility to make sure all process are done properly since the results will be given is highly relates to the previous results. The noise reduction unit works to denoise all the contaminating noise is the ECG. The unit are including numbers of process. The pattern recognition unit is starts after the ECG signal is clean from noises. The unit requires the feature to be extracted and the classification is done by using the extracted feature as the input vector.

Figure 6.1 shows the denoising of the noise contaminating process in the ECG signal is done in the noise reduction unit. At the early stage, an ECG signal is corrupted with BW, PLI, EMG and MA noises. In the first process, the PLI is eliminated from the initial signal. The 50 Hz noise is eliminated from signal by using the designed bandstop notch filter. The EMG noise in the PLI free signal then removed using the IPNLMS adaptive filter. Here, the skin effect signal is removed from the ECG signal. Next, the filtered signal at this stage is filtered again in order to reduce the effect of the low and high frequency noises contributed by the BW and MA noises by using the STHL wavelet based filter. The clean signal obtained after the sequence of filters is used. The clean signal is then processed (extracted and classified) as done in the pattern recognition unit as shown in Figure 6.1.

Figure 6.1 also shows the pattern recognition unit which consists of feature extraction and classification processes. The process starts by getting the clean signal form the noise reduction unit. The amplitude of signal then separated to the beat by beat according to RRI and PTI morphologies. The rectangular pulses are superimposed with the ECG complex then the intersection points between them are extracted to be the input vector of the classifier, the CHMLP and MCHMLP neural networks. The classifier then classified the signal whether it is belonging to the AF or not.

6.3 System Performance

The performance of the system starts with the noise reduction unit to eliminate the PLI, removing the EMG and reducing the impact of BW and MA noises. In this study, the goal of the system is detecting the presents of AF episode. So, signals from normal and AF subjects are taken from the MIT-BIH database. Table 6.1 shows the performance of each filter in denoising certain noise.

Table 6.1: Performance of the noise reduction unit.

Process	**SNR Reading, (dB)**	
	Normal	**AF**
Corrupted Signal	2.78	1.36
After PLI Elimination	3.76	5.33
After EMG Removal	7.25	6.78
After BW and MA Reduction	12.38	15.92

Table 6.1 shows the noise reduction unit performance at each stage. The noises are highly corrupted to the ECG signal. At the beginning, the SNR reading is small but slowly increases at the PLI elimination stage. During PLI elimination stage, the 50 Hz of PLI from powerline source is eliminated. The ratio between the signal and the noise is increased since PLI is eliminated for both normal and AF signals. For the normal signal, the increment up to 1.00 of SNR while up to 4.00 increment of SNR shows for the AF signal. Better signals are shown after the EMG; the skin effect signal is removed from the signals. The signal form the muscle is removed from the signals and the SNR reading for the normal signal is increase to 7.25 while the AF signal is increase to 6.78. The signals (signal free from PLI and EMG) then processed to ensure they are free from measurement equipment, respiration and body movement signals. Results tabulated in Table 6.1 shows the improvement on SNR for normal with 12.38 while the AF signal is improved to 15.92. Comparison between before and after the filtering is done; the corrupted signal is highly contaminated with noises. The filtering process must be performed before the following process to be done unless inaccurate results is produces and the condition of false positive or false negative will be happen. Figure 6.2 and Figure 6.3 shows the performance of the noise reduction unit in denoising the normal and AF signals.

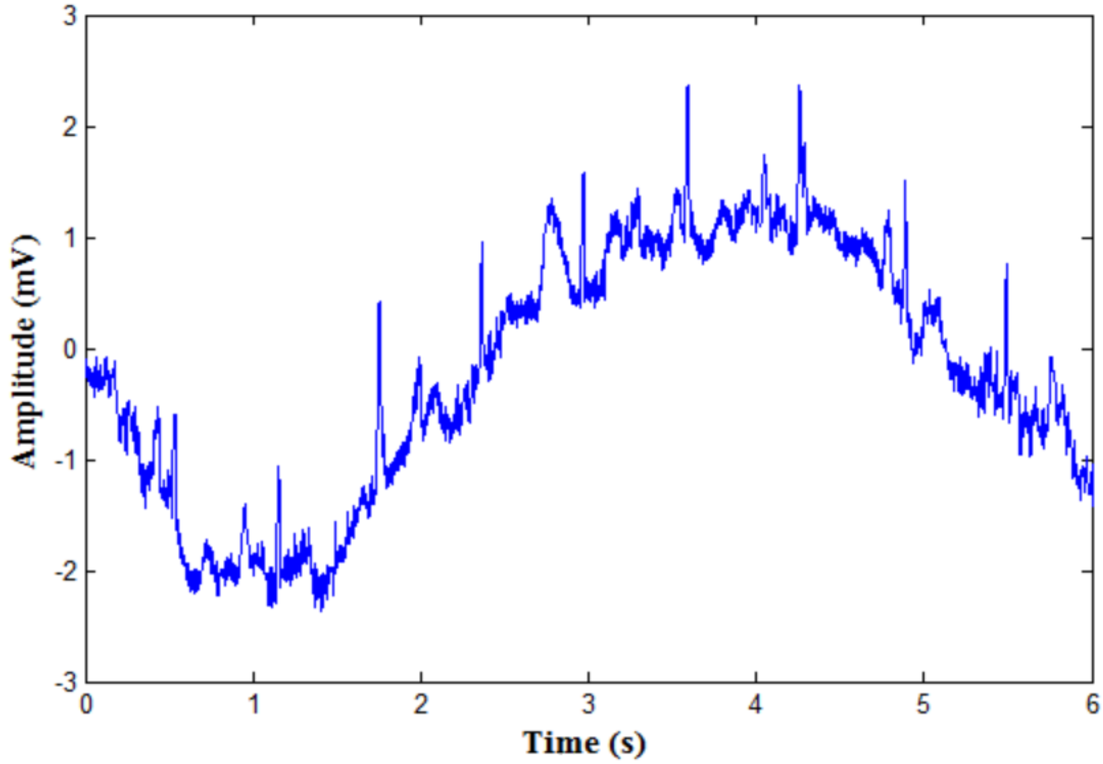

Figure 6.2(a): Normal signal corrupted with BW, PLI, EMG and MA noises.

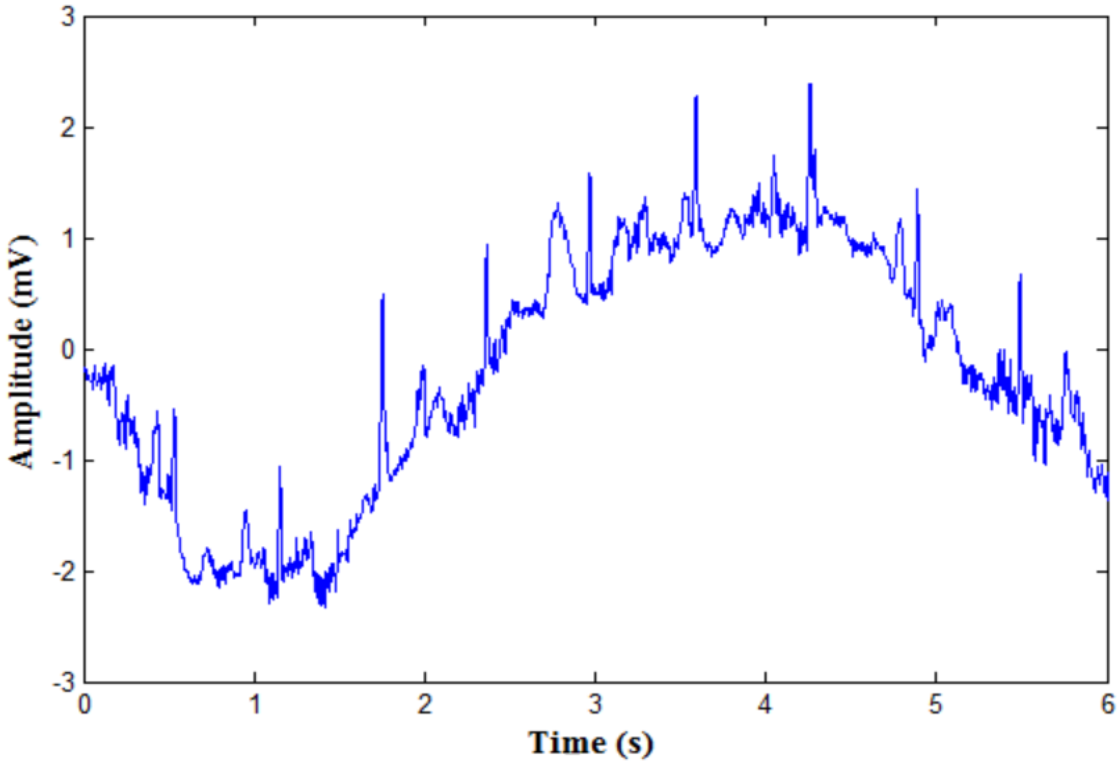

Figure 6.2(b): Normal signal after PLI elimination.

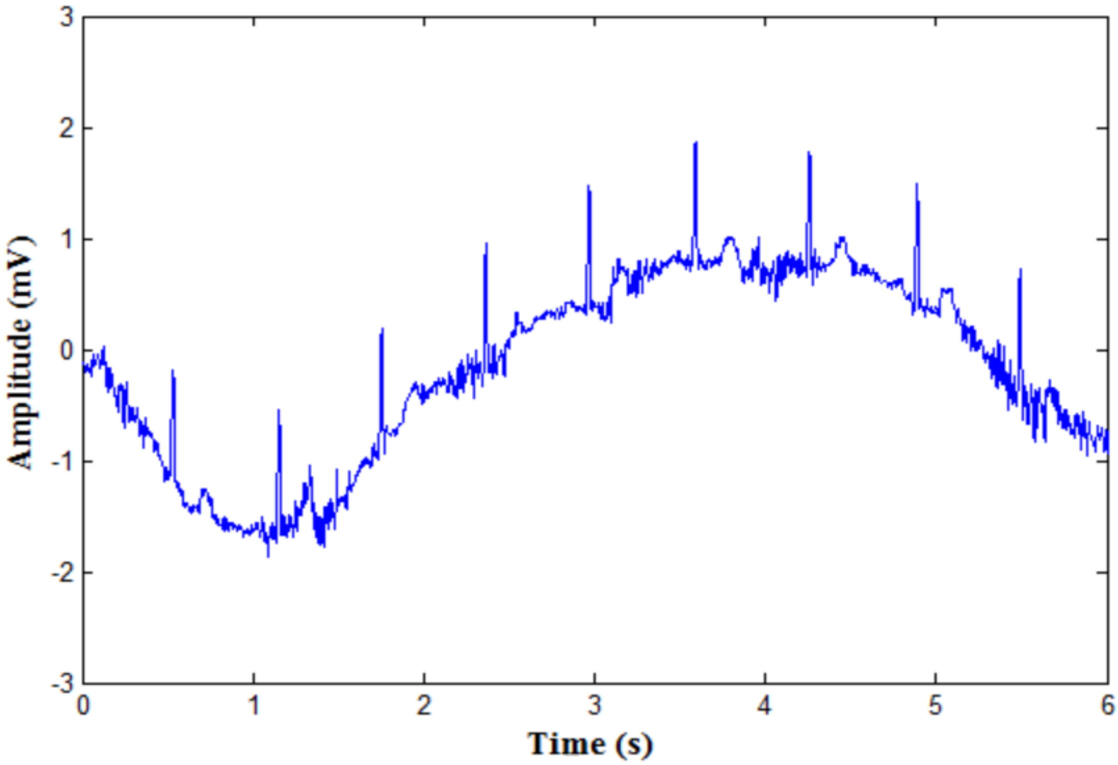

Figure 6.2(c): Normal signal after EMG removal.

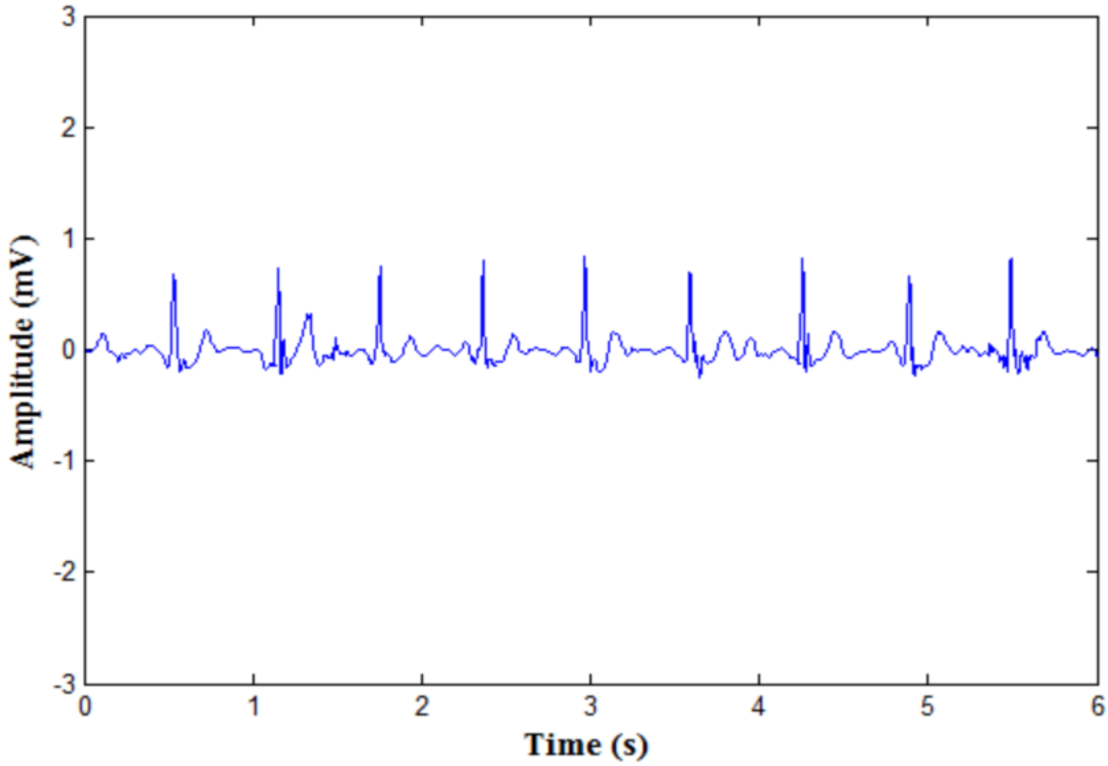

Figure 6.2(d): A clean normal signal generated.

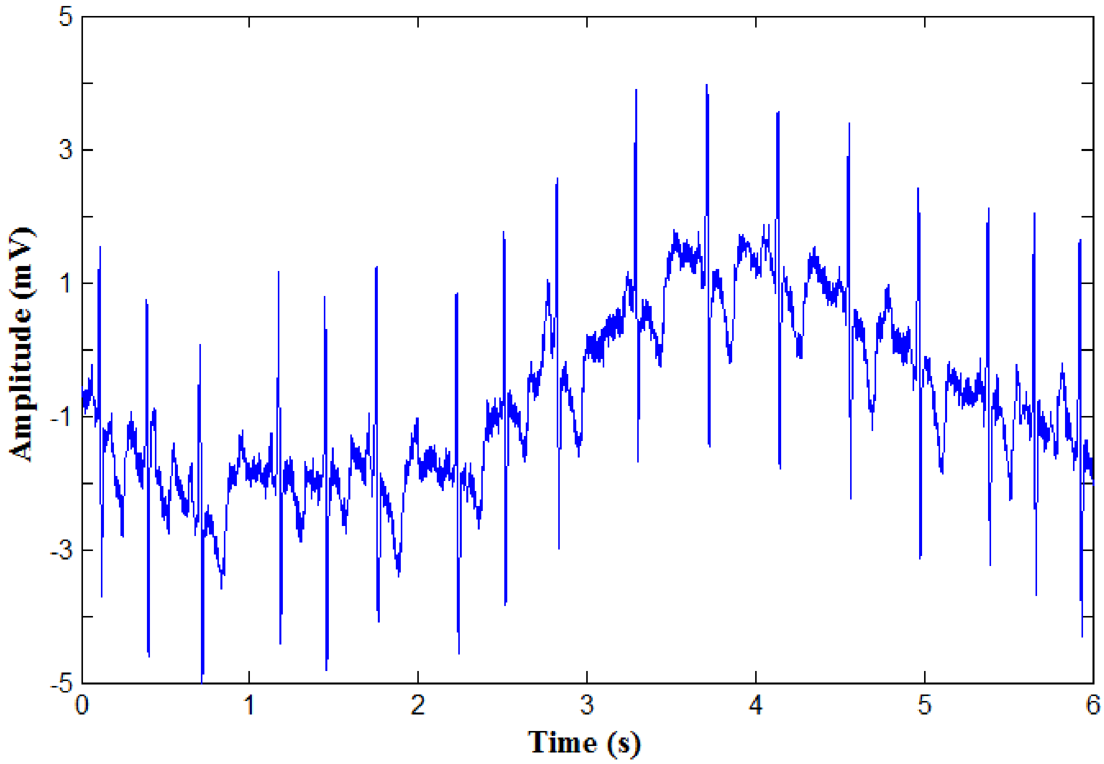

Figure 6.3(a): AF signal corrupted with BW, PLI, EMG and MA noises.

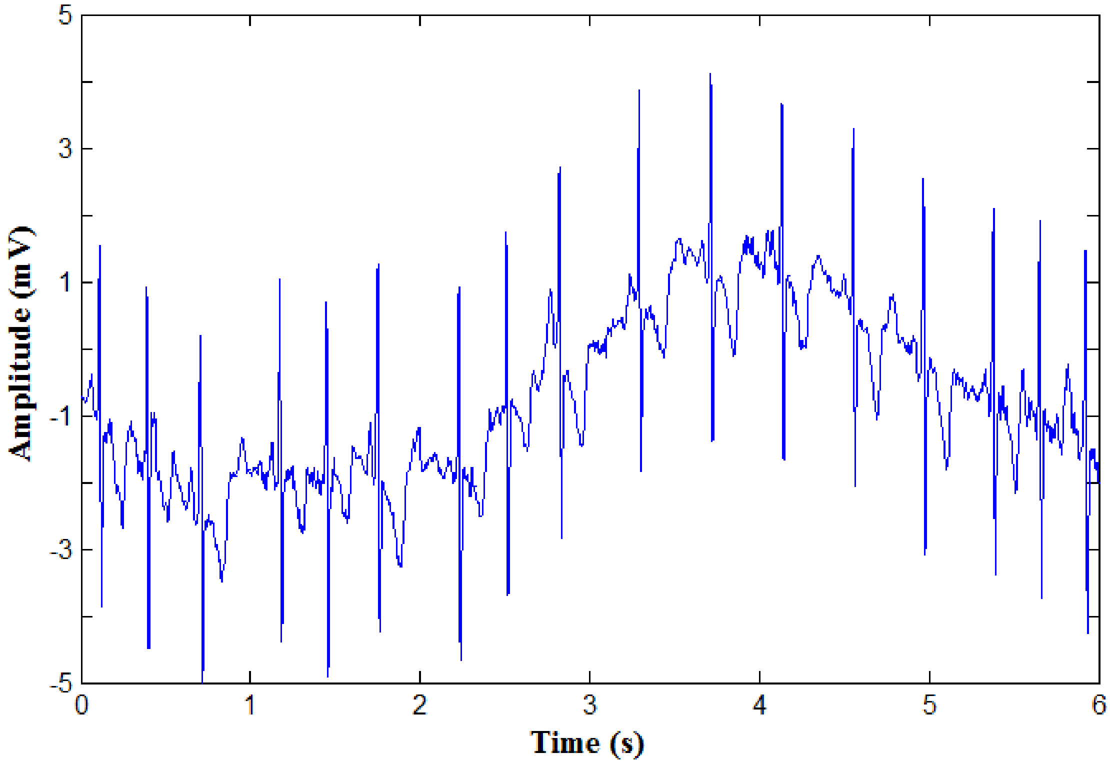

Figure 6.3(b): AF signal after PLI elimination.

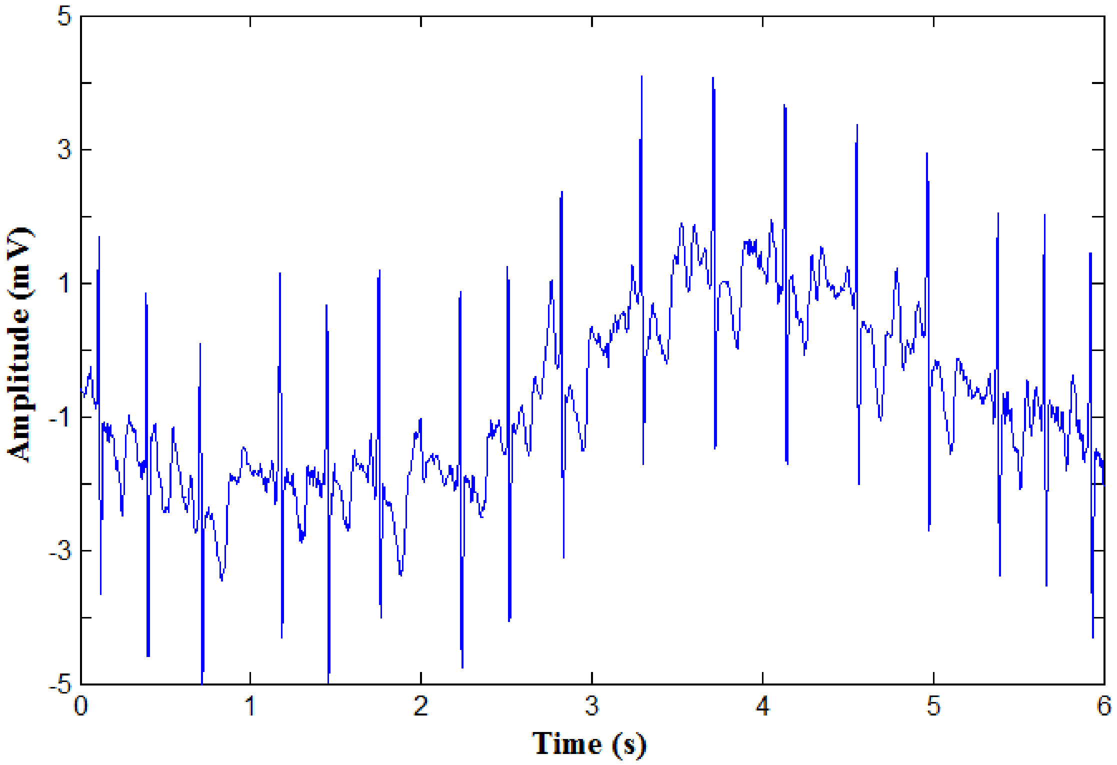

Figure 6.3(c): AF signal EMG removal.

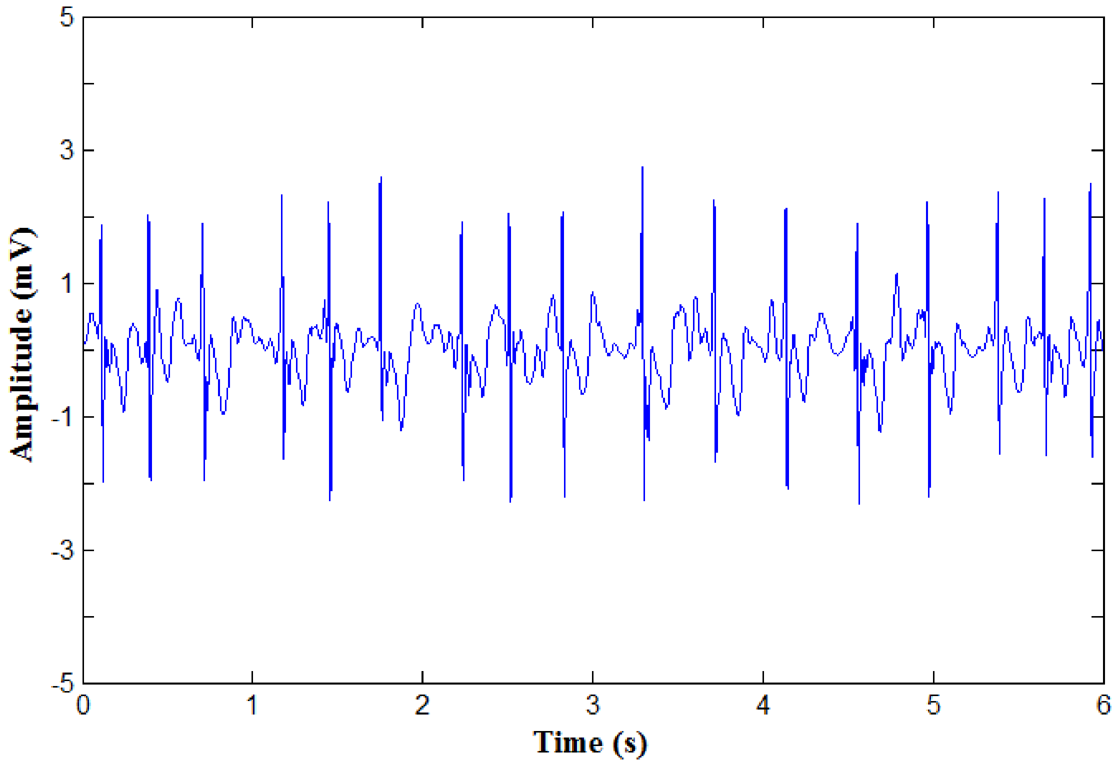

Figure 6.3(d): A clean AF signal generated after BW and MA reduction.

Figures 6.2 and 6.3 shows the results of noise filtering performed by a particular filter for a specific noise of both normal and AF signals. In contrast, the high frequency noise contributed by MA noise has the difficulty to be removed due to spectrum overlapped between the noise and the signals. The important information contained in the signal may be removed together with the noise if the filtering process is not properly done. The combined wavelet based filters (STHL) is used and capable to reduce the effects of MA noise in the signals. However, small amount of the MA noise are still contaminating in the signals (both Figures at (d)) but the information in the original signal is still be maintained.

The filtered signals then are extracted by the RPD. Four rectangular pulses are used to extract eight intersection points (amplitudes) of each ECG complex. The extracted features are fed to the CHMLP network for classification. Table 6.2 exhibits the ability of the CHMLP network using PRD extraction feature to perform the classification for both RRI and PTI morphologies.

Table 6.2: The results of AF classification using CHMLP and MCHMLP networks.

Technique	Result (%)			
	Morphology	**Accuracy**	**Sensitivity**	**Specificity**
CHMLP	RRI	97.92	97.38	98.46
CHMLP	PTI	96.04	94.74	97.34
MCHMLP	RRI	95.46	94.12	96.80
MCHMLP	PTI	94.98	95.25	94.71

Result shows that the CHMLP network has the capability to produce a better classification accuracy using the RPD based RRI morphology feature extraction. The CHMLP network is able to classify the AF dataset with 97.92%, 97.38% and 98.46% accuracy, sensitivity and specificity, respectively. The RPD based PTI is also capable to give better accuracy on AF classification as the results illustrated in Table 6.2. The PTI morphology identified to be an approach when no detail information about the ECG signals. The CHMLP network is able to classify the AF dataset with 96.04%, 94.74% and 97.34% accuracy, sensitivity and specificity, respectively. The PTI morphology can solved problem of the different between the rest and the moving ECG signals. The results show that the PTI morphology can offers a reliable input vector for the AF detection.

6.4 Discussion

In the ECG analysis system, both noise reduction unit and pattern recognition unit are combined to develop a complete system. For noise reduction unit, the four major noises are filtered by a filter at each time. Firstly, the PLI noise is filtered from the signals and SNR for normal signal are increased from 2.78 dB to 3.76 dB and 1.36 dB to 5.33 dB for AF signal. The process follows by removing the EMG effects from the filtered PLI signals. From the results, the SNR is improved to 7.25 dB for normal signal while 6.78 dB for AF signal. Noise free signals are provided after STHL wavelet based filter are applied to the filtered (PLI and EMG) signals. A normal noise free signal is resulting with 12.38 dB while 15.92 dB for the AF. The results are acquired at the noise reduction unit.

In the pattern recognition unit, the noise free signal then is extracted and information from the signals is taken to be fed to the neural network. A new feature extraction method which is RPD technique is applied to the signals based on RRI and PTI morphologies. The features then are fed to CHMLP and MCHMLP networks to classify either the signal is categorizing as AF signal or normal signal. From Table 6.2, the result shows the CHMLP network with RRI morphology capable to give 97.92% on accuracy of the prediction, follows by 97.38% on sensitivity and 98.46% on specificity. The table also shows the CHMLP network with PTI morphology capable to produce 96.04% on accuracy and 94.74% and 97.34% on sensitivity and specificity, respectively. For the MCHMLP network, it works well by using RRI morphology with 95.46% accuracy of prediction. The MCHMLP also giving a good result by using PTI morphology with 94.98% on accuracy of the prediction. Based on PTI morphology performance, 2% and 0.5% improvement have been provided by CHMLP and MCHMLP networks, respectively. The PTI morphology gives good results for both CHMLP and MCHMLP networks which can be used as indicator of AF occurrence if no information of signals is given.

6.5 Conclusion

The ECG analysis system is used to detect the AF or non-AF (normal) episodes. The system capable to reduce the noise effects from contaminating in the ECG signal. At the same time, the originality of the signal is still remaining. The noises in both signals (normal and AF) such as BW, PLI, EMG and MA have been reduced by using bandstop notch filter, IPNLMS adaptive filter and STHL wavelet filter, respectively. However, some noises are still contained in the signals since the MA noise has the difficulty to be removed due to spectrum overlapped between the ECG signals and MA noise. The problem needs to be compromised since to remain the important information in the signals. The combination of the RPD as the feature extraction approach and the CHMLP and MCHMLP network as the classifier can provide better overall classification results in the detection of AF. For ECG analysis system, the CHMLP network is chosen as the classifier since it performs better than MCHMLP in AF detection. The results obtained using the RPD and CHMLP combination were compared, and found to be superior compared to the outcomes from other detection techniques. Both RRI and PTI morphologies were used for extracting feature parameters and in both cases the results of the RPD/CHMLP can offer good results. From the results, the complete technique package (CHMLP networks as the classifier, RRI/PTI signals morphology extracted by RPD feature extractor) is effective in AF detection and proven to provide better results. The PTI morphology extractions technique capable to offer good quality of feature since no information about the signal at the initial phase.

Chapter 7

Conclusions and Future Work

7.1 Conclusions

In this study, a new approach of ECG analysis system is developed in identifying a cardiac abnormality. The development of the system is still in the initial stage and this study is focussing more on the detection of AF. There are numerous techniques have been developed to detect the presence of AF based in ECG signals. In the study, some novel techniques have been proposed to improve the detection performances and compare the results with previous approaches.

The system consists of two main novel units; novel noise reduction and novel pattern recognition units. The system following with four major noises contained in the ECG signal; such as baseline wander (BW) powerline interference (PLI), electromyogram (EMG) and motion artifact (MA). Three different filters are used to ensure that the remaining noise in the filtered output signal is at a minimum level. During the noise reduction process, two novel techniques have been developed and used. The novel approach of IPNLMS adaptive filter is used to remove the EMG noise. Meanwhile, the IPNLMS adaptive filter are used in echo cancellation but never been used in removing noises in biomedical signal. The wavelet based filter (STHL) provides better results than other techniques in reducing the impact of BW and MA noises. Combination of these wavelet based filter capable to reduce both high frequency noise and low frequency noise. In addition, the bandstop notch filter has been designed in eliminating the effects of 50/60 Hz PLI.

In the pattern recognition unit, this study suggests the use of novel RPD as a technique to extract the information contained in the filtered signal. The extracted features (amplitudes of ECG) are fed to the classifier (neural network) as the input parameter. Each ECG complex is separated from each other with respect to two different morphologies; the R to R interval (RRI) and the P to T interval (PTI). The extracted features are classified by novel CHMLP network classifier for detection of AF activity. The CHMLP network capable to give a better accuracy results which tested with several datasets in order to prove the ability of the network to perform the classification.

The ECG analysis system has been developed by combining together the noise reduction unit and the pattern recognition unit. The raw ECG signals will be filtered through the noise reduction unit then the filtered ECG signals will be extracted and classified to normal or AF signal. The system has been tested to perform the detection of AF activities and encouraging results are given. The high accuracy results are able to avoid false alarms from occurring as well as the potential to be applied in the medical field. However, although the developed system can offer a high accuracy result but the system only helps cardiologist to do the pre-screening process only.

7.2 Future Work

Based on the research conducted, some recommendations on the developed system need to be implemented. The improvement of the ECG analysis system could be perform as a small unit (noise reduction and pattern recognition) or as a whole ECG analysis system. In general, the development of the system is still in its initial stage and there are still some deficiencies at the noise reduction unit; as the noise cannot be reduced to the minimum level while the accuracy of classification accuracy unable to perform 100% as at the pattern recognition unit.

Several improvements can be made at the noise reduction unit. The unit itself use three different filters in order to reduce the noises effect to the ECG. They used notch bandpass filter to remove the PLI effect. An adaptive filter is used to eliminate the EMG noise and wavelet based filters are used to reduce the BW and MA noises. The PLI noise capable to be remove to the minimum level since it has static frequency with 50/60 Hz depends on power supply of the country. The notch bandpass is designed to remove the 50/60 Hz, but in real application the PLI not exactly 50/60 Hz. A study has to be done in order to identify the lowest and the highest frequencies of the 50/60 Hz PLI, so the notch bandpass filter can be designed on based on the study in order to remove the partial of PLI noise. The use of adaptive filter was unable to eliminated the EMG effect entirely. The adaptive filter needs longer time to reach the settling phase. The MA noise is found to be difficult to be reduced. The problem arises since the frequency of MA noise itself is overlapped with ECG signal. The signal may be remove along with the overlapped noise during the removing process if it is not done properly. Important information from the signal maybe get rid together. As the results, a better threshold need to be applied in order to distinguish the real high and low frequencies of MA noise and low frequency of BW noise. A research has to be conducted to use a single filter rather than three different filters. The range of ECG signal need to be identified before a filter is designed to remain the ECG signal while remove the noises contaminating in the signal.

In the pattern recognition unit, numbers of improvement should be done. During feature extraction phase, the intersection points between filtered ECG signal and the rectangular pulse domain (RPD) are measured based on amplitude axes only. The intersection points are fed to the neural network as the input vectors. As the same time, in addition, the intersection points can be relied on the voltage reading *(y-axis)* and amplitude *(x-axis)* rather than the amplitude measurement only. However, the classification performance may increase due to more accurate features are extracted from the signal. The performance may also decrease since the additional of input vector can increase the complexity of the network. This study also suggests a development of a better classifier which capable to perform more accurate classification results. Based on the developed system, improvement on the classifier can be made to identify the cases of AF. If the classifier is trained to do the classification correctly, it may decrease the cases of false alarms. The cases of misdiagnosis will be decline for both patients with AF but diagnosed with non-AF and non-AF patient but diagnosed with AF.

The ECG analysis system also can be improved by designing a hardware prototype of the system rather than on the software version. This prototype with multi-leads would be attached to the body of a patient and the ECG signals would be collected. The processes such as noise removal, feature extraction and signal classification will be done on the built in board. All information of all the processes would be stored in a memory card then the preliminary results are transmitted to the hospital for further analysis process remotely via wireless technology from computer network. The prototype can be designed as a small as could since design-on-chip technology has been implemented. However, more research on the design need to be started since the system is supported with a lot other element such as power supply to make sure the machine is in working mode, the load to carry the machine and the internet network to transmit the results.

The successive episode shown of AF detection using the amplitude of the ECG signal becomes a benchmark to start the detection on others heart disorders. There are various cases of heart disorders that still need to be detected at the early stage, where the same procedure will be repeated as done for AF detection.

References

1. Benjamin, E. J., P. A. Wolf, R. B. D'Agostino, H. Silbershatz, W. B. Kannel and D. Levy, *Impact of Atrial Fibrillation on The Risk of Death.* Circulation, 1998. **98**(10): p. 946-952.
2. Dash, S., K. H. Chon, S. Lu and E. A. Reader, *Automatic Real Time Detection of Atrial Fibrillation.* Annals of Biomedical Engineering, NY, USA: Biomedical Engineering Society, 2009. **37**: p. 1701-1709.
3. Babaeizadeh, S., R. E. Gregg, E. D. Helfenbein, J. M. Lindauer and S. H. Zhou, *Improvements in Atrial Fibrillation Detection for Real-Time Monitoring.* J. Electrocardiol, 2009. **42**: p. 522-526.
4. Palaniappan, R., T. E. Khoon, *Uni-channel PCA for noise reduction from ECG signals*. in *IBIS*. 2004.
5. Ur Rahman, M. Z., R. A. Shaik and D. V. R. K. Reddy, *Cancellation of Artifacts in ECG Signals using Sign Based Normalized Adaptive Filtering Technique.* Industrial Electronics & Applications, ISIEA,IEEE Symposium 2009: p. 442-445.
6. Agrawal, S. and A. Gupta, *Fractal and EMD based removal of baseline wander and powerline interference from ECG signals.* Computers in Biology and Medicine, 2013. **43**(11): p. 1889-1899.
7. Piskorowski, J., *Suppressing harmonic powerline interference using multiple-notch filtering methods with improved transient behavior.* Measurement, 2012. **45**(6): p. 1350-1361.
8. Sultornsanee, S., I. Zeid, and S. Kamarthi, *Classification of Electromyogram Using Recurrence Quantification Analysis.* Procedia Computer Science, 2011. **6**: p. 375-380.
9. Tong, D. A., K. A. Bartels, and K. S. Honeyager, *Using motion sensors to reduce motion artifact in the ECG.* Journal of Electrocardiology, 2004. **37, Supplement**(0): p. 43.
10. Thakor, N. V. and Y. S. Zhu, *Applications of Adaptive Filtering to ECG Analysis: Noise Cancellation and Arrhythmia Detection.* Biomedical Engineering, IEEE Transactions, 1991. **38**: p. 785-794.
11. Larburu, N., T. Lopetegi and I. Romero, *Comparative Study of Algorithms for Atrial Fibrillation Detection.* Computing in Cardiology, 2011: p. 265-268.
12. Mashor, M. Y., *Hybrid Multilayer Perceptron Networks.* International Journal of System Sciences, 2000. **31**(6): p. 771-785.
13. Newman, D. J., S. Hettich, C. L. Blake, C. J. Merz and D. W. Aha. *UCI Respirototy of The Machine Learning Database.* 1998 [cited 2012 18 August]; Available from: http://archieve.ics.uci.edu/ml/databases.html.
14. Barker, R. L., B. J. Burton and P. D. Zieve, *Principles of Ambulatory Medicine*. 6 ed. 2003, Philadelphia: Lippinocott, Wilkins & Williams.
15. Custer, J. W. and R. E. Rue, *The Harriet Lane Handbook.* 18th ed. 2008, Philadelphia: Mosby Elsevier Inc.
16. Mark, J. B., *Atlas of Cardiovascular Monitoring*. . 1998, New York: Churchill Livingstone.
17. Kumar, T. S., V. S. Pankajan, B. A. Dora, E. V. L. N. Tarun, E. V. S. R. Varun and N. V. S. Chakravarthi, *2D Atlas and Coronary Detection of Human Heart for Educational Purposes*, in *International Conference on Emerging Trends in Electrical and Computer Technology (ICETECT)*. 2011. p. 876-881.
18. Ordas, S., E. Ouble, R. Sebastian and A. F. Frangi, *Computational Anatomy Atlas of the Heart*, in *5th International Symposium on Image and Signal Processing and Analysis*. 2007, ISPA. p. 338-342.

19. Goldberger, A. L., *Fractal mechanisms in the electrophysiology of the heart*, in *Engineering in Medicine and Biology Magazine*. 1992, IEEE. p. 47-52.
20. Altuve, M., G. Carrault, A. Beuchee, P. Pladys and A. I. Hernandez, *On-line apnea-bradycardia detection using hidden semi-Markov models*, in *Annual International Conference* E.i.M.a.B. Society, Editor. 2011, IEEE. p. 4374-4377.
21. Muaynoi, P. S. Tretriluxana and K. Chitsakul, *Signal Processing for Heart Rate Variability Analysis Case Study: Ventricular Tachycardia Condition*, in *Biomedical Engineering International Conference (BMEiCON)*. 2011. p. 117-119.
22. Xiaozhong, C and N. A. Trayanova, *A Novel Methodology for Assessing the Bounded-Input Bounded-Output Instability in QT Interval Dynamics: Application to Clinical ECG With Ventricular Tachycardia*. Biomedical Engineering, IEEE Transactions, 2012. **59**: p. 2111-2117.
23. Cabasson, A., L. Dang, J. M. Vesin, L. Kappenberger, R. Leber, X. Aba and R. cherli, *Susceptibility to paroxysmal atrial fibrillation: A study using sinus rhythm P wave parameters*. in *Computing in Cardiology, 2010*. 2010.
24. McMillan, S., I. Rubinfeld, and Z. Syed. *Predicting atrial fibrillation from intensive care unit numeric data*. in *Computing in Cardiology (CinC), 2012*. 2012.
25. Houben, R. P. M., N. M. S. de Groot and M.A. Allessie, *Analysis of Fractionated Atrial Fibrillation Electrograms by Wavelet Decomposition*. Biomedical Engineering, IEEE Transactions on, 2010. **57**(6): p. 1388-1398.
26. Schamroth, L., *An Introduction to Electrocardiography*. 7th ed. 1990: Blackwell Scientific.
27. Mark, J. B. and T. F. Slaughter, *Cardiovascular Monitoring*. 6th ed. 2005, Philadelphia: Elsevier Churchill Livingstone.
28. Gan-Xin, Y. and C. Antzelevitch, *Cellular Basis for The Electrocardiographic J Wave*. Circular, 1996. **93**: p. 372-379.
29. Texas Heart Institute, *The Conduction System*. 2014 [cited 2014 12 December]; Available from: http://www.texasheart.org/HIC/Anatomy/conduct.cfm.
30. John Hopkin Medicine, *Heart Library*. [cited 2014 12 December]; Available from: http://www.hopkinsmedicine.org/healthlibrary/conditions/cardiovascular_diseases/anatomy_and_function_of_the_hearts_electrical_system_85,P00214/.
31. Gan-Xin, Y., R. S. Lankipalli, J. F. Burke, S. Musco and P. R. Kowey, *Ventricular Repolarization Components on the Electrocardiogram: Cellular Basis and Clinical Significance*. J Am Coll Cardiol, 2003. **42**(3): p. 401-409.
32. Pan, J. and J. W. Tompskins, *A Real-Time QRS Detection Algorithm*. Biomedical Engineering, IEEE Transactions 1985. **32**: p. 230-236.
33. Boulgouris, N. V., K. N. Plataniotis and E. M. Tzanakou, *Biometrics: Theory, Methods, and Applications*. 2009, Canada: John Wiley & Sons, Inc.
34. Allyn, W., *AHA Diagnostic ECG Electrode Placement*. 2012 [cited 2014 October 10th]; Available from: http://www.welchallyn.com/documents/Cardiopulmonary/Electrocardiographs.pdf.
35. Conover, M. B., *Understanding Electrocardiography*. 8th ed. 2002, Missouri: Mosby.
36. Jameson, J. N., D. L. Kasper, T. Randolph, B. Eugene, A. S. Fauci, S. L. Hauser and D. L. Longo, *Harrison's principles of internal medicine*. 2005, New York: McGraw-Hill Medical Publishing Division.
37. Leith, J. W., M. Basta and P. J. Fletcher, *Effect of phenylephrine infusion on atrial electrophysiological properties Heart*. 1997. **78**: p. 166-170.
38. Shen, L. and J. W. Tompkins, *Experimental study: brachial motion artifact reduction in the ECG*. Computers in Cardiology, 1995: p. 33-36.

39. Pollack, C. V., *Wireless cardiac event alert monitoring is feasible and effective in the emergency department and adjacent waiting areas.* Critical pathways in cardiology, 2009. **8**: p. 7-11.
40. Escalona, O. J. and M. E. Reina, *A Fast and Robust Time-Series Based Decision Rule for Identification of Atrial Fibrillation Arrhythmic Patterns in the ECG.* Computers in Cardiology, 2010. **37**: p. 995-998.
41. Hilbel, T., T. M. Helms, G. Mikus, H. A. Katus and C. Zugck, *Telemetry in the clinical setting.* Herzschrittmachertherapie & Elektrophysiologie, 2008. **19**: p. 146-164.
42. Zuxiang, F., L. Dakun, G. Xin and W. Xiaomei, *Successive ECG telemetry monitoring for preventing sudden cardiac death*, in *Annual International Conference of the IEEE*. 2009, Engineering in Medicine and Biology Society. p. 1738-1741.
43. Hung-Fat, T., G. Y. Lip, J. Andrew and S. Coats, *ODR Cardiology*. 2011.
44. Zoni-Berisso, M., F. Lercari, T. Carazza and S. Domenicucci, *Epidemiology of Atrial Fibrillation: European Perspective.* Clinical Epidemiology, 2014. **6**: p. 213-220.
45. David, G., *Chamberlain's Symptoms and Signs in Clinical Medicine: An Introduction to Medical Diagnosis*. 13 ed. 2010, London: Hodder Arnold.
46. Fuster, V., L. E. Ryden and D. S. Cannom, *ACC/AHA/ESC 2006 Guidelines for the Management of Patients with Atrial Fibrillation: a report of the American College of Cardiology/American Heart Association Task Force on Practice Guidelines and the European Society of Cardiology Committee for Practice Guidelines (Writing Committee to Revise the 2001 Guidelines for the Management of Patients With Atrial Fibrillation): developed in collaboration with the European Heart Rhythm Association and the Heart Rhythm Society.* Circulation, 2006. **114**: p. 257-354.
47. Fu, R., S. Wu, P. Wu and J. Qiu, *A Study of blood soluble P-selectin, fibrinogen, and von Willebrand factor levels in idiopathic and lone atrial fibrillation.* Europace, 2011. **13**: p. 31-36.
48. Slocum, J. Slocum, A. Sahakian and S. Swiryn, *Diagnosis of atrial fibrillation from surface electrocardiograms based on computer-detected atrial activity.* Journal of Electrocardiology, 1992. **25**: p. 1-8.
49. Goldberger, A., L. Amaral and L. Glass, *PhysioBank, PhysioToolkit and PhysioNet: Components of a New Research Resource of Complex Physiologic Signals.* Circulation, 2000. **101**(6): p. 215-220.
50. Furno, G. S and J. W. Tompkins, *A Learning Filter for Removing Noise Interference.* Biomedical Engineering, IEEE Transactions, 1983. **30**: p. 234-235.
51. Widrow, B., J. R. Blover, J. M. Mc Cool, J. Kaunnitz, C. S. Williams, R. H. Hean, J. R. Zeidler, E. Dong and R C. Goodlin, *Adaptive Noise Cancelling: Principles and Applications*. in *Proceeding of The IEEE*. 1975. IEEE.
52. Van Alste, V. A. and T. Schilder, *Removal of Base-Line Wander and Power-Line Interference from the ECG by an Efficient FIR Filter with a Reduced Number of Taps.* Biomedical Engineering, IEEE Transactions 1985. **32**: p. 1052-1060.
53. Alhady, S. S. N., M. R. Arshad and M. Y. Mashor, *P, Q, R, S and T peaks recognition of ECG using MRBF with selected features*. in *Proceedings of the 4th WSEAS International Conference on Software Engineering, Parallel & Distributed Systems*. 2005. Salzburg, Austria.
54. Meddour, C and M. Tighidet, *Realization and development of a tool hard/soft for detection of cardiac abnormalities*, in *International Conference onCommunications, Computing and Control Applications (CCCA)*, . 2011. p. 1-6.
55. Soo-Chang, P., S. Jong.-Jy, H. Yun-Da and C. Cheng-Han, *Improved Methods for The Design of Variable Fractional-Delay IIR Digital Filters.* Circuits and Systems I: Regular Papers, IEEE Transactions, 2012. **59**: p. 989-1000.

56. Goel, A., A. Vetteth, K. R. Rao and V. Sridhar, *Active Cancellation of Acoustic Noise using A Self-Tuned Filter.* Circuits and Systems I: Regular Papers, IEEE Transactions, 2004. **51**: p. 2148-2156.
57. Shi, W. V. and Z. MengChu, *Fuzzy PID controllers for dual-sensor pacing systems in patients with bradycardias at rest*, in *IEEE International Conference on Systems, Man, and Cybernetics (SMC)*. 2011. p. 1117-1122.
58. Zhen, Q., L. Qingshan, D. N. Metaxas and L. Axel, *Identifying Regional Cardiac Abnormalities From Myocardial Strains Using Nontracking-Based Strain Estimation and Spatio-Temporal Tensor Analysis.* Medical Imaging, IEEE Transactions 2011. **30**: p. 2017-2029.
59. Min, D and L. Shi-Liu, *Removal of Baseline Wander from Dynamic Electrocardiogram Signals*, in *Image and Signal Processing 2009. CISP '09. 2nd International Congress*. 2009. p. 1-4.
60. Ling, Z., C. Lall and C. Yu, *Low-distortion baseline removal algorithm for electrocardiogram signals.* Computing in Cardiology (CinC), 2012: p. 769-772.
61. Kim, K. J., J. H. Ku, I. Y. Kim, S. I. Kim and S. W. Nam, *Notch filter design using the scaled sampling kernel and its application to power line noise removal from ECG signals*, in *Control, Automation and Systems, ICCAS '07. International Conference* 2007. p. 2415-2418.
62. Zhu, Y. S., X. H. Wu and Z. S. Zhang, *Design of FIR narrow-band frequency selective filters using sliding DFT array processors*. in *Circuits and Systems, Conference Proceedings, International Conference*. 1991. China.
63. M. Ferdjallah and R. E. Barr, *Adaptive digital notch filter design on the unit circle for the removal of powerline noise from biomedicals signal.* Biomedical Engineering, IEEE Transactions o, 1994. **41**: p. 529-536.
64. Piskorowski, J., *Powerline interference removal from ECG signal using notch filter with non-zero initial conditions*, in *Medical Measurements and Applications Proceedings (MeMeA), 2012 IEEE International Symposium*. 2012. p. 1-3.
65. Panda, R. and U. C. Pati, *Removal of artifacts from electrocardiogram using digital filter*, in *Electrical, Electronics and Computer Science (SCEECS), IEEE Students' Conference*. 2012. p. 1-4.
66. Jeyarani, A. D. and T. J. Singh, *Analysis of noise reduction techniques on QRS ECG waveform - by applying different filters.* Recent Advances in Space Technology Services and Climate Change (RSTSCC), 2010: p. 149-152.
67. Widrow, B. and D. Stearns, *Adaptive Signal Processing*. 1985: Prentice Hall.
68. Rehman, S. A., R. Kumar and M.Rao, *Performance comparison of various adaptive filter algorithms for ECG signal enhancement and baseline wander removal*, in *Computing Communication & Networking Technologies (ICCCNT), Third International Conference* 2012. p. 1-5.
69. Haykin, S., *Adaptive Filter Theory*. 2002: Prentice Hall.
70. Boukis, C., D. P. Mandic and A. G. Constantinides, *Bias reduction in acoustic feedback cancellation systems with varying all-pass filters*. 2006. **42**, 556-558.
71. Ohta, S., Y. Kajikawa, and Y. Nomura, *Acoustic Echo Cancellation Using Sub-Adaptive Filter*. in *Intelligent Signal Processing and Communications, 2006. ISPACS '06. International Symposium on*. 2006.
72. Raya, M. A. D. and L. G. Sison, *Adaptive noise cancelling of motion artifact in stress ECG signals using accelerometer*. in *Engineering in Medicine and Biology, 2002. 24th Annual Conference and the Annual Fall Meeting of the Biomedical Engineering Society EMBS/BMES Conference, Proceedings of the Second Joint*. 2002.

73. Pandey, V. K., *Adaptive filtering for baseline wander removal in ECG*, in *Information Technology and Applications in Biomedicine (ITAB), 10th IEEE International Conference* 2010. p. 1-4.
74. Paul, B. and B. P. Mythili, *ECG noise removal using GA tuned sign-data least mean square algorithm*, in *Advanced Communication Control and Computing Technologies (ICACCCT), IEEE International Conference*. 2012. p. 100-103.
75. Ur Rahman, M. Z., D. V. R. K. Reddy and Y. Sangeetha, *Stationary and Non-Stationary noise removal from Cardiac Signals using a Constrained Stability Least Mean Square Algorithm*, in *Communications and Signal Processing (ICCSP), 2011 International Conference*. 2011. p. 485–488.
76. Zhao, Z and C. Ma, *A novel cancellation method of powerline interference in ECG signal based on EMD and adaptive filter*, in *Communication Technology, ICCT 11th IEEE International Conference*. 2008. p. 517-520.
77. Abbaspour, S., A. Fallah and A. Maleki, *A comparison of adaptive neuro-fuzzy inference system and real-time filtering in cancellation ECG artifact from surface EMGs*, in *Electrical Engineering (ICEE), 20th Iranian Conference*. 2012. p. 1558-1561.
78. Huang, N. E. and S. S. Shen, *Hilbert-Huang transform and its applications*. Vol. 5. 2005: World Scientific.
79. Hernandez, E. and G. Weiss, *A First Course on Wavelets*. 1996: CRC Press.
80. Meyer, Y. and D. H. Salinger, *Wavelets and Operators*. 1995: Cambridge University Press.
81. Meyer, Y. and R. D. Ryan, *Wavelets: Algorithms and Applications*. 1993: Society for Industrial and Applied Mathematics.
82. Benedetto, J. J. and M. W. Frazier, *Wavelets: Mathematics and Applications*. 1994, Boca Raton, FL: CRC Press.
83. Heil, C., D. F. Walnut and I. Daubechies, *Fundamental Papers in Wavelet Theory*. 2009: Princeton University Press.
84. Daubechies, I., *Ten Lectures on Wavelets*. 1992: Society for Industrial and Applied Mathematics (SIAM, 3600 Market Street, Floor 6, Philadelphia, PA 19104).
85. Mallat, S. G., *A theory for multiresolution signal decomposition: the wavelet representation.* Pattern Analysis and Machine Intelligence, IEEE Transactions on, 1989. **11**(7): p. 674-693.
86. De Chazal, P., B. G. Cellar and R. B. Rei, *Using Wavelet Coefficients for the classification of the Electrocardiogram*. in *Proceedings of the 22nd Annual EMBS International Conference*. 2000. Chicago IL.
87. Gubbi, J., A. Khandoker and M. Palaniswami, *Classification of Obstructive and Central Sleep Apnea Using Wavelet Packet Analysis of ECG Signals.* Computer in Cardiology, 2009. **36**: p. 733−736.
88. Percival, D. B. and A. T. Walden, *Wavelet Methods for Time Series Analysis*. 2006: Cambridge University Press.
89. Nagendra, H., S. Mukherjee and V. Kumar, *Wavelet Based Non Linear Thresholding Techniques for Pre-Processing ECG Signals.* International Journal of Biomedical And Advance Research, 2013. **4**(8): p. 534-544.
90. Zhang, W., X. Yang, Z, Xu, P. An, Q. Liu and Y. Lu, *Advances on Digital Television and Wireless Multimedia Communications: 9th International Forum on Digital TV and Wireless Multimedia Communication, IFTC 2012, Shanghai, China, November 9-10, 2012. Proceedings*. 2012: Springer Berlin Heidelberg.
91. Donoho, D. L., *De-noising by soft-thresholding.* Information Theory, IEEE Transactions on, 1995. **41**(3): p. 613-627.

92. Meyer, Y. and S. Roques, *Progress in Wavelet Analysis and Applications: Proceedings of the International Conference "Wavelets and Applications," Toulouse, France - June 1992*. 1993: Editions Frontieres.
93. Donoho, D. L. and I. M. Johnstone, *Ideal Spatial Adaptation by Wavelet Shrinkage*. 1992: Stanford University. Division of Biostatistics.
94. Arvinti, B., D.Toader, M. Costache and A. Isar, *Electrocardiogram baseline wander removal using stationary wavelet approximations* in *Optimization of Electrical and Electronic Equipment (OPTIM), 12th International Conference*. 2010. p. 890-895.
95. Zhe, L., N. Jun and G. Xin, *A Denoising Framework for ECG Signal Preprocessing*, in *Internet Computing for Science and Engineering (ICICSE), 6th International Conference*. 2012. p. 176-179.
96. Patil, P, B, and M. S. Chavan, *A wavelet based method for denoising of biomedical signal*, in *Pattern Recognition, Informatics and Medical Engineering (PRIME), International Conference*. 2012. p. 278-283.
97. Weidong, Z. and J. Gotman, *Removal of EMG and ECG artifacts from EEG based on wavelet transform and ICA*, in *Engineering in Medicine and Biology Society, IEMBS 26th Annual International Conference of the IEEE*. 2004. p. 392-395.
98. Seung Min, L., K. Ko. Kuen and P. Kwang Suk, *Wavelet approach to artifact noise removal from Capacitive coupled Electrocardiograph*, in *Engineering in Medicine and Biology Society, EMBS 30th Annual International Conference of the IEEE*. 2008. p. 2944-2947.
99. Strasser, F., M. Muma and A. M. Zoubir, *Motion artifact removal in ECG signals using multi-resolution thresholding*, in *Signal Processing Conference (EUSIPCO), Proceedings of the 20th European*. 2012. p. 899-903.
100. Plataniotis, K. N., D. Hatzinakos and J. K. M. Lee, *ECG biometric recognition without fiducial detection,* in *Special Session on the Biometric Consortium Conference, 2006 Biometrics Symposium*. 2006. p. 1-6.
101. Agrafioti, F. and D, Hatzinakos, *Fusion of ECG sources for human identification*, in *Communication, Control and Signal Processing, 3rd International Symposium*. 2008. p. 1542-1547.
102. Colloca, R., A. E. W. Johnson, L. Mainardi and G. D. Clifford, *A Support Vector Machine Approach for Reliable Detection of Atrial Fibrillation Events.* Computers in Cardiology, 2013. **40**: p. 1047-1050.
103. Maji, U., M. Mitra and S. Pal, *Differentiating Normal Sinus Rhythm and Atrial Fibrillation in ECG Signal: A Phase Rectified Signal Averaging Based Approach*. in *2014 International Conference on Control, Instrumentation, Energy & Communication (CIEC)*. 2014.
104. Hayes, G. and P. D. Teal, *Real-Time Detection of Atrial Fibrillation using a Low-Power ECG Monitor.* Computers in Cardiology, 2013. **40**: p. 743-746.
105. Lee, J., Y. Nam, D. D. McManus and K. H. Chon, *Time-Varying Coherence Function for Atrial Fibrillation Detection* IEEE Transaction on Biomedical Engineering, 2013. **60**(10): p. 2783-2793.
106. Schmidt, R., M. Harris, D. Novac and M. Perkhun, *Atrial Fibrillation Detection*, N.P. Eindhoven, Editor. 2008: Eindhoven, Netherlands
107. Helfenbein, E., R. Gregg., J. Lindauer and S. Zhou, *An Automated Algorithm for the Detection of Atrial Fibrillation in the Presence of Paced Rhythms.* Computers in Cardiology, 2010. **37**: p. 113-116.
108. Rincon, A. E. S. and C. C. Fernandez, *ECG feature extraction via waveform segmentation*, in *Electrical Engineering Computing Science and Automatic Control (CCE), 2010 7th International Conference* 2010. p. 250-255.

109. Mukhopadhyay, S. K., M.Mitra and S. Mitra, *Time plane ECG feature extraction using Hilbert transform, variable threshold and slope reversal approach*, in *Communication and Industrial Application (ICCIA), International Conference*. 2011. p. 1-4.
110. Mazomenos, E. B., T. Chen and A. Acharyya, A. Bhattacharya, J. Rosengarten and K. Maharatna, *A Time-Domain Morphology and Gradient based algorithm for ECG feature extraction*, in *Industrial Technology (ICIT), IEEE International Conference* 2012. p. 117-122.
111. Kumar, M., S. Singh and S. C. Mahajan, *Computerized detection & amp; classification of ECG signals*, in *Emerging Trends in Electrical Engineering and Energy Management (ICETEEEM), International Conference*. 2012. p. 126-130.
112. Ge, D., *Study of ECG Feature Extraction for Automatic Classification Based on Wavelet Transform*, in *Computer Science & Education (ICCSE), 7th International Conference*. 2012. p. 500-503.
113. Sutar, R., A. G. Khotari and A. G. Keskar, *ECG Feature Extraction Using LCAD*, in *Communication Systems and Network Technologies (CSNT), International Conference*. 2012. p. 100-103.
114. Safie, S. I., J. J. Soraghan and L. Petropoulakis, *Electrocardiogram (ECG) Biometric Authentication using Pulse Active Ratio (PAR).* IEEE Transactions on Information Forensics and Security, 2011. **6**(4): p. 1315-1322.
115. Stuart, J. E., J. Connolly, P. Dorian, S. H. Hohnloser, D. D. Gretler, U. Sinha and M. D. Ezekowitz, *Betrixaban compared with warfarin in patients with atrial fibrillation: results of a phase 2, randomized, dose-ranging study.* European Heart Journal, 2012.
116. Andersson, O., K. H. Chon, L. Sörnmo, J. N. Rodrigues, *A 290 mV Sub-VT ASIC for Real-Time Atrial Fibrillation Detection.* IEEE Transaction on Biomedical Circuit and Systems, 2014. **99**: p. 1-10.
117. Ladavich, S. and B. Ghoraani, *Developing an atrial activity-based algorithm for detection of atrial fibrillation*, in *36th Annual International Conference of the IEEE on Engineering in Medicine and Biology Society (EMBC)*. 2014. p. 54-57.
118. Lian, J., L. Wang and D. Muessig, *A Simple Method to Detect Atrial Fibrillation using RR Intervals*, in *31st Annual Sciencetific Sessions of the Heart Rhythm Society*. 2010: Denver, Colorado. p. 1494-1497.
119. Kostka, P. S. and E. J. Tkacz, *Rules extraction in SVM and Neural Network Classifiers of Atrial Fibrillation Patients with Matched Wavelets as a Feature Generator*. in *31st Annual International Conference of the IEEE EMBS* 2009. Minneapolis, Minnesota, USA.
120. Haykin, S., *Neural Network: A Comprehensive Foundation*. 1994, NJ Prentice Hall.
121. Haykin, S., *Neural Networks and Learning Machines*. 2009, New York: Prentice Hall.
122. Mashor, M. Y., *Some Properties of RBF Network with Applications to The System Identification.* International Journal of the Computer, the Internet and Management, 1999. **7**(1): p. 34-71.
123. Chen, S., S. A. Billings and P. M. Grant, *Recursive Hybrid Algortihm for Non-Linear System Identification using Radial Basis Function Networks.* International Journal of Control, 1992. **55**: p. 1055-1070.
124. Bishop, C. M., *Neural Networks for Pattern Recognition*. 1995, Oxford University Press: Oxford, UK.
125. Funashashi, K., *On The Approximate Realization on Continuous Mapping by Neural Networks.* Neural Networks, 1989. **2**: p. 182-192.
126. Cybenko, G., *Approximation by Superposition of The Sigmoid Function.* Mathematics of Control, Signals & Systems, 1989. **2**: p. 303-314.

127. Mashor, M. Y., *Modified Recursive Prediction Error Algorithm for Training Layered Neural Network.* International Journal of Computer, the Internet and the Management, 2003. **11**(2): p. 29-35.
128. Maeda, Y., Y. Yotsumoto, and Y. Kanata. *Unsupervised learning of neural networks for separation of unknown data*. in *Industrial Electronics, Control, and Instrumentation, 1995., Proceedings of the 1995 IEEE IECON 21st International Conference on*. 1995.
129. Duttweiler, D. L., *Proportionate Normalized Least-Mean-Squares Aaptation in Echo Cancelers.* Speech and Audio Processing, IEEE Transactions 2002. **8**: p. 508-518.
130. Benesty, J. and S. L. Gay, *An Improved PNLMS Algorithm.* IEEE International Conference on Acoustic, Speech and Signal Processing, 2002: p. 1881-1884.
131. Deng. H. and M. Doroslovacki, *Improving Convergence of The PNLMS Algorithm for Sparse Impulse Response Identification.* Signal Processing Letters, IEEE, 2005. **12**: p. 181-184.